Light Transmission Properties of Lentil (*Lens culinaris* Medik.) Seed Coat and Effect of Light Exposure on Cotyledon Quality

A Thesis Submitted to the College of Graduate and Postdoctoral Studies

In Partial Fulfillment of the Requirements

For the Degree of Master of Science

In the Department of Chemical and Biological Engineering

University of Saskatchewan

Saskatoon

By

NSUHORIDEM JACKSON

PERMISSION TO USE

In presenting this thesis in partial fulfillment of the requirements for a Postgraduate degree from the University of Saskatchewan, I agree that the Libraries of this University may make it freely available for inspection. I further agree that permission for copying of this thesis in any manner, in whole or in part, for scholarly purposes may be granted by the professor or professors who supervised my thesis work or, in their absence, by the Head of the Department or the Dean of the College in which my thesis work was done. It is understood that any copying or publication or use of this thesis or parts thereof for financial gain shall not be allowed without my written permission. It is also understood that due recognition shall be given to me and to the University of Saskatchewan in any scholarly use which may be made of any material in my thesis.

Requests for permission to copy or to make other uses of materials in this thesis in whole or part should be addressed to:

Head of the Department of Chemical and Biological Engineering
University of Saskatchewan
57 Campus Drive Saskatoon,
Saskatchewan S7N 5A9

OR

Dean
College of Graduate and Postdoctoral Studies
University of Saskatchewan
116 Thorvaldson Building, 110 Science Place
Saskatoon, Saskatchewan S7N 5C9 Canada

ABSTRACT

Cotyledon color is one of the most important quality criteria in the lentil market because the color may correlate well with other quality attributes. Therefore, cotyledon color is an important quality criterion in lentil breeding programs. The objectives of this work were to investigate the variation in optical properties among lentil seed coat types and to determine the effect of light treatment, seed coat presence, and seed coat type on color loss in lentil cotyledon. Light transmission properties of seed coat types were obtained to find out if they differ in their light-blocking ability and protection of the underlying cotyledon from photodegradation. Light reflectivity was measured to investigate if there are recognizable patterns, which might be useful in market class discrimination, quality prediction and disease detection in the seeds. A fiber-optic spectrometer was used to obtain spectral reflectivity and transmission properties of seed coats of 20 lentil genotypes. The reflectivity (0°\32°) and nadir-aligned transmission spectra were measured in the 250 nm to 850 nm wavelength range. An Analysis of Variance (ANOVA) showed that there were significant ($p<0.05$) differences in light transmission properties of the major seed coat types.

A computer vision system was used to study the influence of light exposure on the cotyledon color of red, green, and yellow lentils. Twenty samples from each of the three cotyledon color classes were subjected to six levels of light treatment, namely ultraviolet, full-spectrum visible, red, green, blue, and control (dark) for seven days, at room temperature. This light exposure had a significant effect on all three cotyledon color classes. The effect size was largest in green lentils, smaller in yellow, and least in red lentils.

Having established the light-blocking characteristics of the various seed coats and realizing that light exposure does affect the color of lentil cotyledon, the protective effects of different kinds of seed coat against light-induced cotyledon color change was tested. Results showed that some whole green cotyledon lentils experienced color losses in the underlying cotyledon. Red and yellow lentil classes had high levels of colorfastness, and their seed coats successfully protected the cotyledon from these minimal effects. Thus, breeding for seed coat protection may not improve the cotyledon color of Canadian red lentils (the most de-hulled market class), but it may improve the overall quality of green lentils.

ACKNOWLEDGMENTS

I owe a debt of gratitude to my supervisor Dr. Scott Noble; the contact I made with him back in October 2017 has changed the course of my career history – in a positive way. I thank him for effectively managing the challenges of supervising an international student. His guidance and insights enabled me to manage my strengths and weaknesses and make significant achievements during this work. I am grateful for his flexible approach to supervision, which allowed me to express my ideas freely, thereby making the work more enjoyable. I am also super grateful for the timely manner my requests for needed materials were supplied; this was a great source of motivation.

Also, the depth of my gratitude to my advisory committee member Dr. Albert Vandenberg cannot be emphasized enough. His support made it possible for me to figure out my research problem early enough to have results for conference presentations. But that is not all. He drove me to the US to present my first ever oral presentation at an international conference – all expenses paid; I also cannot forget the nice stopovers and edibles, which came at no cost to me. My gratitude also extends to my Committee Chair Dr. Venkatesh Meda; his cooperation and corrections significantly contributed to my progress.

I also appreciate the mentorship of Dr. Maya Subedi at the beginning of my research. She was instrumental in deciding and obtaining the samples I needed for the first phase of my work. She also introduced me to nice souls at the Crop Science Field Laboratory, such as Brent Barlow. Brent is so much appreciated by me today because he is down to earth cooperative; this made it possible for me to obtain my samples and use equipment at the Field Lab without friction. The cooperation and assistance of my research group members Reisha Peters, Tyrone Keep, and Keith Halcro are also highly appreciated.

Finally, and quite importantly, I express my gratitude to my indefatigable and loving Mum, Mrs. Patricia Isaac Udeme for her unparalleled support in my life and to my brothers like no other - the five Jacksons.

DEDICATION

I dedicate this work to my mother Mrs. Patricia Udeme, who single-handedly sponsored the undergraduate education of myself and five brothers after the demise of my father several years ago.

TABLE OF CONTENTS

PERMISSION TO USE i
ABSTRACT ii
ACKNOWLEDGMENTS iii
DEDICATION iv
TABLE OF CONTENTS v
LIST OF FIGURES ix
LIST OF TABLES xi
LIST OF ABBREVIATIONS xiii
Chapter 1: INTRODUCTION 1
1.1 Problem Statement 2
1.2 Research Objectives 3
1.2.1 Hypotheses 3
1.3 Scope Statement 4
1.3.1 Within Scope 4
1.3.2 Out of Scope 4
Chapter 2: LITERATURE REVIEW 5
2.1 Lentils 5
2.1.1 Major Commercial Groups of Lentils 5
2.1.2 Genetics and Biochemistry of Lentil Seed Coat Colors 6
2.1.3 Genetics and Biochemistry of Lentil Cotyledon Classes 9
2.2 Light and its Interaction with Matter 10
2.2.1 The Nature and Properties of Light 10
2.2.2 Sunlight 11
2.2.3 Light Interaction with a Material 12
2.3 Optical Properties and Optical Spectroscopy 12
2.3.1 Optical Spectroscopy Instruments 14
2.4 Effect of Light on Plant Biomaterials 16

2.4.1 Photo-thermal Effect 16
2.4.2 Photochemical Effect in Crop Products 17
2.4.3 Photochemical Effect in Living Plants 19
2.5 Color Measurement 19
2.5.1 The Munsell Color Scale 19
2.5.2 CIE and Hunter L, a, b Color Systems 20
2.5.3 The CIELAB Color Difference Equation 22
2.5.4 Color Measurement Instruments 23
2.5.4.1 Color Measurement by Computer Vision 23
PROLOGUE TO CHAPTERS 3 & 4 26
Chapter 3: OPTICAL FIBER SPECTROMETER SET-UP AND TESTING 27
3.1 Instrument Description 26
3.1.1 Calibration and Measurement Procedure 29
3.2 Measurement System Analysis/Method Validation 31
3.2.1 Sample Preparation 31
3.2.2 Measurement Repeatability Assessment 31
3.2.3 Within-sample Variation Assessment 32
3.2.4 Results and Discussion 33
3.3 Summary and Conclusion 36
Chapter 4: OPTICAL PROPERTIES AND GENOTYPIC VARIABILITY IN LENTIL SEED COAT 38
4.1 Materials and Methods 37
4.1.1 Data Collection 37
4.1.2 Data Analysis 38
4.2 Results and Discussion 40
4.2.1 Transmission Properties 40
4.2.2 Reflectivity Properties 46
4.3 Chapter Summary/General Discussion and Conclusion 50
PROLOGUE TO CHAPTERS 5 & 6 52
Chapter 5: EFFECT OF LIGHT EXPOSURE ON COLOR OF LENTIL COTYLEDON 53

5.1 Materials and Methods 52
5.1.1 Experimental Design 53
5.1.2 Color Measurement 53
5.1.3 Light Treatment 54
5.1.4 Data Analysis 54
5.2 Results and Discussion 55
5.2.1 Effect of Light Treatment on Green Lentil Cotyledons 57
5.2.2 Effect of Light Treatment on Red Lentil Cotyledons 58
5.2.3 Effect of Light Treatment on Yellow Lentil Cotyledons 61
5.3 Summary/General Discussion and Conclusion 63
Chapter 6: INFLUENCE OF LIGHT ON COTYLEDON COLOR OF WHOLE LENTIL SEEDS 66
6.1 Materials and Methods 65
6.1.1 Experimental Design 65
6.1.2 Color Measurement 66
6.1.3 Light Treatment 67
6.1.4 Data Analysis 67
6.2 Results and Discussion 67
6.2.1 Light and Color of Green Cotyledon Lentils 68
6.2.2 Light and Color of Red Cotyledon Lentils 76
6.2.3 Light and Color of Yellow Cotyledon Lentils 82
6.3 Chapter Summary/General Discussion and Conclusion 88
Chapter 7: GENERAL DISCUSSION, CONCLUSIONS, AND FUTURE RESEARCH 90
7.1 Discussion 89
7.2 Conclusions 91
7.3 Future Research 92
REFERENCES 94
APPENDIX A: ANOVA TABLES FOR LIGHT TRANSMISSION PROPERTIES OF LENTIL SEED COAT 102
PROLOGUE TO APPENDIX B 105

APPENDIX B: MACHINE LEARNING MODELS FOR PREDICTING LENTIL GENOTYPES USING SEED COAT REFLECTIVITY 105
B.1 Signal Preprocessing 105
B.2 Data Modeling 106
B.3 Model Validation 109
B.4 Results and Discussion 109
B.5 Conclusion 113
APPENDIX C: ANOVA TABLES FOR EFFECT OF LIGHT TREATMENT ON LENTIL COTYLEDON 114
APPENDIX D: ANOVA TABLES FOR EFFECT OF LIGHT TREATMENT ON WHOLE LENTILS 117
APPENDIX E: PLOT, ANALYSIS AND MODELING SCRIPTS 129
E.1: Sample Analysis and Plot R Script for Measurement Repeatability Study. 129
E.2: Sample Analysis and Plot R Script for Within-sample Variability Study. 131
E.3: Sample R Plot Script for Seed Coat Transmission. 133
E.4: Transmission Analysis R Script 136
E.5: Sample Color Analysis/Plots R Script (Chapter Five). 141
E.6: Sample Color Difference Plots (GNUPLOT) Script (Chapter Six) 146
E.7: Sample Color Analysis R Script (Chapter Six). 148

LIST OF FIGURES

Figure 2.1: Dehulled lentil cotyledons.. 6
Figure 2.2: Lentil samples with major seed coat colors used in the study..... 8
Figure 2.3: Electromagnetic spectrum 10
Figure 2.4: Schematic diagrams of fiber-optic spectroscopy units..... 16
Figure 3.1: Schematic representation of optical fiber spectroscopy set-up 28
Figure 3.2: The sample stage. 29
Figure 3.3: Average of 10 repeated reflectivity measurements ± 1 SD on single seed coats for six lentil genotypes 34
Figure 3.4: Average reflectivity measurements ± 1 SD (N=10) for seed coats of six lentil genotypes. 35
Figure 4.1: Transmission properties of the seed coats of lentil market classes. 42
Figure 4.2: Mean and distribution of cumulative UV transmission (250-400 nm) 43
Figure 4.3: Mean and distribution of normalized cumulative VIS transmission (400 – 700 nm). 44
Figure 4.4: Mean and distribution of cumulative NIR transmission (700 – 850 nm)..... 45
Figure 4.5: Reflectivity properties of the seed coats of lentil market classes. 48
Figure 5.1: Lentil sample holders for light treatment. 53
Figure 5.2: Mean changes in color values as a function of cotyledon color and light treatment . 56
Figure 5.3: Spread in color change values of green lentil cotyledons as a function of light treatment 59
Figure 5.4: Spread in color change values of red lentil cotyledons as a function of light treatment 60
Figure 5.5: Spread in color change values of yellow lentils as a function of light treatment..... 62
Figure 6.1: Changes in L^*-value in different seed coat classes and treatment groups (green lentils): 72
Figure 6.2: Changes in a^*-value in different seed coat classes and treatment groups (green Lentils) 73
Figure 6.3: Changes in b^*-value in different seed coat classes and treatment groups (green lentils) 74

Figure 6.4: Changes in E^* in different seed coat classes and treatment groups (Green Lentils).. 75
Figure 6.5: Changes in L^*-values in different seed coat classes and treatment groups (red lentils) 78
Figure 6.6: Changes in a^*-values in different seed coat classes and treatment groups (red lentils) 79
Figure 6.7: Changes in b^*-values in different seed coat classes and treatment groups (red lentils) 80
Figure 6.8: Changes in E^* in different seed coat classes and treatment groups (red lentils) 81
Figure 6.9: Changes in L^*-values in different seed coat classes and treatment groups (yellow lentils) 84
Figure 6.10: Changes in a^*-values in different seed coat classes and treatment groups (yellow lentils) 85
Figure 6.11: Changes in b^*-values in different seed coat classes and treatment groups (yellow lentils) 86
Figure 6.12: Changes in E^* in different seed coat classes (yellow lentils) 87
Figure B.1: Reflectivity spectra of seed coat. 106
Figure B.2: Performance Plots for LDA Models 111

LIST OF TABLES

Table 4.1: Lentil genotypes and their seed coat color characteristics..... 38
Table 6.1: Lentils used for the study..... 66
Table A.1: ANOVA for Cumulative UV Transmission 102
Table A.2: ANOVA for Cumulative VIS Transmission..... 102
Table A.3: ANOVA for Cumulative NIR Transmission 102
Table A.4: Multiple Comparisons for Seed Coat Light Transmission 103
Table B.1: Classification accuracies of LDA models. 110
Table B.2: Classification accuracies of the PLS-DA models. 112
Table B.3: Classification accuracies of neural networks (before PCA). 113
Table B.4: Classification accuracies of neural networks (after PCA) 113
Table C.1: GLM model summary for green lentil (ΔL*-value)..... 114
Table C.2: GLM model summary for green lentil (Δa*-value). 114
Table C.3: GLM model summary for green lentil (Δb*-value). 114
Table C.4: GLM model summary for green lentil (ΔE)..... 114
Table C.5: GLM model summary for red lentil (ΔL*-value). 115
Table C.6: GLM model summary for red lentil (Δa*-value). 115
Table C.7: GLM model summary for red lentil (Δb*-value). 115
Table C.8: GLM model summary for red lentil (ΔE). 115
Table C.9: GLM model summary for yellow lentil (ΔL*-value)..... 116
Table C.10: GLM model summary for yellow lentil (Δa*-value). 116
Table C.11: GLM model summary for yellow lentil (Δb*-value). 116
Table C.12: GLM model summary for yellow lentil (ΔE*-value)..... 116
Table D.1: Multiple Comparison of ΔL^*-values of green cotyledon lentil under visible light... 117
Table D.2: Multiple Comparison of ΔL^*-values of green cotyledon lentil under UVA. 117
Table D.3: Multiple Comparison of Δa^*-values of green cotyledon lentil under visible light. .. 118
Table D.4: Multiple Comparison of Δa^*-values of green cotyledon lentil under UVA..... 118
Table D.5: Multiple Comparison of Δb^*-values of green cotyledon lentil under visible light. .. 119

Table D.6: Multiple Comparison of Δb^*-values of green cotyledon lentil under UVA. 119
Table D.7: Multiple Comparison of ΔE^*-values of green cotyledon lentil under visible light... 120
Table D.8: Multiple Comparison of ΔE^*-values of green lentil cotyledon under UVA. 120
Table D.9: Multiple Comparison of ΔL^*-values of red cotyledon lentil under visible light. 121
Table D.10: Multiple Comparison of ΔL^*-values of red cotyledon lentil under UVA. 121
Table D.11: Multiple Comparison of Δa^*-values of red cotyledon lentil under visible light. 122
Table D.12: Multiple Comparison of Δa^*-values of red cotyledon lentil under UVA. 122
Table D.13: Multiple Comparison of Δb^*-values of red cotyledon lentil under visible light. 123
Table D.14: Multiple Comparison of Δb^*-values of red cotyledon lentil under UVA. 123
Table D.15: Multiple Comparison of ΔE^*-values of red cotyledon lentil under visible light. ... 124
Table D.16: Multiple Comparison of ΔE^*-values of red cotyledon lentil under UVA. 124
Table D.17: Multiple Comparison of ΔL^*-values of yellow cotyledon lentil under visible light. 125
Table D.18: Multiple Comparison of ΔL^*-values of yellow cotyledon lentil under UVA. 125
Table D.19: Multiple Comparison of Δa^*-values of yellow cotyledon lentil under visible light. 126
Table D.20: Multiple Comparison of Δa^*-values of yellow cotyledon lentil under UVA. 126
Table D.21: Multiple Comparison of Δb^*-values of yellow cotyledon lentil under visible light. 127
Table D.22: Multiple Comparison of Δb^*-values of yellow cotyledon lentil under UVA. 127
Table D.23: Multiple Comparison of ΔE^*-values of yellow cotyledon lentil under visible light. 128
Table D.24: Multiple Comparison of ΔE^*-values of yellow cotyledon lentil under UVA. 128

LIST OF ABBREVIATIONS

a*:	Redness - greenness
ANN:	Artificial Neural Network
ANOVA:	Analysis of Variance
b*:	Yellowness-blueness
CIE:	Commission Internationale de l'Elcairage
CNIRT:	Cumulative NIR Transmission
CUVT:	Cumulative UV Transmission
CVIST:	Cumulative Visible Transmission
FTIR:	Fourier Transform Infrared Reflectance
GLM:	General Linear Model
IR:	Infrared
L*:	Lightness
LDA:	Linear Discriminant Analysis
MIR:	Mid-infrared
MPD:	Minimum Perceptible Difference
ND:	Neutral Density
NIR:	Near-infrared
PCA:	Principal Components Analysis
PLS-DA:	Partial Least Square Discriminant Analysis
RGB:	Red, Green, and Blue
SNV:	Standard Normal Variate
SWNIR:	Short Wavelength Near-infrared
UV:	Ultraviolet
UVA:	Ultraviolet A
UVB:	Ultraviolet B
UVC:	Ultraviolet C
VIS:	Visible Light

Chapter 1 : INTRODUCTION

Lentil (*Lens culinaris* Medik.) is an economic crop that belongs to the family *Fabaceae.* It is a leguminous seed classified as a pulse. The history of lentil cultivation dates back to 7000 B.C., when they were first grown in southwest Asia (McVicar *et al*., 2017). The crop is best adapted to colder climates, such as the temperate regions and the winter season in Mediterranean climates (Boye, 2015). Lentils are classified based on the color of their cotyledons (green, yellow, or red), and can be further separated based on the color and patterning of their seed coats.

Lentil is rapidly emerging as an important food and cash crop because of its reputation as a nutrition powerhouse. According to McVicar *et al.* (2017) and Boye (2015), a diet of lentils is rich in vitamins, calories, protein, fiber, minerals (calcium, potassium, phosphorus, magnesium, selenium, iron, folate), and healthy amounts of fat and carbohydrate. The proteins in lentils contain good amounts of the essential amino acids leucine, lysine, threonine, and phenylalanine.

Lentil is a leguminous crop and is rich in phenolic compounds in the seed coats. These secondary metabolites possess high antioxidant activity, Thus, consumption of phenolic-rich foods may contribute to a decrease in chronic diseases by scavenging reactive oxygen and nitrogen species (Amarowicz *et al.*, 2009).

This important crop is a major export crop in Canada, which has assumed the status of the world's largest exporter of lentils since 2005-06. Statistics Canada (2019) estimated lentil production in Canada to be about 2.2 million tonnes. Saskatchewan accounts for more than 96% of lentil production in Canada (Statistics Canada, 2015; Lentils.org, 2020).

There is concern about the cotyledon color of Canadian lentils. Although this is mostly associated with red lentils, the class of lentils that are most commonly dehulled (Erdoğan, 2015), it is important to also consider colorfastness of green and yellow cotyledon classes. Color may correlate well with other quality attributes of a commodity (Sahin & Sumnu, 2006), and the loss of color may indicate a loss in nutrients and secondary metabolites, such as polyphenols, possibly affecting colour and flavour.

After maturation, Canadian lentils are swathed (cut down), or desiccated with chemicals and allowed to remain in the field for about ten days to dry (Saskatchewan Pulse Growers, 2020). During this period, there are concerns about the role light may play on the quality of the underlying cotyledon. Also, lentil seeds may be exposed to light during materials handling and storage. If light does affect the quality of lentil cotyledons, having a seed coat (testa) that protects the cotyledons against photodegradation could be beneficial. This would require the testa to reduce the transmission of light by absorbing and/or reflecting light incident on the seed. The relationships between reflectance, transmittance, absorptance, and wavelength are components of the optical properties of the seed coat.

Optical properties of a material describe how the matter responds when exposed to light. The basic optical properties describing the fate of light incident on an object are absorptance, transmittance, and reflectance. Others are color, fluorescence, and scattering. Measurements of optical properties may find applications in many areas, such as pattern recognition and classification of materials (Delwiche & Norris, 1993), damage detection (Moomkesh *et al.*, 2017), disease detection (Martinelli *et al.*, 2015), quality determination (El-Mesery *et al.*, 2019), among others.

The basic optical properties of a material's outer layer are factors determining the degree to which interior material is exposed to photochemical and/or photo-thermal effects. An understanding of the optical properties of the lentil testa and cotyledon materials would have a range of applications, including breeding for colorfastness, monitoring degradation, and evaluating product quality.

Presently, there is limited information available on the optical properties of lentil seed coats specifically (i.e., the optical variability that may exist among seed coats of different lentil genotypes) and the effect of light exposure on quality of lentil cotyledons.

1.1 Problem Statement

Lentil quality may be degraded due to photo-degradation. This may occur if there is light transmission through the seed coat, which is expected to vary with seed coat pigmentation. Therefore, there is a need to investigate whether there are significant differences in the optical properties of seed coats among the different market classes of lentil. There is also a need to investigate the influence of light exposure on lentil cotyledon color, and the influence of seed coat

color/type on cotyledon color loss. It is necessary to determine whether the seed coat protects lentil cotyledons from photochemical effects, and which seed coat types/genotypes have a significant protective effect. This would provide valuable information to lentil breeding programs towards developing seed coat types that maximize the protection of lentil cotyledons from light.

The small size of lentils and lentil seed coats present a challenge for the conventional spectrophotometers available. It was therefore necessary to develop and validate a method for obtaining the optical properties of lentil seed coats and cotyledons. This would open an avenue for studies using spectroscopy and computational tools for quality prediction, disease detection, and market class discrimination in lentil seeds.

1.2 Research Objectives

The overall objective of this work was to investigate the variation in optical properties among lentil seed coat types and determine the effect of light treatment, seed coat presence, and seed coat type on the color of lentil cotyledon. To this end, this work addressed the following questions:

(a) What are the optical properties (light transmission and reflectivity) of the different lentil seed coat types, and are there differences between types?
(b) Does light exposure induce changes in the color of lentil cotyledons?
(c) Do the various seed coat types interfere with light-induced color change of the cotyledon, an if so, does the effect differ between seed coat types?

1.2.1 Hypotheses

To answer the questions above, this research tested/addressed the following hypotheses:

a) There are significant differences in light transmission and reflectivity among the different lentil seed coat types (black, brown, grey, green, tan, zero tannin, and their variants).
b) Light exposure results in significant color changes in lentil cotyledons.
c) The lentil seed coat offers significant protection against light-exposure induced color change of the cotyledon.
d) The level of this protection is a function of seed coat type/color.

1.3 Scope Statement

This research covers four (4) short projects, with each study forming the motivation for and leading to the subsequent one. For clarity, the key tasks to be covered are itemized in the following sub-section, while the out-of-scope areas are shown in section 1.3.2.

1.3.1 Within Scope

(a) Develop and validate a fiber-optic spectroscopy system and use it to measure the optical properties of lentil seed coats from 20 genotypes.

(b) Generate spectral curves for visualizations and test hypotheses for differences in the light transmission properties of the major seed coat types.

(c) Conduct light treatment experiments on dehulled and whole lentil seeds from selected seed coat classes and examine color degradation using computer vision and color (L*a*b*) values analysis.

(d) Test hypotheses on the effect of light exposure, seed coat presence, and seed coat type on lentil cotyledon quality by general linear modeling (GLM).

1.3.2 Out of Scope

(a) Studying the optical properties of all available lentil varieties.

(b) Testing hypotheses for differences in the light transmission properties of all studied lentil genotypes.

(c) Spectrometric assay of lentil seeds to study the effect of light exposure on lentil seed biochemistry.

(d) Extending the light treatment experiment to cover all lentil seed coat classes.

Chapter 2 : LITERATURE REVIEW

This chapter lays the theoretical framework for the study. It explains the terms and concepts relevant to the research, using information from literature, and presents a summary of related work done by other researchers. The areas covered include lentils, the structure of the seed and seed coat classes, a foundation on light and its interaction with materials, optical spectroscopy and the techniques used to obtain optical properties of materials, the usefulness of optical properties and works on the use of optical properties for predictive analytics, effect of light exposure on plant biomaterials, the foundation of color measurement, and color measurement technologies.

2.1 Lentils

Lentil is a pulse crop that belongs to the family *Fabaceae.* The domesticated form of lentil (*Lens culinaris* Medik.) is widely cultivated in regions with colder climates, such as the temperate regions and the winter season in Mediterranean climates (Boye, 2015). Lentil is widely grown in Canada, which became a major export crop after production began in the 1970s and is today the world's leading producer and exporter (Lentils.org, 2020).

The majority of Canadian lentils are cultivated in the province of Saskatchewan, which accounts for 95% of production in Canada (Lentils.org, 2020); more recently, significant production also takes place in the southern regions of Alberta (Boye, 2015).

2.1.1 Major Commercial Groups of Lentils

There are currently 77 registered lentil varieties in Canada (CFIA, n.d.). The two main market classes of lentil, red and yellow cotyledon, are also the most widely grown types in Canada. Green cotyledon lentils form a third, less developed market class. These three cotyledon classes (green, yellow, and red) are shown in Figure 2.1.

Red lentils are mostly consumed in the form of the dehulled cotyledons, either intact (football) or split form lentils (Adascan, 2017). On the other hand, the green lentil types are more widely consumed without de-hulling – as whole seeds or split seeds, although there is a market for dehulled lentils with yellow cotyledons. Lentil flour has increasingly been used in developing

lentil-based products such as breads, pastries, and cakes. This has increased the demand for de-hulling of both green and red lentils.

Figure 2.1:Dehulled lentil cotyledons. From left to right, green, yellow, and red.

The major seed coat colors are black, green, brown, tan, grey, zero tannin, mottled green and mottled black (Adascan, 2017). Figures 2.2 a-h show examples of lentil genotypes representing the major seed coat types. Depending on their genotype, there may be slight differences in the appearances of the seed coat of each type, giving rise to variants.

2.1.2 Genetics and Biochemistry of Lentil Seed Coat Colors

Genetically, three broad groups of lentil seed coat can be identified, namely *Tan* (non-black), *tan* (non-black) (Mirali *et al.*, 2016), and black (Vaillancourt & Slinkard, 1992). This is based on the presence/absence of tannins (a water-soluble polyphenol) in the seed coat, i.e., the non-black clusters differ mainly due to the presence or absence of tannins on the seed coat. *Tan* genotypes contain tannins/tannin precursors that slowly oxidize when exposed to air or cooked, causing seed coat darkening (Muehlbauer & Sarker, 2011). The seed coat colors in this category include tan, gray, green, mottled green, mottled grey, and brown. On the other hand, the *tan* genotypes contain reduced levels of tannins and are not susceptible to darkening (Mirali *et al.*, 2016); they include grey zero tannin and colorless zero tannin seed coat colors. Black seed coats contain high concentrations of tannins (Vaillancourt *et al.*, 1986) and anthocyanins (Elessawy *et al.*, 2019).

Two independent genes determine the primary colors of the seed coat classes, namely: gray ground color (*Ggc* – dominant, *ggc* - recessive) and tan ground color (*Tgc* – dominant, tgc - recessive). The major seed coat colors are formed based on the combinations of the alleles of these two genes, depending on which is dominant and which is recessive (Mirali et al., 2016). The combinations are as follows: *Ggc Tgc* (brown), *Ggc tgc* (gray), *ggc Tgc* (tan), or *ggc tgc* (green); seed coat pattern

(the mottled categories) is determined by multiple alleles at a single locus (Vandenberg & Slinkard, 1990). An allele is a variant form of a gene; a variety of different forms of a gene may be located at the same position, or genetic locus, on a chromosome (Nature Education, 2014). The zero-tannin seed coat is formed due to the expression of a single homozygous recessive gene *tan* (Vandenberg & Slinkard, 1990). When the zero tannin trait is expressed, the presence of the dominant *Ggc* produces a gray zero tannin seed coat (*Ggc tan)*, while the recessive *ggc* results in the colorless zero tannin seed coat (*ggc tan*) (Mirali *et al.*, 2016).

It was reported that a single gene determines black seed coat, as a result of the dominance of black over non-black (Vaillancourt & Slinkard, 1992). Thus, the black seed coat has a different pattern of inheritance and this makes it possible to inherit the black seed coat trait in combination with another seed coat color or pattern trait. For example, it may be possible to combine black and green seed coats in a future generation of lentils; the genetically green seed coat would appear black due to the additional pigments expressed due to the black gene.

Differences in lentil seed coat colors may be explained by differences in concentrations of pigments such as anthocyanins (orange, red, and purple colors), pro-anthocyanin, carotenoid (red, orange and yellow colors) (Sanderson *et al.*, 2019), and chlorophyll (Davey, 2007). It can also be due to the type and concentration of polyphenols present. Mirali *et al.* (2017) detected various phenolic compounds in green, brown, tan, and grey seed coats, namely, vanillic acid 4-O-βD-glucoside, resveratrol 3-O-β-D-glucoside, luteolin 4′-O-β-Dglucoside, and several flavonols, flavan-3-ols, and proanthocyanidin oligomers. Mirali *et al.* (2016) found that the major distinguishing feature between tannin-containing and zero tannin lentils is the presence of dihydromyricetin, myricetin-3-*O*-rhmanoside, flavan-3-ols, and proanthocyanidin oligomers in the brown phenotypes and their absence in the zero-tannin phenotypes.

(a) CDC Robin (Brown)

(b) ZT4 (Zero tannin)

(c) CDC QG-3 (Green)

(d) CDC Rosebud (Tan)

(e) Indianhead (Black)

(f) CDC Maxim (Grey)

(g) CDC QG-4 (Mottled Green)

(h) 7312-g (Mottled black)

Figure 2.2: Lentil samples with major seed coat colors used in the study.

2.1.3 Genetics and Biochemistry of Lentil Cotyledon Classes

The cotyledon color in lentils is controlled by three genes, namely, *Dg* for dark green, *Y* for yellow, and *B* for brown (Kumar *et al.*, 2018).

In the presence of dominant gene *Dg*, the gene combination *YY* gives yellow cotyledon, double dominant condition *YB* gives red cotyledons, while double recessive state *yybb* produces light green cotyledons (Emami & Sharma, 1996). The monogenic homozygote *dgdg* will also produce dark green cotyledons (Kumar *et al.*, 2018), irrespective of dominant or recessive genes for yellow/brown/red cotyledons (Thomas, 2016).

In terms of phenotype, the cotyledon color is determined by the type and concentration of pigments. According to Sanderson *et al*. (2019), the differences in lentil cotyledon colors (red, yellow, or green) may be explained by differences in carotenoid concentration. In a study to understand carotenoid variability and concentration in the three types of lentil cotyledon, Thomas (2016) reported that the mean total carotenoid concentration in green cotyledon was approximately 27% higher than in red cotyledon lentils, which in turn had 8% higher carotenoid concentration than yellow cotyledon lentils. High carotenoid concentration is considered to be a factor in chlorophyll retention in plants (Zhou *et al.*, 2011).

The color of lentil cotyledons may also be influenced by the types and concentration of phenolic substances present. Phenolic substances are secondary phytochemicals that contain an aromatic ring with an attached OH group (Mirali, 2016), and they are classified into two major subgroups, namely phenolic acids and flavonoids, according to their molecular structures (Zhanga *et al.*, 2018). The major phenolic compounds found in lentils include sub-classes of phenolic acids and flavonoids; common flavonoids include flavan-3-ols, condensed tannins (proanthocyanidins), anthocyanidins, flavonols, stilbenes, flavones, and flavanones (Zhanga *et al.*, 2018).

Amarowicz *et al.* (2009) found the major polyphenols in red lentil to be p-hydroxybenzoic acid, trans-p-coumaric acid, trans-ferulic acid, and sinapic acid, while trans-p-coumaric acid and trans-ferulic acid were mainly present in green lentil. Mirali (2016) also found the levels of vanillic acid-4-*ß-D*-glucoside and kaempferol-3-*O*-arabinoside-7-*O*-rhamnoside to be higher in red lentil cotyledons than in yellow cotyledons.

2.2 Light and its Interaction with Matter

The term “light” is sometimes understood to refer to the visible portion of the electromagnetic spectrum. However, light extends across a wider wavelength range, from ultraviolet (UV) to infrared. The following sub-sections discuss light nature and properties, its interaction with matter, and applications in spectroscopy.

2.2.1 The Nature and Properties of Light

The nature of light is explained by the wave-particle duality phenomenon. As a wave, light is composed of electric and magnetic vectors perpendicular to each other, each of which oscillates in a plane at right angles to the direction of propagation (Hofmann, 2010). Light forms part of the electromagnetic spectrum with wavelengths ranging from 10 nm to 1mm (Zwinkels, 2015). Fig. 2.3 shows the various radiations in the electromagnetic spectrum and the wavelength regions.

The wave properties of light include wavelength, frequency, and amplitude. Wavelength is the spatial distance between two consecutive crests or troughs in the sinusoidal waveform and has a unit of length. The maximum vertical displacement of the wave from the horizontal axis is called the amplitude. Frequency is the number of oscillations made by the wave per unit time (typically measured in cycles per second or Hz) (Hofmann, 2010).

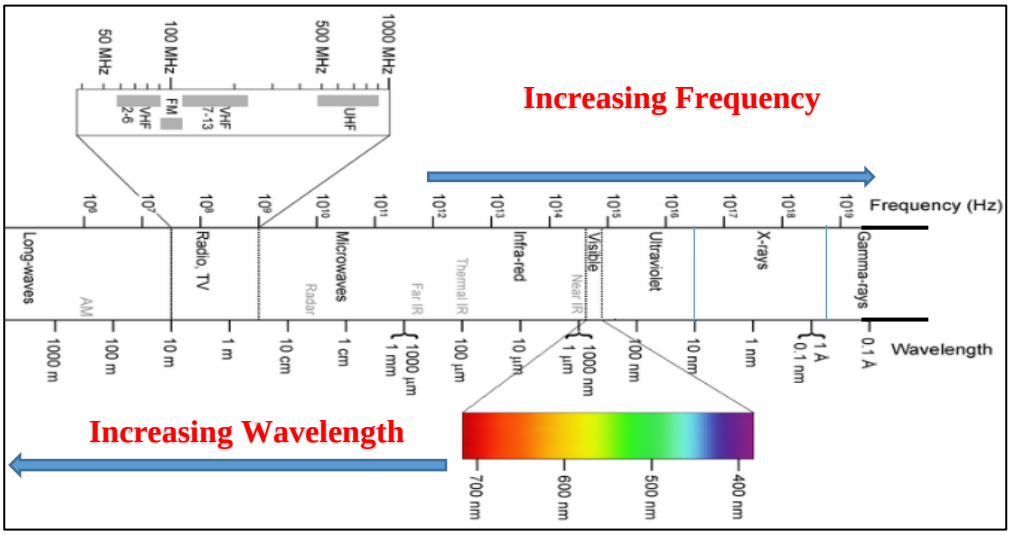

Figure 2.3: Electromagnetic spectrum (Source: (Keiner, 2013)).

The particle theory of light has it that light is made up of energetic particles called the photons, which interact with other particles such as electrons, atoms, molecules, phonons, etc. electromagnetically. According to Huang *et al.* (2014), light components comprise different spectral regions, namely, ultraviolet radiation (UV), visible light (VIS), near-infrared (NIR), mid-infrared (MIR), and far-infrared (FIR) (see Fig. 2.3).

The energy of light ranges from 1.2 meV and 124 eV (Soares, 2014). Energy is inversely proportional to wavelength; shorter wavelength UV light is made up of more energetic photons, followed by visible and infrared light in that order (Salasnich, 2014).

Within the context of this project, the high-energy UV light is of particular potential interest. UV light covers the band of the electromagnetic spectrum from 10 nm to 400 nm and is composed of three bands, namely, UVA: 315 nm-400 nm; UVB: 280 nm-315 nm; and UVC: 10 nm-280 nm (Diffey, 2002). UVC radiation has a high ionizing ability and germicidal effect. UVB is considered to be mainly responsible for photochemical effects in living tissues and other materials (such as photodegradation/color loss, sunburns, etc). UVA may cause minor skin and eye reactions such as photosensitization reactions, conjunctivitis, etc. (Diffey, 2002).

2.2.2 Sunlight

The term “sunlight” is usually associated with solar radiation that we see, however, the light we see (visible light) is just one part of the spectrum of light emitted by the sun. The sun’s spectrum is itself part of the electromagnetic spectrum (Fig. 2.3). Russel (2007) noted that the sun emits EM radiation across most of the electromagnetic spectrum The extraterrestrial radiation from the sun thus comprises x-rays, UV, visible light, IR, and some number of microwaves and radio waves. As the sun’s rays pass through the atmosphere some wavelengths are absorbed and a proportion of the total energy is scattered, resulting in an overall reduction in intensity. Absorption or scattering of radiation occurs due to the presence of ozone, oxygen, water vapor, carbon dioxide, and dust particles (ITACA, 2018).

As a result of these interactions, the UVC light from the sun is completely absorbed by the atmosphere, and UVB is partially absorbed. Thus, terrestrial radiation (the sunlight reaching the

earth's surface) comprises UVB, UVA, visible light, and infrared radiation (ITACA, 2018). Therefore, this study will focus on the band of radiation starting from UVB.

2.2.3 Light Interaction with a Material

At the atomic/molecular level, when light impinges on a material, different excitations are created, depending on the energy of the photons (Soares, 2014). The photons of UV (10 nm to 400 nm) and visible light (400 nm to 700 nm) are more likely to interact with the electrons of the outer shells promoting them to more energetic levels and/or creating excitations.

On the other hand, the photons of infrared light (700 nm to 1 mm) are more likely to penetrate and interact with the material's lattice. This results in molecular vibrations and rotations, creating phonons (Soares, 2014). These interactions form the basis for spectroscopy and optical properties measurement (Hofmann, 2010).

From a macroscopic point of view, light encountering a material may experience three basic phenomena: scattering (specular and diffuse reflection), absorption, or transmission. The response of a material to light depends on its physical, chemical, and structural properties, as well as the wavelength (energy, frequency) and intensity of the photons. The absorption of light that penetrates the tissue of samples depends on the physical and chemical properties of the material; this forms the basis of emission and absorption spectroscopy (Huang *et al.*, 2014).

2.3 Optical Properties and Optical Spectroscopy

Optical properties have been defined as material properties that are a product of the physical phenomena that occur when light interacts with a material under consideration (Durán & Calvo, 2004). Optical properties of a material have to do with the characteristic way the material responds to light of certain wavelength/wavelength range. The three processes that can occur are classified as reflectance, transmission, and absorption (Palmer, 1995).

Palmer (1995) defines transmission as the process by which incident radiant flux leaves a surface or medium from a side other than the incident side; this side is usually the opposite side. Transmittance of a material is the ratio of the transmitted spectral flux to the incident spectral flux.

Absorption is the process in which incident radiated energy is retained by the medium of contact (Posudin, 2007); the incident radiant flux is converted to another form of energy, usually heat by the material (Palmer, 1995). The spectral absorptance/absorptivity is the ratio of spectral power absorbed to the incident spectral power (Palmer, 1995).

Reflection is said to occur when a fraction of the radiant flux incident on a surface bounces back into the same hemisphere of incidence, whose base is the reflecting surface (Palmer, 1995). The reflection can be specular (mirror-like), diffuse (scattered into the entire hemisphere), or total (combination of specular and diffuse). Reflectance is generally defined as the ratio of the radiant flux reflected to the incident radiant flux (Palmer, 1995).

The absorptance (α), transmittance (τ), and reflectance (ρ) are the three fractions of the total incident radiation and are related by equation 2.1 (Posudin, 2007).

$$\alpha + \tau + \rho = 1 \qquad 2.1$$

Measurement of optical properties is fundamental in spectroscopy, which is a science that involves the analysis of the interaction between matter and any portion of the electromagnetic spectrum. Singh *et al.* (2006) define spectroscopy as the study of physical characteristics of atoms or molecules by using electromagnetic radiation in the form of absorption, emission, or scattering by molecules. Optical spectroscopy involves any interaction between light and matter, including absorption, emission, reflection, scattering, transmission, etc. The spectra of light reflected, transmitted, and emitted by a material can be used to gain information about the material. There are many different types of spectroscopy depending on the wavelength of electromagnetic radiation used (e.g. VIS-NIR spectroscopy, infrared spectroscopy, far-infrared spectroscopy, etc.) (Helmenstine, 2017).

Some of the uses of spectroscopy include identification of the nature of compounds in a sample, monitoring of chemical processes, assessing the purity of products. It may also be used to measure the effect of electromagnetic radiation on a sample, which can be used to determine the intensity or duration of exposure to the radiation source (Helmenstine, 2017). Spectroscopy is also extensively applied in the assessment of food quality and safety (Huang *et al.*, 2014).

The study of physical and optical properties can be useful in designing sensors and developing methods and calibrations to measure and/or predict chemical attributes or other physical properties of crop and food materials. Reflectance, transmittance, absorptivity, and scattering of light by food samples can be utilized by techniques such as spectroscopy, hyperspectral imaging, multispectral imaging, and computer vision to measure various aspects of food quality (Huang *et al*., 2014). In near-infrared spectroscopy, reflectance of near-infrared radiation can be used for the quantitative analysis of food (Osborne, 2000).

2.3.1 Optical Spectroscopy Instruments

A spectrophotometer is an instrument that is used to study the light absorption properties of a sample. The basic components include a light source, a monochromator (light dispersing component), a sample chamber, and optical detectors (that convert reflected/transmitted light into electrical energy). Based on wavelength considerations, spectrophotometers can be classified into two different types: UV-Visible spectrophotometer and IR spectrophotometer (Kevin, 2019). Some IR spectrophotometers are of the Fourier transform infrared reflectance (FTIR) type. The detailed working principle of spectrophotometers is presented by (Hofmann, 2010).

For measurements of total reflectance and transmittance, some spectrophotometers are fitted with specially designed integrating spheres. The inside of the integrating sphere is coated with a near-Lambertian (ideally diffuse) material. While integrating spheres facilitate the measurement of total reflectance and transmittance, they tend to have limitations related to sample size and positioning. Small and delicate samples are difficult to measure in isolation using this approach in a standard spectrophotometer.

Spectrophotometers are generally integrated benchtop instruments. While various sample-holding accessories are available, the end-user is relatively restricted in terms of customizing for particular sample constraints. Spectrophotometers have been used for measuring reflectance in seeds, but generally using bulk samples rather than individual seeds (Eu, 1997), or bulk samples after grinding (Delwiche & Norris, 1993).

Optical fiber-based techniques for spectroscopy involve the interconnection of components using fiber optics cables, which transmit light signals from one point to another by total internal

reflection. The basic components of an optical fiber spectroscopy system commonly include the light source, fiber optic cable/probes, sample holder, and a diode-array spectrometer. A fiber optic cable transmits incident light from the light source to the sample, and another cable directs reflected/transmitted light from the sample to the spectrometer. The spectrometer contains a diffraction grating, which disperses the light into its wavelengths and projects the dispersed light onto the detector array (B&W Tek, 2019).

In their study, Donskikh *et al.* (2017) showed how fiber-optic spectroscopy components can be connected to adapt to the different needs of reflectance and transmission measurements. Figure 2.6 illustrates the two connection modes. In the reflectance mode (Figure 2.6a), light is transmitted through the first optical fiber cable into the integrating sphere, where it is directed on the sample. The reflected light is integrated and transmitted onto the spectrometer through the second fiber cable. In the transmission mode (Figure 2.6b), the sample is placed on a holder, and the light transmitted through Fiber cable 1 is incident on it after exiting through the probe end. The transmitted light passes through Fiber cable 2 onto the spectrometer.

The fiber-optic approach lends itself to easier adaptation to specific use cases using relatively standard optical components as compared to an integrated spectrophotometer. This makes the technique useful for studying materials of various shapes and sizes, which cannot be studied using spectrophotometers. It is also particularly useful for on-line, at-line and in-line material quality measurement in practical settings (B&W Tek, 2019). Industrially, fiber optics spectroscopy has been used for various applications, such as process monitoring, authenticity control, sample discrimination, the assessment of sensory, rheological or technological properties and physical attributes; some of these applications are carried out under sophisticated conditions, such as on moving conveyor belts, in continuous flow tubes, and monitoring of fermentation processes (Porep *et al*., 2015).

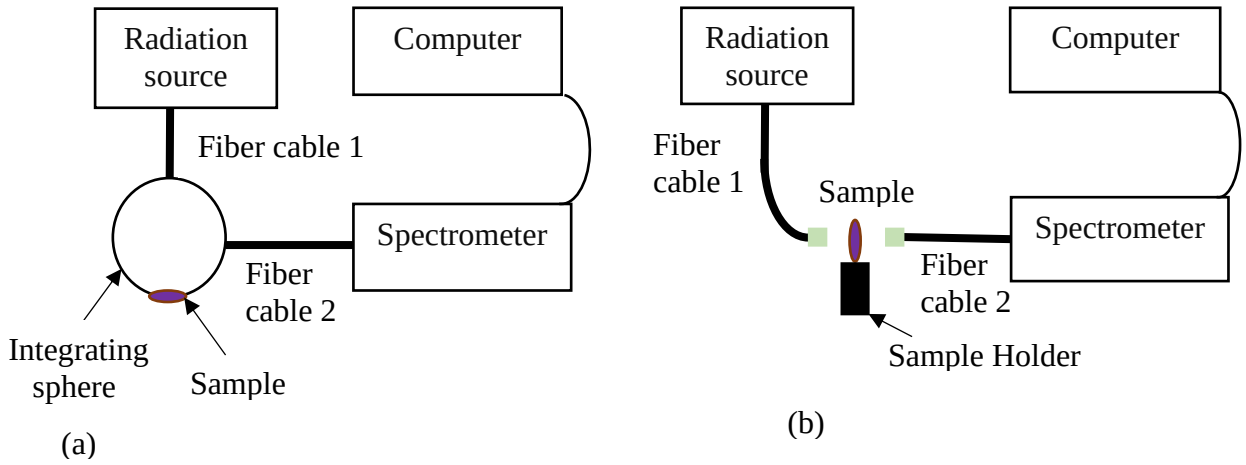

Figure 2.4: Schematic diagrams of fiber-optic spectroscopy units for: (a) Reflectance Measurement, (b) Transmission Measurement. Adapted from Donskikh *et al.* (2017).

Due to its flexibility, fiber optics spectroscopy is increasingly becoming the method of choice for agriculture research. Moomkesh *et al.* (2017) used fiber optics spectroscopy in the VIS/SWNIR range for early detection of freezing damage in sweet lemons. The sample was openly exposed to light from a lamp and a fiber optics cable was then used to direct the reflected/transmitted light to the spectrometer. Ghosh *et al.* (2016) used an optical fiber set up to classify 30 different kinds of cereal and 19 different kinds of nuts by near-infrared reflectance spectroscopy and concluded that NIRS (using an optical fiber system) combined with chemometrics is a robust method for specificity analysis of peanuts from different cereals and nuts. Steidle Neto *et al.* (2018) also used the technique to successfully classify sugarcane varieties using visible/near-infrared mode, while Donskikh *et al.* (2017) used it to classify 3 types of triticale (a hybrid of wheat and rye) using transmittance and reflectance modes in the visible and near-infrared wavelength ranges.

2.4 Effect of Light on Plant Biomaterials

The effect of light exposure on a material can occur as a result photo-thermal or photochemical process, depending on the wavelength (range) of light involved.

2.4.1 Photo-thermal Effect

The photo-thermal effect involves the generation of heat which results from vibration, rotation, and translation of molecules of the material as they absorb light. This leads to rise in tissue

temperature, in amounts dependent on the amount of radiant energy (measured in Joules, J) absorbed per unit time (s) in a certain volume of the material (i.e., the specific absorption rate, W/m^3) (SCENIHR, 2012).

According to Johnson (2015), the excess heat generated may be dissipated as long-wave radiation, convection into the air, or transpiration. Retained excess heat can result in sunburn browning; a loss of pigmentation resulting in yellow or brown spots. This may be due to the denaturation of pigments such as chlorophyll, carotenes, and xanthophyll (Johnson, 2015). The photo-thermal effect is mostly associated with infrared light.

2.4.2 Photochemical Effect in Crop Products

The photochemical effect is the chemical alteration of a material due to its interaction with light of certain wavelengths. This can occur when the absorption of radiant energy causes excitation of atoms or molecules by moving the valence electrons to higher orbital energy levels. As the electrons fall back to the ground state, energy is released. According to SCENIHR (2012), this energy can be utilized in photochemical reactions, lost in fluorescence, or converted to heat. Chemical alterations can occur both in the absorbing and surrounding molecules as the energy can be transferred to other molecules, which may then become chemically reactive (e.g. radicals and reactive oxygen species may thus be formed) (SCENIHR, 2012).

SCENIHR (2012) posited that the band of radiation mostly responsible for photochemical action is UV radiation. This is because, among the three components of sunlight (UV, VIS, and IR), the photons of UV carry the highest energy. UV light covers the band of the electromagnetic spectrum from 10 nm to 400 nm, and it is absorbed by certain common chromophores in organic molecules (e.g. C=O, C=S, and aromatic rings) (Diffey, 2002).

For food materials (harvested or processed plant and animal materials), the photochemical effects are known as photodegradation. Photodegradation is the deterioration of light-sensitive constituents of food when exposed to light. Duncan & Chang (2012) indicated that photodegradation can result in color degradation, the destruction of nutrients and bioactive substances, the formation of off-odors and flavors, and the formation of potentially harmful

substances in foods. The source adds that the constituents of food degraded by light exposure include some vitamins, pigments (chlorophyll, carotenoids, flavonoids), proteins, and lipids.

The effect of light of different wavelengths on harvested crop quality has been studied. Asim & Kasi (2018) investigated the effects of UVB irradiation on the post-harvest color quality and decay rate of red "Capia" peppers. The fully ripe peppers were subjected to the UVB treatment at doses of 4.46 kJ m^{-2} and 8.93 kJ m^{-2}. They reported that the UVB treated group showed lower lightness (L*) values, but higher redness-blueness (a*) and hue (h) values as compared to the control group. This showed that UVB treatment enhanced the redness but darkened the red peppers.

Gómez *et al.* (2012) investigated the effect of pulsed light (PL) dose on color, microbiological stability and microstructure of cut apple during 7-day refrigerated storage. They performed PL treatments with an RS-3000B Steripulse-XL system, which produced polychromatic radiation in the wavelength range of 200–1,100 nm. They reported that the cut-apple surface exposed to high PL fluxes turned darker (lower lightness (L*) values) and less green (higher redness-greenness (a*) value) than the control; this effect was more pronounced as PL dose and/or storage time increased.

Xu e*t al.* (2014) evaluated the effect of 470 nm blue-light treatment on quality, antioxidant capacity, and enzyme activity of harvested strawberry fruit. The treatment group was irradiated with blue light at an intensity of 40 $\mu molm^{-2}s^{-1}$ for 12 days at 5℃. The control group was stored at 5 ℃ in the dark. The color was quantified using the color index of red grapes (CIRG). They reported that the CIRG of treated samples significantly increased compared to the untreated control, with a corresponding increase in antioxidant activity, total phenolic compounds, ascorbic acid, total sugar content, and titratable acidity.

Büchert *et al.* (2011) reported that subjecting cut broccoli florets to a visible light treatment resulted in the yellowing of treated samples, compared with untreated control.

The results of the studies reviewed in this section suggest that exposure to light may result in changes in color and other quality attributes of the crop/food, depending on the wavelength of light and type of material. These changes can be either deleterious or considered enhancements depending on the light, food, and what characteristics are desirable.

2.4.3 Photochemical Effect in Living Plants

For parts of a living growing crop, such as seed and leaves, photochemical effects may occur in other ways. Apart from the commonly known photosynthesis, other photochemical phenomena occur when crops are exposed to sunlight. UNEP (1998) indicates that crop interaction with UVB radiation may result in deleterious effects such as the production of active oxygen species and free radicals, DNA damage, and partial inhibition of photosynthesis. They further explained that to protect itself from damage, crops undergo a physiological process called radiation shielding through pigment changes and specific damage repair systems.

According to UNEP (1998), an increase in the amount of UVB radiation absorbed by a plant part would result in the synthesis of additional UV-absorbing compounds (usually flavonoids and other phenolic compounds). This is a natural defense to reduce the penetration of UVB radiation to underlying tissues and resulting DNA damage.

Gaberščik et al. (n.d.) have hinted that although UV radiation may negatively affect plant growth and yield; it also has beneficial effects. The most important is that exposure to UVB radiation triggers the production of healthy antioxidants in plants. Plants grown under UV light are also more likely to produce secondary metabolites essential for plant protection, enabling the plant to adapt to some negative environmental conditions.

2.5 Color Measurement

Color measurement is possible due to light reflected or transmitted from an object. With absorption occurring at various wavelengths, color measurement systems and methods simulate the perception of color by the human eye (Marcus, 1998). In human vision the light triggers light-sensitive cells in the eye, generating an impulse, which is transmitted to the brain for interpretation. There are two major color measurement scales, namely: the Munsell scale and the CIE color measurement systems; these are interconvertible (Mahyar *et al.*, 2009).

2.5.1 The Munsell Color Scale

The Munsell color assigns numerical values to the three properties of color: hue, chroma (saturation), and value (lightness) (Mahyar *et al.*, 2009).

According to Cleland (1937), A. H. Munsell defined Hue as “the quality by which we distinguish one color from another, as a red from yellow, a green, a blue or a yellow.” The colors red, yellow, green, blue, and purple are called Principal Hues and their intermediates are called Intermediate Hues. The principal hues, intermediate hues, and sub-intermediates are formed into a circle of hues. Colors are assigned numbers and letters to represent their Hue.

Value is “the quality by which we distinguish a light color from a dark one.” (A. H. Munsell in Cleland (1937)). Value thus refers to lightness of the color. A scale of Value may be conceived as a vertical pole, or axis to the circle of Hues, with black at the lower end representing the total absence of light, and white at the top representing pure light. Between these are a number of sub-divisions of grey; black is assigned value 0, darkest grey 1, and white 10 (Cleland, 1937).

Chroma refers to the strength of the color and is rated on a scale of 1-9, with 1 representing the strongest; this gets *greyer* until it gets to 9 which represents a complete loss of color (Cleland, 1937).

2.5.2 CIE and Hunter L, a, b Color Systems

The CIE, Commission Internationale de l’Eclairage (translated as the International Commission on Illumination) Systems utilize three coordinates to locate a color in a color space. According to X-Rite (n.d) , these color spaces include: CIE XYZ, CIE L*a*b*, and CIE L*C*h°. These color spaces are utilized in color measuring instruments, which perceive color the same way human eyes do - by gathering and filtering wavelengths of light reflected from an object.

The CIE XYZ color space is based on the concept of the CIE Standard Observer recommended by the CIE in 1931. According to Marcus (1998), all colors can be produced by shining combinations of RGB (red, green, and blue) light on the cones of the eye; the amounts of blue, green, and red colors needed to produce the color is called the color matching function. Thus, colors could be represented by their RGB values. This source also adds that a special set of mathematical light models, X, Y, and Z, were created to replace actual red, green and blue lights, to avoid the use of negative numbers in color calculations. Every color can be matched using appropriate amounts of X, Y, and Z light called the color's tristimulus values. The tristimulus values are found by combining a sample's reflectance or transmittance curve with a standard illuminant and with the

color matching functions. The observers in the experiment viewed a 2° visual field, thus, the CIE 1931 Standard Observer is commonly called the CIE 2° Standard Observer (Marcus, 1998).

In 1964, CIE developed a supplemental Standard Observer based on the 10° field experiments (the CIE 10° Standard Observer), which more closely approximates industrial color matching and quality control viewing conditions, thus used for most colorimetric calculations (Marcus, 1998). The RGB and X, Y, Z color scales are non-uniform and device/measurement system dependent.

The Hunter L, a, b color scale was developed during the 1950s and 1960s as a more uniform color scale; the current formulas were released in 1966 (Hunterlab, 2012). In 1976 the CIELAB (L*, a*, b*) color space was developed as a modification of Hunter L, a, b color scale. Both use the Cartesian coordinates to calculate a color in a color space. According to Marcus (1998), in the CIELAB color space L* describes the lightness of the sample with 100 as perfectly white and 0 as perfectly black. The notation a* represents the redness or greenness, with (+a*) representing redder and (-a*) greener; while b* is the yellowness-blueness, with (+b*) showing more yellow and (-b*) showing bluer.

CIELAB L*, a*, and b* coordinates can be calculated from the tristimulus values according to equations (2.1) to (2.3) (Marcus, 1998).

$$L^* = 116f(Y/Y_n) - 16 \quad (2.1)$$

$$a^* = 500[f(X/X_n) - f(Y/Y_n)] \quad (2.2)$$

$$b^* = 200[f(Y/Y_n) - f(Z/Z_n)] \quad (2.3)$$

Where: X, Y, and Z are tristimulus values of the sample and X_n, Y_n, and Z_n, refers to the tristimulus values of the perfect diffuser for the given illuminant and standard observer.

$$f(G/G_n) = (G/G_n)^{1/3} \quad (2.4)$$

for values of (G/G_n) greater than 0.008856; and

$$f(G/G_n) = 7.787(G/G_n) + 16/116 \quad (2.5)$$

for values of (G/G_n) equal to or less than 0.008856.

Where, G represents the X, Y, and Z tristimulus value (Marcus, 1998).

The advantage of the L*a*b* space over other color models such as RGB and XYZ is that in the L*a*b* space the color perception is uniform; i.e., the Euclidean distance between two colors closely approximates to the color difference perceived by the human eye (Hunt & Pointer, 2011).

2.5.3 The CIELAB Color Difference Equation

Color differences between two samples can be assessed in terms of the changes in L*, a*, b* values designated as ΔL^*, Δa^* and Δb^* as well as the overall color difference designated as ΔE^*. The values are calculated as follows:

$$\Delta L^* = L^*_n - L^*_r \quad 2.6$$

$$\Delta a^* = a^*_n - a^*_r \quad 2.7$$

$$\Delta b^* = b^*_n - b^*_r \quad 2.8$$

Where the subscripts **n** and **r** indicate the color values are of the new and reference samples, respectively.

Marcus (1998) provides a guide to interpreting ΔL^*, Δa^* and Δb^*. A positive value of ΔL^* indicates that the new sample is lighter than the reference sample whereas a negative value indicates that the new sample is darker. A positive value of Δa^* indicates that the new sample is *redder* than the reference; a negative value indicates that the new sample is greener. A positive value of Δb^* indicates that the new sample is *yellower* than the reference; a negative value indicates that the new sample is *bluer* (Marcus, 1998).

The overall color difference ΔE^* is calculated as follows: (Marcus, 1998).

$$\Delta E^* = [(\Delta L^*)^2 + (\Delta a^*)^2 + (\Delta b^*)^2]^{1/2} \quad 2.9$$

The color difference measured by an instrument can be related to that detected by the human eye using the concept of minimum perceptible difference (MPD). Otherwise called just perceptible difference, the MPD is a psychophysical measurement of an observers' ability to judge whether a difference exists between two samples (Kim *et al.*, 2011). This can be quantified using a visual colorimeter, a process that may involve showing a color-matched pair in two halves of the bipartite field and asking observers to change the wavelength of one of them until a difference is first

noticed (Kim *et al.*, 2011). The color difference detected by the instrument corresponding to the first color change detected by the human eye is the minimum perceptible difference. Mahy *et al.* (1994) indicated that the total color difference, ΔE* between two samples is perceptually indistinguishable if the value is less than an MPD threshold ($\Delta E \approx 2.3$). Kim *et al.* (2011) found that the MPD in terms of ΔE* (reported as ΔE^*_{ab}) for yellow, cyan, and magenta ranged from 1 to 6 depending on the color used and the optical density.

2.5.4 Color Measurement Instruments

Conventional color measuring instruments include colorimeters, spectrophotometers, and spectrocolorimeters. Others include densitometers, RGB cameras, and computer vision.

2.5.4.1 Color Measurement by Computer Vision

Haralick & Shapiro (1992) define computer vision as "the science that develops the theoretical and algorithmic basis by which useful information about an object or scene can be automatically extracted and analyzed from an observed image, image set or image sequence." Computer vision involves the use of an automatic digital or video camera – computer technology-based system for acquiring the color, or other physical properties of a material. Computer vision has proven to be successful for the objective measurement of various agricultural and food products. It includes capturing, processing, and analyzing images, facilitating the objective and non-destructive assessment of the visual quality of materials (Vyawahare *et al.*, 2013).

Computer vision had its origin in the 1960s and has experienced growth with its applications in various fields beyond color measurements, process automation, medical diagnostic imaging, factory automation, remote sensing, forensics, robotics, etc. (Haralick & Shapiro, 1992). The basic components of a computer vision system include a light source, scanner, or digital/video camera for acquiring images, software for image acquisition and processing, and the sample holder.

Digital cameras have a built-in computer, and all of them record images electronically by ultimately focusing the light reflected from the sample onto a semiconductor device that records light electronically; a computer then breaks this electronic information down into digital data (Haralick & Shapiro, 1992). The images are then processed to obtain useful information for various applications.

There is increasing interest in research related to the application of computer vision in agriculture and food processing. Saldaña *et al.* (2013) designed, implemented, and calibrated a new computer vision system in real-time for the food product color measurement. This system was designed to work with foods with flat surfaces. The system was composed of an image acquisition system and software (for image processing and analysis). The system calibration was performed using a conventional colorimeter (Model CIEL* a* b*). They concluded that the system proved to be satisfactory for the color measurement of samples.

Zapotoczny & Majewska (2010) indicated that the color of the seed coat of wheat kernels can be determined by digital image analysis instead of spectrophotometry. They used both methods to measure the seed coat colors in terms of the RGB, XYZ, and L*a*b* models, and reported high linear correlations ($p < 0.05$) between color measurements performed by these techniques.

Mendoza et al. (2017) implemented and tested a machine vision system for automatic inspection of the color and appearance of canned black beans. They reported that the partial least squares regression model trained with the data showed high predictive performance with correlation coefficients of 0.937 and 0.871, and standard errors of 0.26 and 0.38, for color and appearance respectively. Also, a support vector machine model using both attributes sorted the samples into two sensory quality categories of "acceptable" and "unacceptable" with an accuracy of 89.7%.

Halcro *et al.* (2020) developed a computer vision system for imaging and extracting color and physical dimensions of seeds. The system comprised a portable imaging hardware (BELT), image acquisition and storage software (LentilSoftware), and image processing software (phenoSEED). BELT was equipped with a prism, allowing a single camera to record both top and side views of the seed at the same time; there are two cameras for throughput. Color calibration was done by mapping RGB values of the images to CIELAB values for the X-Rite Color Checker Digital SG by modeling using an artificial neural network. The phenoSEED software was equipped with a program that applied color and dimensions calibration to extract seed color and other properties that are functions of size and shape, as well as seed coat patterning. They concluded that the system provided increased precision and higher rates of data acquisition compared to traditional techniques.

PROLOGUE TO CHAPTERS 3 & 4

The following two chapters deal with the set-up and validation of a fiber-optic instrument and its application for studying the light transmission and reflectivity properties of the lentil seed coat.

This part of the thesis was presented at a conference of North American Pulse Improvement Association, Fargo, US, November 5th, 2019, titled: "**Optical Properties and Genotypic Variability in Lentil Seed Coat using Optical Fibre Spectroscopy**."

Chapter 3 : OPTICAL FIBER SPECTROMETER SET-UP AND TESTING

The small size and brittleness of lentils and their seed coats make them difficult to reliably measure using the conventional spectrophotometer equipment available. The first step for this work was to develop and validate methods for measuring the spectral transmission and reflectivity characteristics of lentil seed coats. In this chapter, a description of the fiber-optic spectrometer set up is presented.

The objective of this work was to assess the suitability of the fiber optic spectroscopy set-up for studying the optical properties of lentil seed coat and to evaluate the likelihood of finding real differences in optical properties of different kinds of lentil seed coat. First, the measurement repeatability was assessed by ascertaining the level of variability in measurement that is due to the measurement system, sample geometry, and positioning of a sample that may be spatially heterogeneous (particularly in the case of mottled seed coats). This was done by measuring the same seed coat repeatedly. The instrument was also used to study the within-sample variation (variation in optical properties of lentil seed coats of the same market class). The results of both studies were considered individually and by inter-comparison, using standard deviations as the metric.

3.1 Instrument Description

Figure 3.1 shows the fiber optic spectroscopy set-up in reflectivity and transmission modes. The two architectures were formed by changing the fiber connected to the spectrometer to fit the need (reflectivity or transmission measurement). The general components of the system include the following: A 78VA Deuterium/Halogen light source (Ocean Optics, Florida, United States), bifurcated reflectance/backscatter probe (Ocean Optics, Florida, United States), a horizontal sample platform with support and sample cover, a transmission fiber cable and a Maya2000 Pro spectrometer (Ocean Optics, Florida, United States) configured for the 200 - 1160 nm spectral range.

In reflectivity mode, a reflection/backscatter probe was used (QR-400-7-SR, Ocean Optics FL). The bifurcated optical fiber cable has both illumination and reflection/pick-up fibers that merge into one cable at a junction. The illuminating fiber is positioned at the center of the probe while the reflection/pick-up fibers are arranged around the circumference of the probe. The distance from the center of the probe to the outer ring of the fibers is 2.55 mm. Figure 3.1 (a) shows the illuminating fiber (1) and reflection fiber (7) packed together in a fiber bundle (2) and linked to the illuminating/reflection probe (3). The illuminating fiber is connected to the light source, while the reflection fiber is connected to a spectrometer.

The reflection/backscatter probe is located above the sample (0° to the vertical) at a distance of 4mm from the sample (4), which sits on the sample holder (5). This distance was set as 4mm for lentil seed coat measurement (suitably far from the sample to avoid spectrometer saturation during calibration and close enough to avoid too low signal strength). Light from the light source was directed to the sample through the illuminating fiber, while the reflected light was picked up by the reflection fiber and passed to the spectrometer. With the distance from the probe to the sample of 4 mm, and the distance from the center of the probe to the outer ring of fibers of 2.5 mm, the direction of reflection measurement for lentil seed coat was (about 32° to the vertical). Thus, the bidirectional reflectance (reflectivity) geometry was 0°\32°. Figure 3.2 is a pictorial view of the sample platform, with the sample cover slightly raised to reveal the reflectance/backscatter probe.

In transmission mode (Figure 3.1b), the transmission probe (11) is fixed vertically below the sample (for nadir-aligned transmission measurement). There is a 4mm hole at the center of the sample holder, where the sample sits. Light from the light source is directed to the sample through the illuminating fiber of the reflectance/backscatter probe. The light transmitted through the sample passes through the hole on the sample stage and coupling lens and is propagated through the transmission fiber to the spectrometer.

The spectrometer signal was captured and recorded using OceanView software in the form of light intensity (counts) as a function of wavelength.

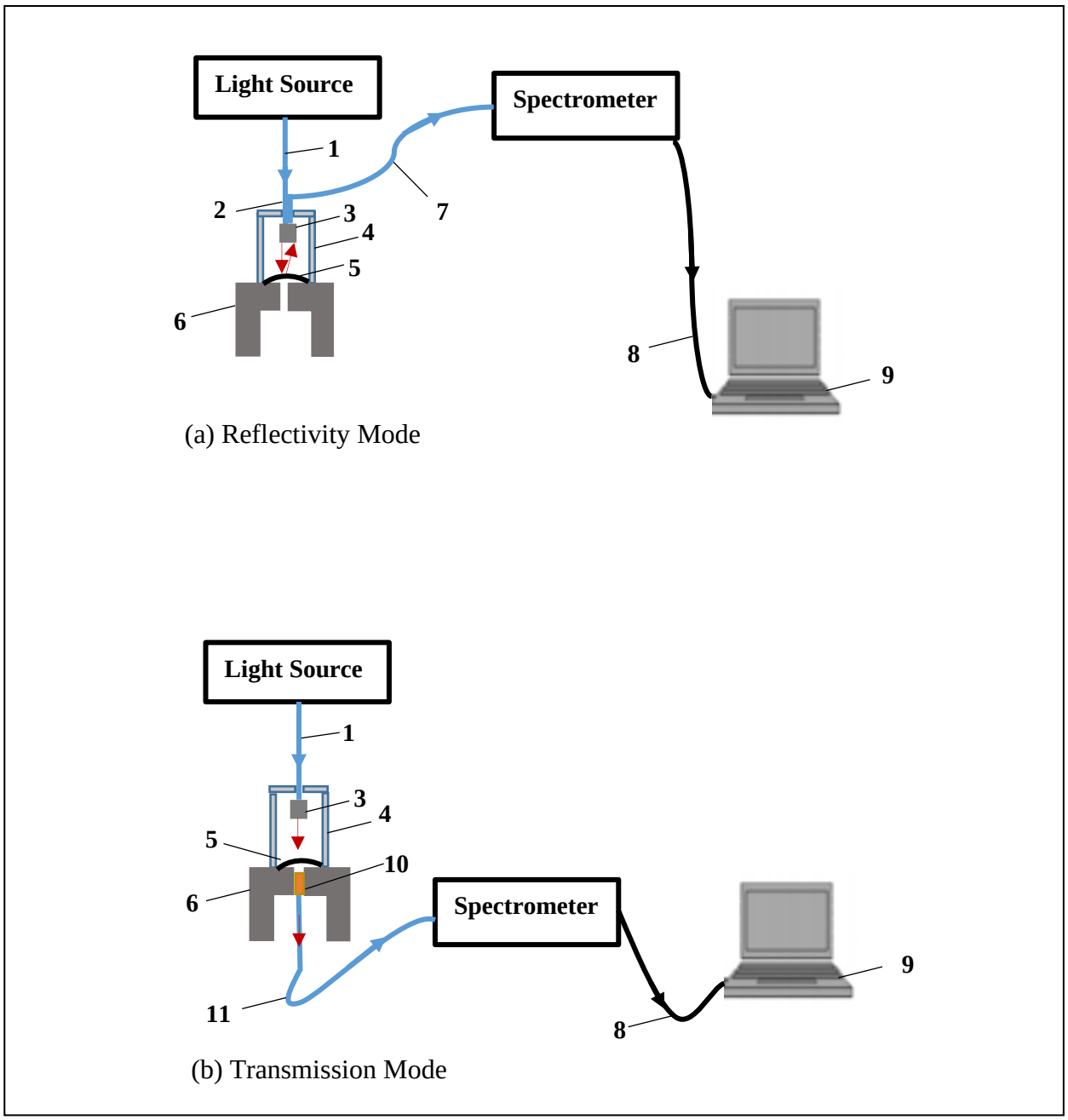

Figure 3.1: Schematic representation of optical fiber spectroscopy set-up; 1. Illuminating fiber cable; 2. Illuminating/Reflection fiber bundle; 3. Reflection/backscatter probe; 4. Sample cover; 5. Sample; 6. Sample platform; 7. Reflection fiber cable; 8.USB Cable; 9.Computer; 10. Collimator lens; 11.Transmission fiber.

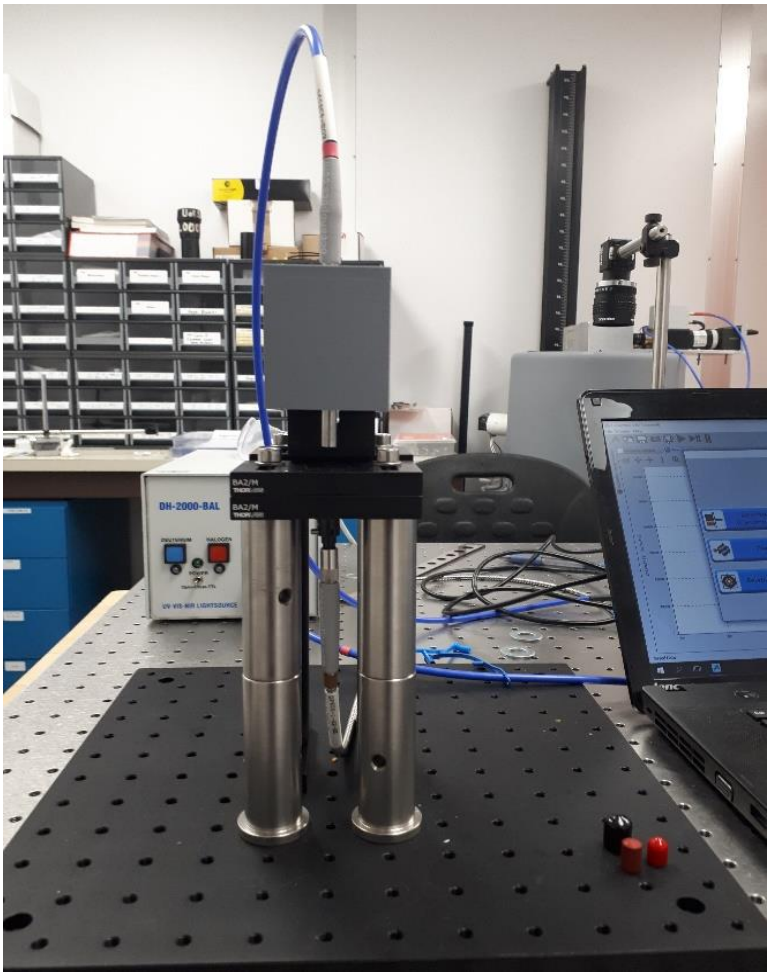

Figure 3.2: The sample stage.

3.1.1 Calibration and Measurement Procedure

Before reflectivity measurement, the instrument was calibrated using a 50% reflectance Spectralon diffuse reflectance standard (SRS-50, Labsphere, New Hampshire, United States). First, the light source was turned on and allowed to remain for about ten minutes to stabilize. The reflectance standard then was placed on the sample stage and the end of the reflection/backscatter probe was positioned 4 mm from the standard surface. The OceanView software was started and the light source shutter opened. To capture the reference spectrum, the software was is placed on "automatic" to select an integration time that produces 85% of the instrument range (to avoid saturation), (another option would be to manually select the integration time (OceanOptics, 2018). The "boxcar width" (for in-measurement smoothing/noise reduction) was set to six (6) data intervals and "scans to average" (number of scans to average for a reading) was set to five scans.

After capturing the reference signal, the light shutter was closed and the dark measurement (a measurement of instrument output without illumination) was taken.

The general technique of seed coat reflectivity measurement using the fiber-optic instrument involves measuring the intensity of light reflected by the sample and comparing it with that of the 50% Spectralon reflectance standard. The correction factor is then applied, together with dark noise correction to obtain percent reflectivity (R) using equation 3.1:

$$R\,(\%) = \frac{M_s - M_d}{M_{Ref} - M_d} \times C \times 100\% \qquad 3.1$$

Where,

M_s = Intensity of reflected light (counts) on the sample,

M_d = Intensity of dark spectrometer signal (counts),

M_{Ref} = Intensity of reflected light (counts) on reflectance standard, and

C = Calibration factor of the Spectralon reflectance standard.

The general technique in seed coat transmission measurement involves comparing the intensity of light passing through the sample to the intensity passing through the empty hole on the sample stage. After reconfiguring the optical path, the calibration process for transmission measurement was similar to that for reflectivity measurement, except that the reference material was changed to a neutral density (ND) (optical density: 0.3) filter (NDUV03B, Thorlabs, New Jersey, USA). The ND filter was used to attenuate the light to avoid saturating the spectrometer detector during calibration. The light transmission property, D of this filter was calculated using equation 3.2, and assumed to be constant across the entire spectral range.

$$D = 10^{-(OD)} \qquad 3.2$$

Where, OD is the optical density of the filter.

The correction factor was then applied, together with dark noise correction to obtain the percent transmission (T) using equation 3.3:

$$T\,(\%) = \frac{N_s - N_d}{N_R - N_d} \times D \times 100\% \qquad 3.3$$

Where,

N_s = Intensity of transmitted light (counts) on the sample,

N_d = Intensity of dark spectrometer signal (counts),

N_{Ref} = Intensity of transmitted light (counts) on the filter, and

D = Calibration factor (transmission factor of ND filter).

3.2 Measurement System Analysis/Method Validation

In this section, the preliminary study carried out using the fiber-optic spectrometer is presented. It covers the measurement repeatability and the within-sample variation assessment.

3.2.1 Sample Preparation

The lentil samples were placed in the headspace of a saturated aqueous potassium chloride solution (relative humidity over the salt solution 84% at 25°C (Engineering Toolbox, 2014)) in a closed chamber and left for two nights to absorb moisture. This rendered the seed coat removable, without the problem of pigment loss caused by soaking. The conditioned seeds were then cut in halves and the seed coat removed using a scalpel. The half seed coat samples were then allowed to dry in the open air before being used for the study.

3.2.2 Measurement Repeatability Assessment

The measurement repeatability was examined using lentil seed coats from the following genotype classes: Brown (CDC Robin), Black (Indianhead), Tan (CDC Rosebud), Green (CDC QG-3), Light Gray (IBC 1264-3), and Mottled Green (CDC QG – 4). A single seed coat from each of the six genotype classes was used for the study. The general idea was to ascertain the level of consistency in measurement when the same seed coat was scanned repeatedly, under the same measurement conditions.

Following calibration, the removed one-half seed coat was placed on the sample stage with the convex surface facing up, maintaining a distance of 4 mm between the top of the sample and the reflection/backscatter probe. Then 0°\32° bidirectional reflectance measurements were obtained in the wavelength range of 280 nm to 1100 nm using the reflectivity/backscatter probe.

One sample from each variety was subjected to repeated measurements (10 scans), making a total of 60 scans. Each successive measurement was carried out after removing and replacing the sample and closing and reopening the light shutter. The measurements were exported to Microsoft Excel for calculation of light reflectivity using equation 3.1.

The preprocessed data were loaded into R Program v3.5.1 (R Development Core Team, 2011) for analysis (see Appendix E1 for the script). The light reflection spectrum of each coat is a multidimensional data (comprised of 1962 dimensions or wavelengths; some wavelengths appeared as fractions). The data analysis involved computing the mean and spread in measurements on a per-wavelength basis, across the spectra.

Data were smoothed using a moving average filter from the "Prospectr" package on the R program; the smoothing window was 11 (smoothing bandwidth of 5 nm). This de-noising protocol reduced the dimensions of the data to 1889 wavelengths per spectra. The mean and standard deviation of the smoothed light reflectivity values were computed and plotted on a per-wavelength basis.

3.2.3 Within-sample Variation Assessment

The study was designed to ascertain the level of spread in measurements when the spectral properties of different seed coat samples from the same genotype were measured under the same conditions. Seed coat samples from the following genotype classes were used: Grey (CDC Maxim), Green (CDC QG-3), Mottled Green (CDC QG-4), Brown (CDC Robin), Tan (CDC Rosebud), and Light Grey (IBC 1264-3) (some of the genotypes used for within-sample assessment were different from those used for repeatability tests). Ten samples of each of the genotype classes were used.

The calibration and seed coat reflectivity measurement protocol described in section 3.3.2 was also used here. Ten samples from each of the six genotypes were subjected to one reflectivity measurement each (making a total of 60 scans). The ten spectra for each genotype were then compared to ascertain the within-sample variation. The data were also exported to Excel for calculation of light reflectivity using equation 3.1. The signal de-noising protocol of section 3.3.2 was also applied; the mean and standard deviations of the smoothed reflectivity spectra were computed and plotted using an R Program script (Appendix E2).

3.2.4 Results and Discussion

Figure 3.3 shows the descriptive statistics plots for the measurement repeatability test. The mean and standard deviations (10 measurements) of the percent light reflectivity against wavelength for each of the six lentil seed coat genotype classes are shown. The maximum and minimum standard deviation values over the entire wavelength ranges are shown for each genotype class.

Generally, the spread of the repeated measurements of a single seed coat from the mean values were fairly tight; this is evident in the closeness of the ± standard deviation curves to the mean reflectivity curves. The maximum and minimum standard deviation values show that the highest variation (standard deviation of 2.69%) was observed in the tan seed coat sample, CDC Rosebud (Figure 3.3 (f), at 580 nm. The measurements were widely spread out between 480 and 680 nm. This large spread might have been due to spatial variability in pigments that absorb at the spectral region. There were also relatively high variations in the mottled green, CDC QG-4 (Figure 3.3(e)) between 480 nm and 680 nm, with a maximum standard deviation of 2.07% at 550 nm. The likely source of variation with this phenotypic class is the seed coat patterning; this might result in the exposure of areas with different concentrations of pigments each time the sample was repositioned.

Figure 3.4 shows the descriptive statistics plots for the within-sample variation test. The mean and standard deviations (N=10) of the percent light reflectivity against wavelength for each of the six lentil genotype classes are shown. The maximum and minimum standard deviation values over the entire wavelength ranges are also shown for each genotype class. Generally, the standard deviation values were larger than those in the repeatability test using single seed coats; this is evident in the wider spread of the ± standard deviation curves around the mean reflectivity curves. For example, the maximum within-sample standard deviation for the grey seed coat, CDC Maxim (Figure 3.5 (a)) is 8.9%, but it was 1.63% in the single-seed coat repeatability test (Figure 3.4 (c)).

Such within-sample spread in optical properties is common with biological materials, which are known to be heterogeneous (Sun *et al.*, 2019). It may be due to "scatter effects" caused by differences in physical properties (such as size, shape, microstructure/spatial variability in components, etc.), (Rinnan *et al.*, 2009).

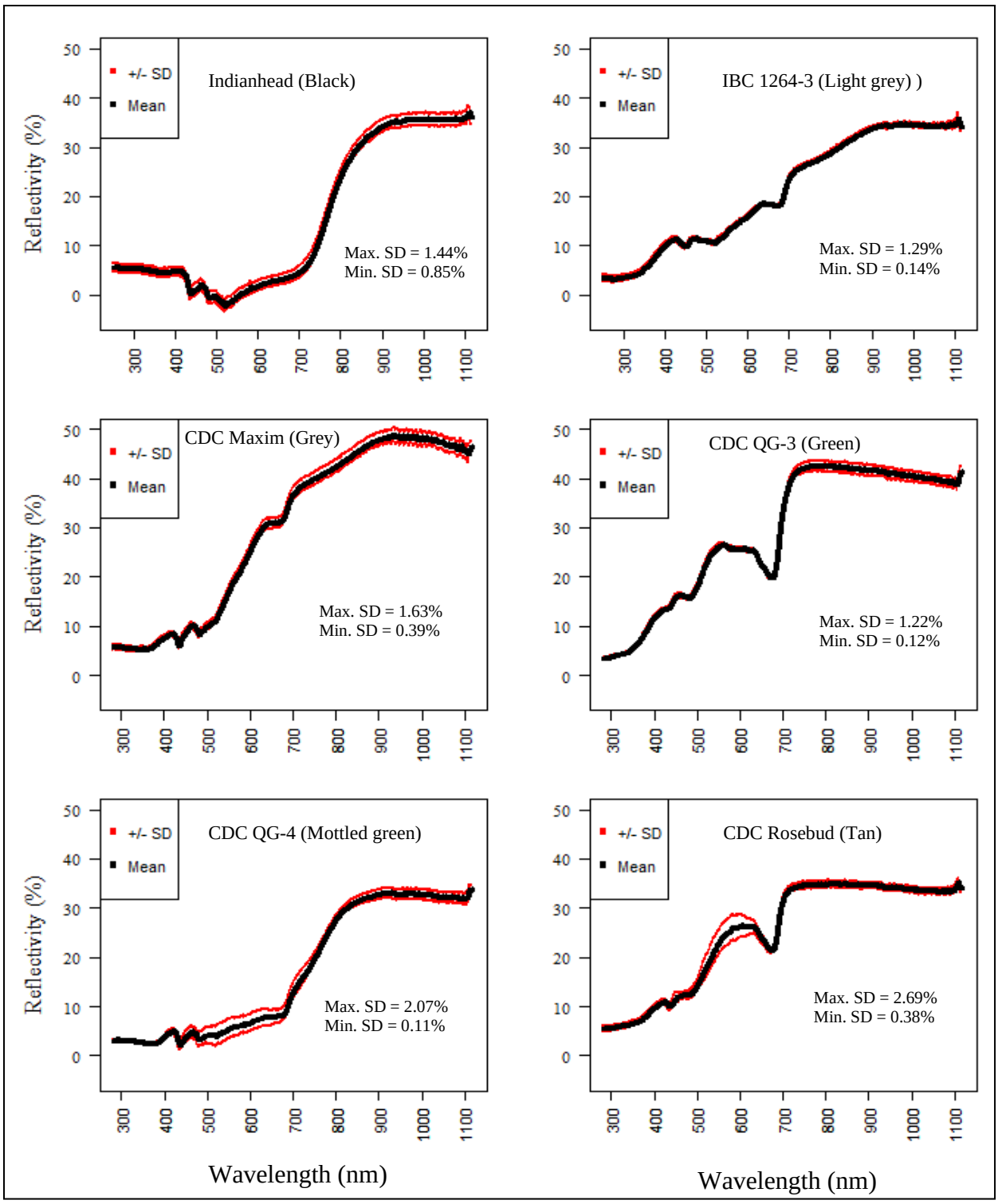

Figure 3.3: Average of 10 repeated reflectivity measurements **±1 SD** on single seed coats for six lentil genotypes (SD = Standard deviation).

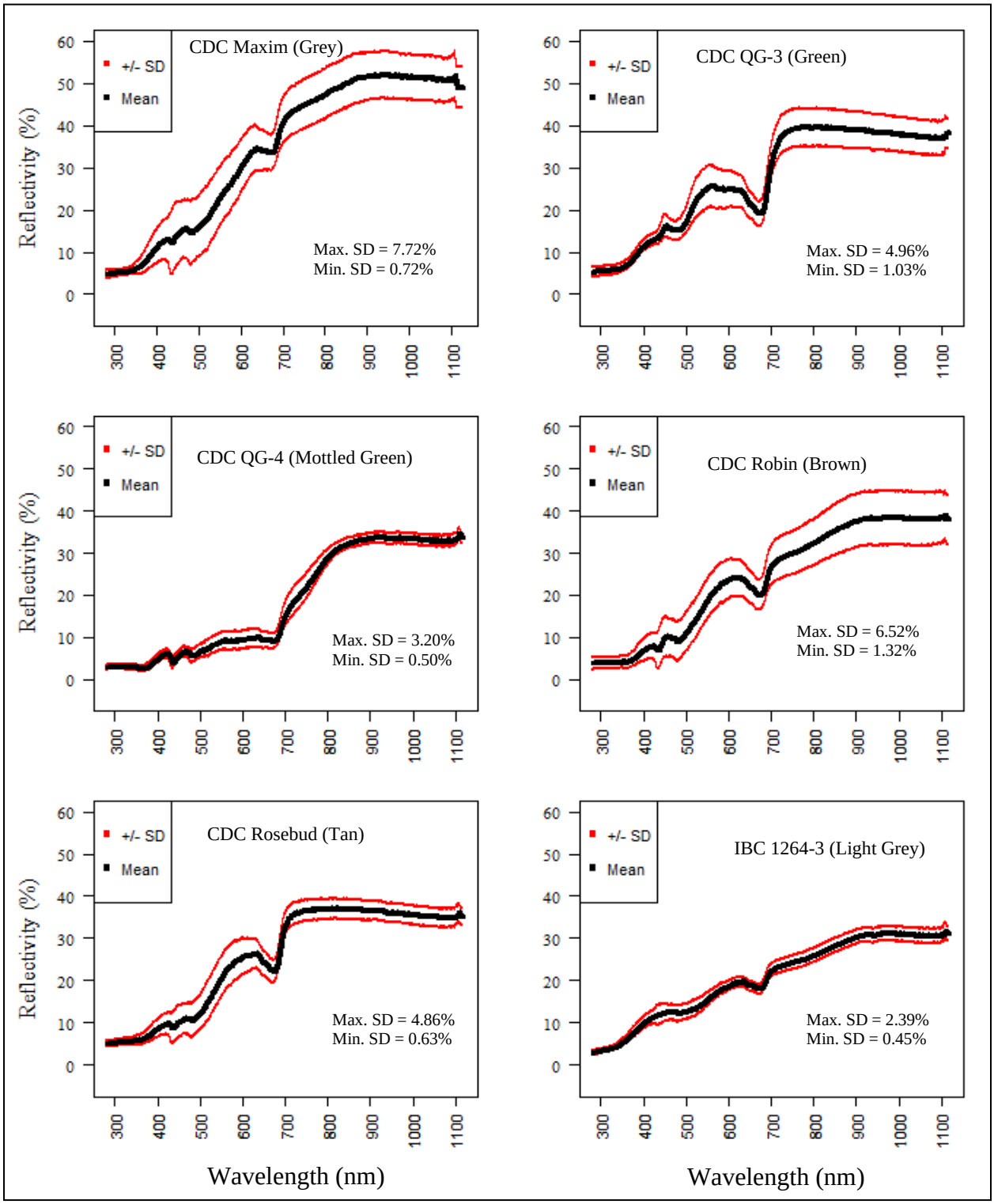

Figure 3.4: Average reflectivity measurements **±1 SD** (N=10) for seed coats of six lentil genotypes (SD = Standard deviation for the sample).

3.3 Summary and Conclusion

This chapter addressed the problem of developing a suitable instrumentation system for measuring the optical properties of lentil seed coats. This was necessary because of the constraints associated with the small size and brittleness of lentil seed coats, which makes them unsuitable for measurement using conventional spectrophotometers. The system was set up using available fiber optic spectroscopy and optical bench components.

The measurement system analysis was carried out to assess the variability in measurements that were due to secondary factors, such as sample geometry and positioning (which relates to the effect of spatial variations in properties within a seed coat. The measurement repeatability of the instrument was assessed, and the methodology validated for studying optical properties of lentil seed coats.

From the results of the measurement repeatability test, it was concluded that multiple measurements could be made using the system with little variability; this was revealed by the plotted standard deviation values. In four of the six cases, the standard deviation lines almost overlapped with the mean reflectivity curves. Also, the instrument indicated a wider spread in light reflectivity when genetically different seed coats were measured, compared to when the same seed coat was measured. It was therefore concluded that the optical fiber instrumentation was suitable for studying the optical properties of lentil seed coats.

The size of the within-sample variation for the six lentil varieties tested did not appear to be too wide; visible differences in the spectral curves of the seed coats of different lentil varieties were clear, even with variability. It was concluded that in the main study it would be possible to find real differences in optical properties of lentils of different seed coat classes.

Generally, it was useful to develop and validate a method for obtaining the optical properties of lentil seed coat/seeds and other biomaterials whose optical properties cannot be easily obtained using spectrophotometers, due to their morphological features. This opens an avenue for studies using spectroscopy and computational tools for quality prediction, disease detection, and market class discrimination in lentil seeds and other crops that are not suited for study using a spectrophotometer.

Chapter 4 : OPTICAL PROPERTIES AND GENOTYPIC VARIABILITY IN LENTIL SEED COAT

Plant scientists are seeking engineering solutions to guide understanding of variability in optical properties of different kinds of lentil seed coat. This is primarily intended to find out if they differ in their light-blocking ability and protection of the underlying cotyledon from photodegradation. It is hypothesized that seed coat types with minimum light transmission may offer maximum protection. The chapter presents the study methodology and optical properties of the seed coats of the different lentil genotypes. Tests of significance of differences in light transmission in the UV, Visible and Near-infrared bands are also presented.

4.1 Materials and Methods

Twenty (20) lentil varieties representing the various seed coat colors (black and its variants, brown, grey, and its variants, mottled, green and its variants, and tan) were obtained from the Crop Development Center (CDC), University of Saskatchewan (Table 4.1). Seed coats were removed using the procedure described in section 3.3.1.

4.1.1 Data Collection

Light reflectivity and transmission properties of the seed coats were obtained using the fiber optics instrument described in section 3.1. Before reflectivity measurement, calibration was performed using the method described in section 3.1.1, and with a 50% Spectralon reflectance standard (SRS-50, Labsphere, New Hampshire, United States). The automatic integration time setting method was used, and the boxcar averaging width was increased to 15 Measurements recorded were the average of five scans. For transmission measurement, calibration was done with 8ms integration time, boxcar average width of 15, and taking the average of five scans. The reference material was a 50% transmission (optical density: 0.3) neutral density (ND) filter (NDUV03B, Thorlabs, New Jersey, USA).

Table 4.1: Lentil genotypes and their seed coat color characteristics

Lentil Genotype	Seed Coat Color
Indianhead	Black
7311-1	Black
7312g	Mottled Black
CDC QG-3	Green
CDC Greenstar	Light Green
CDC QG-4	Mottled Green
CDC Maxim	Grey
CDC KR-2	Grey
CDC SB-3	Grey
SB4(IBC 929)	Grey
IBC 929R	Grey
IBC 1264-3	Light Grey
CDC Marble	Marbled Green
CDC Rosebud	Tan
IBC 1264-1	Tan
7427-12	Tan
IBC 1274-2	Light Tan
CDC Kermit	Light Tan
CDC Robin	Brown
ZT-4	Zero Tannin

For both transmission and reflectivity measurements, seed coats from 20 seeds were selected at random from each genotype class and subjected to one measurement each. Each one-half seed coat was placed on the sample holder with the convex surface facing up. Measurements were taken of reflectivity and transmission as described in Chapter 3.

4.1.2 Data Analysis

Preliminary data reformatting was done using Excel. The mean (N=20) spectrum of each sample was computed and extracted to form plot files (reflectivity and transmission plot files), while the original data were arranged in a data frame suitable for analysis using RStudio (R Development Core Team, 2011).

The reformatted data frames were saved as comma-delimited (.csv) files and loaded to scripts on RStudio synchronized with R Program v3.5.1 (R Development Core Team, 2011) for analysis.

Multi-plots for reflectivity and transmission were generated using the "ggplot2" package (Wickham, 2018). See Appendices E3 and E4 for the plot and analysis scripts, respectively.

To study variability in light transmission of the different seed coat types, features were extracted from the ultraviolet (UV), visible (VIS), and near-infrared (NIR) regions of the transmission curves of ten genotypes representing the major seed coat colors. The ten genotypes were selected to narrow down the comparisons the seed-coat-type basis, in order to more easily build an understanding of variations in light transmission properties It was important to compare Indianhead (black) and 7311 (black) because black seed coats have different genetic structure compared to the others; one may be selected and genetically combined with green seed coat to combine the ease of de-hulling of green seed coat (Subedi *et al.*, 2018) and light-blocking ability of black.

The cumulative light transmission characteristics were compared based on features extracted in each spectral range, defined as Cumulative UV Transmission (CUVT), Cumulative VIS Transmission (CVIST), and Cumulative NIR Transmission (CNIRT) respectively. The features represented the area under the curve in each spectral region and were computed by multiplying the light transmission values in that region by the spectral bandwidth and summing up the total (integration by summation). This was done using R algorithms based on equations 4.1-4.3.

$$\mathrm{CUVT} = \sum_{\lambda=250}^{\lambda=400} (\mathrm{T}\,(\lambda) \times \Delta\lambda) \qquad 4.1$$

$$\mathrm{CVIST} = \sum_{\lambda=401}^{\lambda=700} (\mathrm{T}\,(\lambda) \times \Delta\lambda) \qquad 4.2$$

$$\mathrm{CNIR} = \sum_{\lambda=701}^{\lambda=850} (\mathrm{T}\,(\lambda) \times \Delta\lambda) \qquad 4.3$$

Where T (λ) is the light transmission (%) on the seed coat, Δλ is the wavelength difference, and λ is the wavelength (nm).

Further data cleaning (outlier detection and removal), and normality tests, were carried out using RStudio. Tests for significant differences in light transmission were then done using analysis of variance (ANOVA) via General Linear Modelling (GLM); post-hoc test (for pair-wise multiple comparisons) was done using the Tukey Honestly Significant Difference (HSD) test (GLM Tukey) and results converted to data frame and outputted using "broom" package (Robinson & Hayes, 2019).

4.2 Results and Discussion

In this section, the light transmission and reflection properties of seed coats are presented in terms of curves. Also, the comparison of transmission properties using the cumulative light transmission approach is presented.

4.2.1 Transmission Properties

Figure 4.1 shows the average (N=20) light transmission curves for the 20 lentil lines used in the study. These genotypes represent the major seed coat colors (market classes) and their variants. The most important finding concerning the effect of light on the underlying cotyledon (photodegradation) is that there was no detectable light transmission in the UVB region (290-315 nm) through the seed coat of any studied genotypes, except for the zero tannin seed coats. This limited transmission of UVB through the seed coat suggests that if any photodegradation occurs in whole lentil cotyledons, it is due to other wavelengths. This would be notable because UVB light has been identified as the primary culprit for photochemical effects (Diffey 2002).

Another important observation is that the light transmission properties highlighted the three groups of lentil seed coat identified by Mirali *et al.* (2016) and Vaillancourt & Slinkard, (1992). The non-tannin containing type, zero tannin (Figure 4.2a) seed coat had the highest light transmission across the entire wavelength range, while Indianhead (black) had the lowest (Figure 4.2b). The two black seed coats showed no detectable transmission up to 600 nm (Figure 4.2b). The tannin-containing seed coat classes, which include the following: brown, tan, green, and its variants, and grey and its variants, had transmission properties that lie between the two extremes of zero tannin and black. Among the non-black tannin-containing group, brown seed coat (CDC Robin) showed extremely low detectable transmission up to 450 nm, effectively blocking all UV and some visible light

(Figure 4.2f). The above findings suggest that zero tannin seed coat may not be good for breeding programs that focus on enhancing lentil cotyledon quality; brown may be the closest to black in light-blocking ability, and black may be the most useful based on light-blocking properties.

The light transmission curves for zero tannin, black, and green seed coats showed characteristic shapes and differ markedly from the other market classes. This suggests that seed coats of the same market class contain similar pigments in differing concentrations. In contrast, the grey, brown, and tan seed coats presented similar spectral patterns, but their transmission values at various wavelengths differ. The similar spectral patterns were expected because the three seed coat classes closely resemble one another visually, with only slight variations (see Figure 2.3). Also, these genotypes belong to the *Tan* (tannin-containing) group. Further, it suggests that, although these lentil market classes have different genetic backgrounds, their seed coats contain similar pigments but in differing concentrations.

The notable spectral difference between brown and the grey and tan genotypes is that brown showed no detectable transmission up to 450 nm, while the other two did. The subtle difference between the tan and grey is that the tan seed coat showed a slightly more pronounced trough between 650 and 700 nm and flattened out more between 700 and 850 nm.

Figures 4.2 – 4.4 show the computed CUVT, CVIST, and CNIRT of the ten selected lentil genotypes, in terms of the mean (diamond) and the spread in datapoints (See Figure 4.2 for box key). The letter “M” in seed coat color stands for “Mottled” or “Marbled", i.e. seed coat with color pattern/non-uniform color. The GLM ANOVA result showed that there were significant ($p<<0.010$) differences in CUVT, CVIST, and CNIRT among the tested seed coat colors (see Tables A1-A3, Appendix A). Hence, the Tukey test was used for orthogonal multiple comparisons, and letters indicating which pairs of seed coat types were not statistically different are indicated on the boxplots. Genotype pairs that have the same letters are not statistically different; those that do not are significantly different ($p<0.05$). See Appendix A for Table A4 showing the full multiple comparisons results.

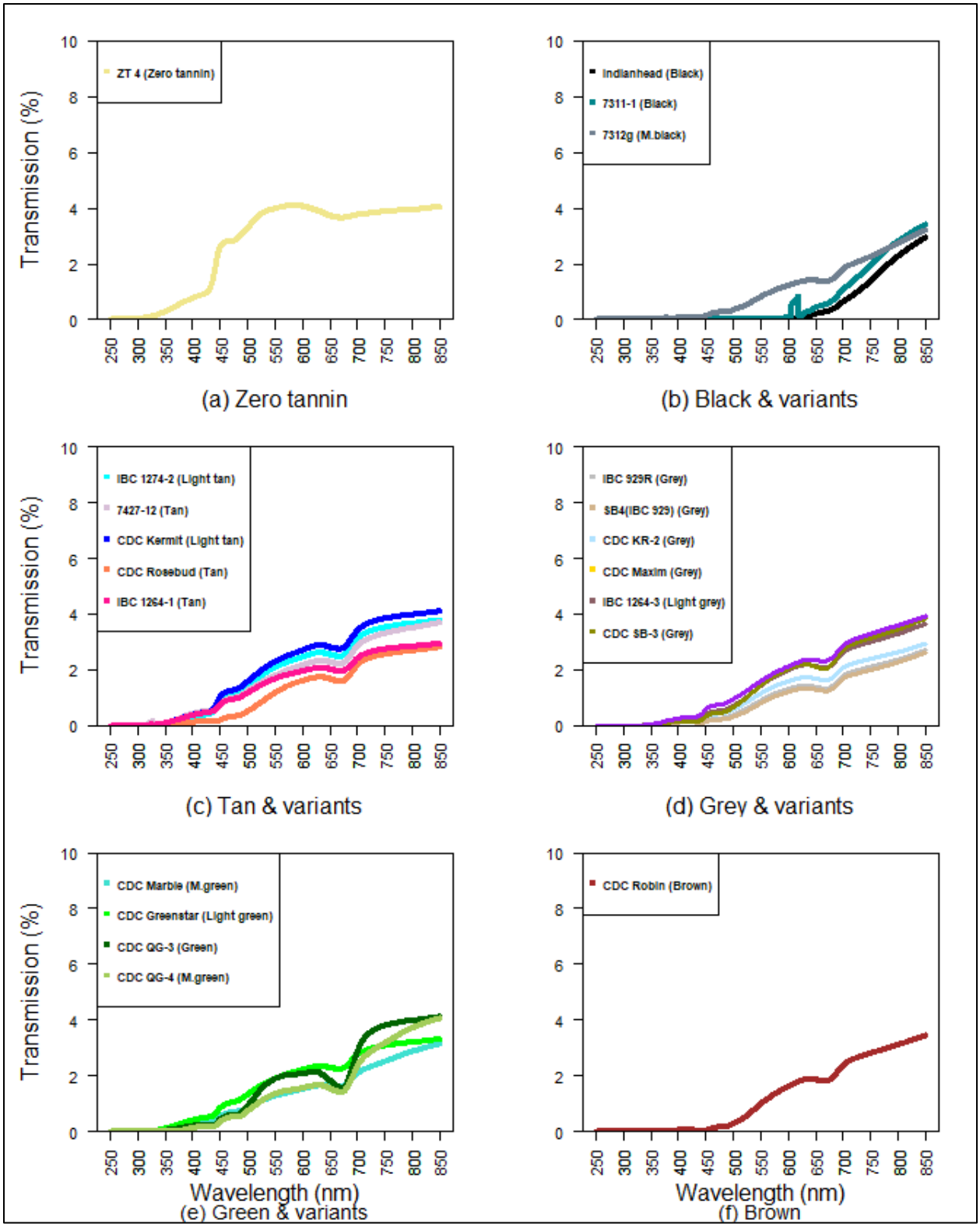

Figure 4.1: Transmission properties of the seed coats of lentil market classes.

Figure 4.2 shows the results for CUVT, which reveals that zero tannin seed coats have the highest CUVT and the largest within-group spread. Zero tannin is the only seed coat type that is statistically different from all other seed coat types. The two black seed coats had the lowest (zero) CUVT, meaning that they transmitted effectively zero UV light; they were not statistically different. Brown seed coats also had extremely low CUVT (not statistically different from the two black seed coats) and tight within-class spread.

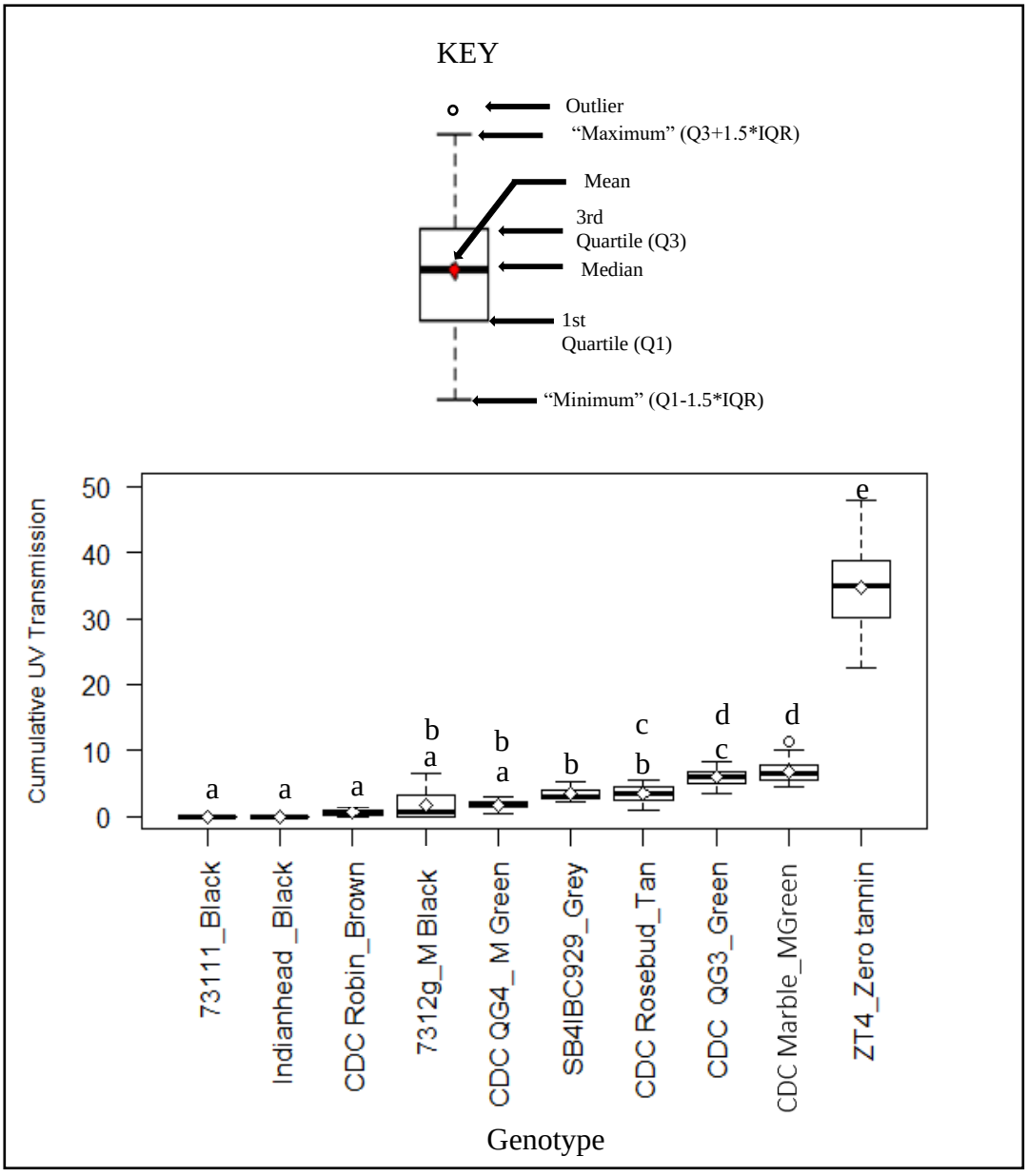

Figure 4.2: Mean and distribution of cumulative UV transmission (250-400 nm; Classes with the same letter indicate the null hypothesis that classes are equal could not be rejected by the Tukey test ($\alpha = 0.05$)).

Another notable observation is that, although the transmission curves of brown, grey, and tan were similar in shape (Figure 4.2), the CUVT of brown was statistically different ($p<0.05$) from the other two; grey and tan CUVT values were not statistically different.

Light transmission in the VIS region was generally higher than in the UV region. The two black seed coat types, which effectivity blocked all UV light, showed some detectable VIS transmission (Figure 4.3). Like the UV region, zero tannin had the highest CVIST. Again, zero tannin was statistically different from all other seed coat types. Green seed coat transmitted the second-highest cumulative VIS light and was significantly different from all other seed coat types. The two black seed coats had the lowest CVIST and were not statistically different. Brown, tan, mottled/marbled green, and marbled grey were not statistically different from one another in the VIS region; grey and mottled black were also not different. A notable finding here is that black was different from mottled black, and green was different from the two patterned green seed coats (marbled and mottled); this shows that seed coat pattern affects visible light transmission.

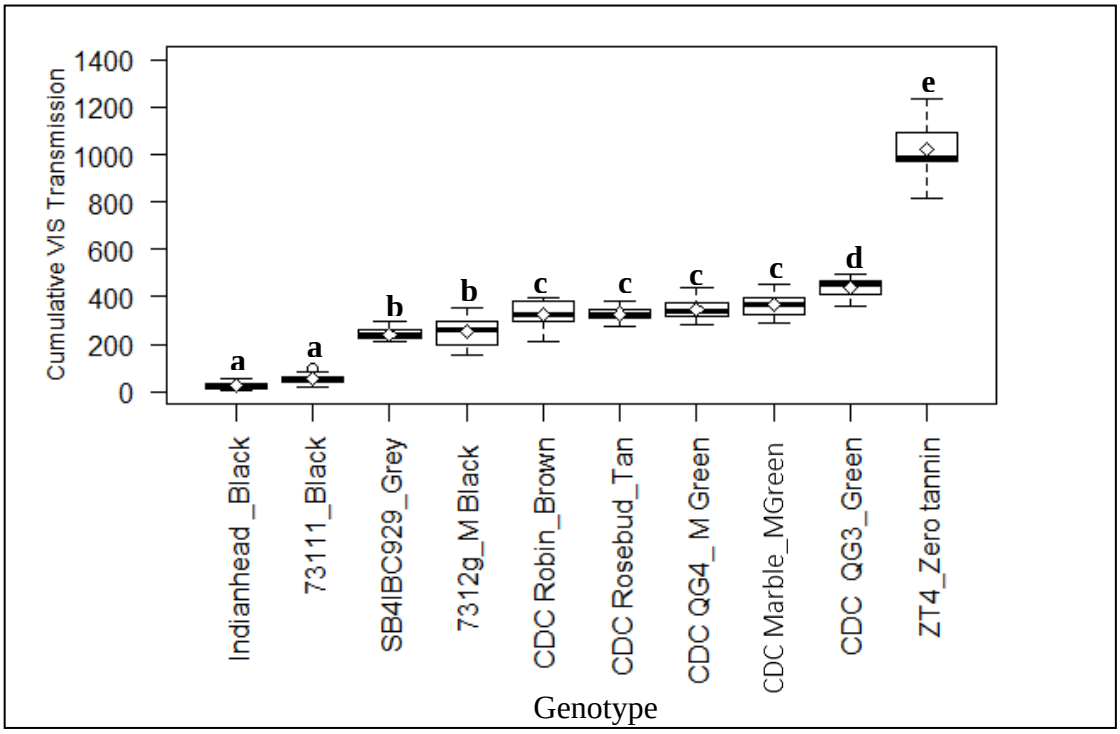

Figure 4.3: Mean and distribution of normalized cumulative VIS transmission (400 – 700 nm; Classes with the same letter indicate the null hypothesis that classes are equal could not be rejected by the Tukey test ($\alpha = 0.05$)).

Figure 4.4 shows that the CNIRT values were generally higher than CUVT and CVIST. The two black seed coat types that effectivity blocked all UV light and a relatively high amount of VIS light showed high (comparable to others) NIR transmission. The CNIRT of zero tannin seed coat was not significantly different from the green seed coat.

One mottled green seed coat (CDC QG4) had CNIRT values that were significantly different from all other seed coat types, with a lower mean than green and zero tannin. Unlike the UV and visible regions, the black seed coats were significantly different from each other, with 73111 higher than Indianhead. In the NIR region, the cumulative transmission for grey, tan, and brown seed coats were significantly different from one another; the separation between these classes was very limited in the UV and visible regions.

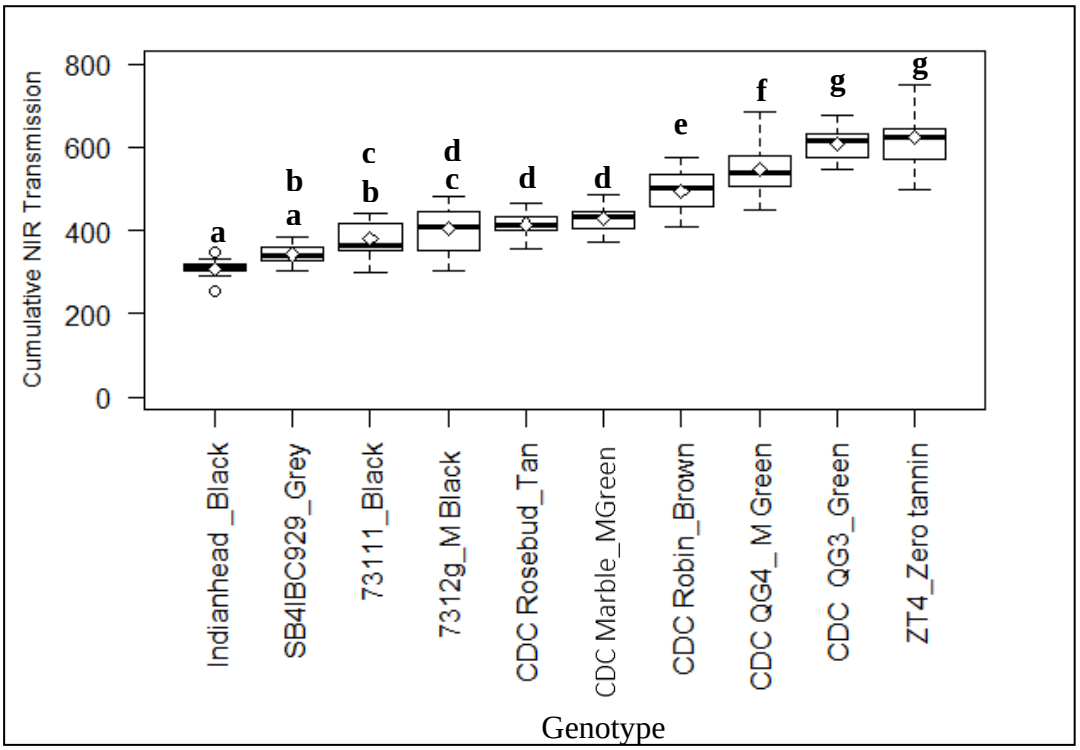

Figure 4.4: Mean and distribution of cumulative NIR transmission (700 – 850 nm; Classes with the same letter indicate the null hypothesis that classes are equal could not be rejected by the Tukey test ($\alpha = 0.05$)).

Generally, there were real differences in the light transmission properties of the tested seed coat classes; however, the pairwise comparisons test showed that most pairs of the classes were not

statistically different from each other in the UV region. The most pair-wise differences were seen in the VIS region. In the NIR region, the transmission properties of all the tested seed coat types were relatively high; the other seed coat types were closer in transmission than in the UV and VIS regions.

4.2.2 Reflectivity Properties

Figure 4.5 shows the light reflectivity curves for the 20 lentil genotypes used in the study, representing the major seed coat colors (market classes) and their variants. Each curve represents an average of the reflectivity of 20 seed coats from that genotype The figure reveals that the reflectivity properties of all the seed coat types were generally high, compared to transmission properties (Figure 4.2) in the entire wavelength range of 250 nm to 850 nm; this is especially so in the NIR region.

It is noteworthy that, similar to transmission properties, the reflectivity properties separated the lentil genotypes into the three groups identified by Mirali *et al.* (2016) and (Vaillancourt & Slinkard, 1992). The non-tannin containing zero tannin class (Figure 4.5a) had the highest reflectivity in the full spectrum range. The two black seed coats and their variant, mottled black, showed the lowest reflectivity between 450 and 700 nm (Figure 4.5b), while the tannin-containing non-black category have their reflectivity properties lying in-between.

The reflectivity curves generally show characteristic shapes among seed coats of the same market class and differ markedly from others. Black seed coat reflectivity decreased with increasing wavelength up to 480 nm, had their minima between 500 and 550 nm, and then rose steadily into the NIR region. The variants of tan seed coats had reflectivity curves with their minima at the lowest wavelength (250 nm); they all increased with increasing wavelength.

The most consistent pattern in within-class reflectivity properties was found with grey seed coats and their variants. The curves had their minima at the lowest wavelength, increased in overlapping fashion as the wavelength increased, had peaks and troughs at the same wavelength regions, and reached their maxima at the highest wavelength.

The mottled green category closely resembled mottled black between 250 and 650 nm. Notably, these two market classes are characterized by seed coat pattern, genetically caused by multiple alleles at a single locus (Vandenberg & Slinkard, 1990). The two genotypes with green seed coats both had steep absorption features between 650 and 700 nm, with normal green having the overall steepest absorption feature in this region. Finally, brown seed coats had reflectivity curves that maintain a constant value between 250 and 350 nm; they had a peak around 400 and 450 nm, rise from 500 nm to a maximum value at 850 nm

These recognizable patterns in light reflectivity of seed coats of lentil genotypes within the same market classes suggest that reflectivity data may be used to train a machine learning algorithm to successfully identify the market class of a particular lentil sample. This may be useful in confirmatory tests to place a new lentil variety in a particular market class or for easy identification of samples for breeding purposes. A preliminary study investigating this possibility is presented in Appendix B.

According to Sanderson *et al.* (2019), the differences in lentil seed coat colors can be explained by differences in concentrations of pigments such as anthocyanins, pro-anthocyanins, and carotenoids. Also, Davey (2007) posited that chlorophyll is mostly responsible for the green seed coat color; extraction experiments successfully isolated chlorophylls from green lentil hulls.

Anthocyanins absorb high amounts of radiation from 250 nm to 650 nm, with absorption peaks between 270-290 nm and 500-550 nm (Woodall & Stewart, 1998). Figures 4.1 and 4.5 reveal that black seed coats have the lowest transmission and reflection in this region, and there was no detectable transmission or reflection between 500 and 550 nm. This suggests that anthocyanin absorption plays a great role in the observed difference between the optical properties of black seed coats and the other phenotypes. Interestingly, Elessawy *et al*. (2019) found that black seed coats contain high amounts of anthocyanins. The spectra also suggest that colorless zero tannin seed coat contains the least (if any) amount of anthocyanins, considering its relatively high transmission and reflection properties in this region. This agrees with the finding of Elessawy *et al*. (2019), which showed that there was no anthocyanin presence in zero tannin seed coat.

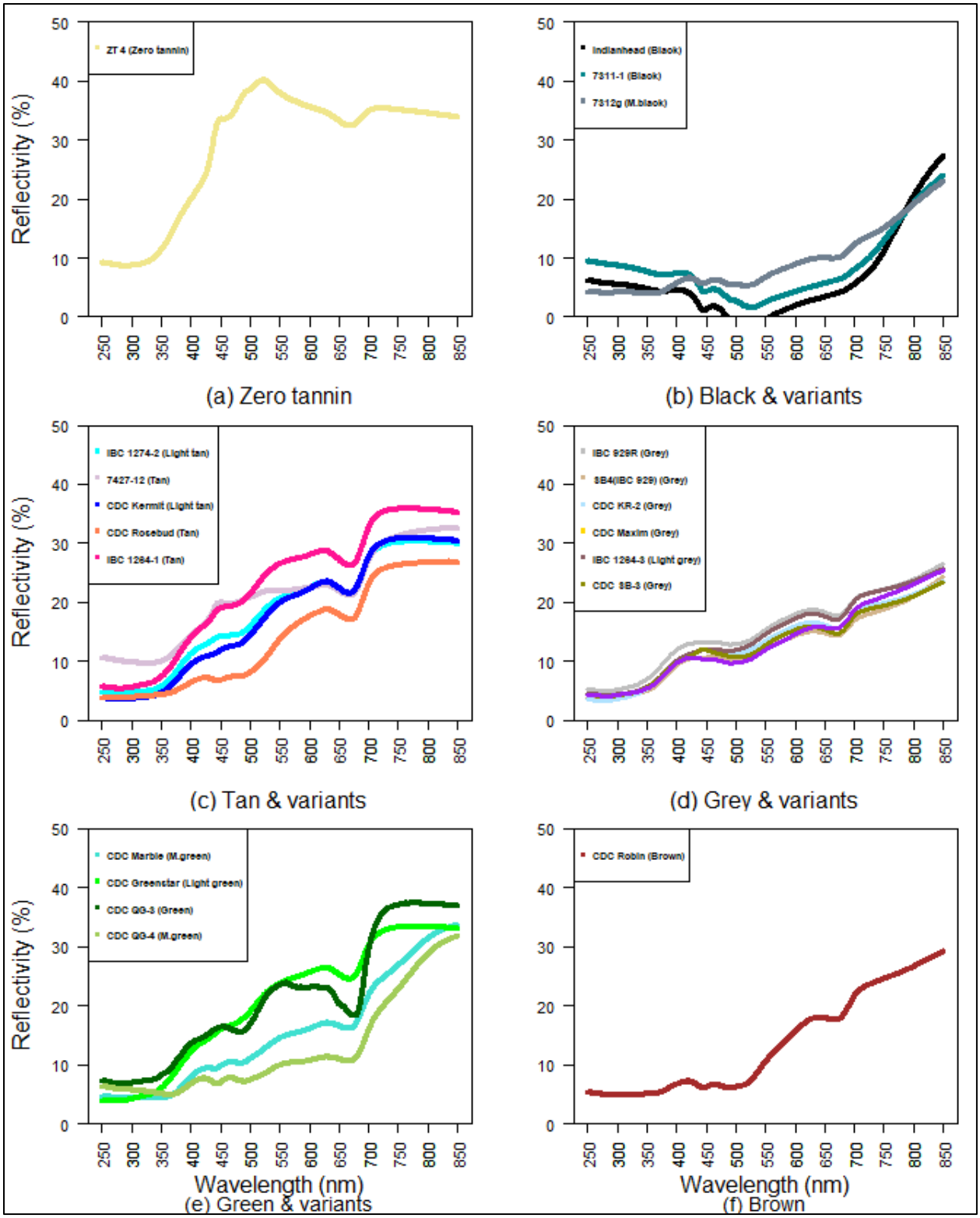

Figure 4.5: Reflectivity properties of the seed coats of lentil market classes.

In a study by Peters & Noble (2014) involving spectrographic analysis of pigments, chlorophyll-a showed strong absorption at 300 nm - 450 nm and 600 nm - 700 nm, while chlorophyll b absorbed strongly at 400 nm - 500 nm and 600 nm - 700 nm. Figures 4.2 and 4.5 show that, unlike zero tannin seed coat, green, grey, tan, brown, mottled-green, and mottled-black seed coats all have pronounced troughs at 430-450 nm and 650-700 nm, with the green and mottled green types having the steepest trough between 650-700 nm. This suggests that one reason these lentil phenotypes differ in optical properties from zero tannin is the presence of chlorophylls. Also, carotenoid absorbs strongly between 300 and 550 nm (Peters & Noble, 2014). In this range, the high transmission and reflection properties of zero tannin indicate that there is low absorption in this region; thus zero tannin seed coats may contain the least amounts of carotenoids, compared to the other seed coat types.

Looking at Figures 4.2 and 4.5, zero tannin seed coats have the highest light transmission and reflectivity from 250 nm to 700 nm, which means that the absorption was lowest in this region. One contributing factor to this may be the absence of some phenolic compounds and tannins, which are present in the *Tan* (tannin-containing seed coat types). In a study by Mirali *et al*. (2016), the following phenolic compounds were found in grey opaque seed coats but not in colorless zero tannin: myricetin-3-*O*-rhamnoside, flavan-3-ols (including catechin, epicatechin, gallocatechin, epigallocatechin, and catechin-3-glucoside), proanthocyanidin dimers, trimers, tetramers, and pentamers.

Also, a study by Mirali (2016) found varying concentrations of UV absorbing pigments catechin, catechine$^{13}C_3$, gallocatechin, kaempferol 3-O-robinoside-7-Orhamnoside and luteolin-4-O-glucoside in black, grey, tan, green, and brown lentil seed coats. They reported that black seed coat from Indianhead had the highest concentration of luteolin-4’ O-glucoside, followed by grey and tan. This may explain the strong UV absorption of black seed coat compared to the other phenotypes.

4.3 Summary/General Discussion and Conclusion

In this chapter the light transmission and reflectivity of 20 lentil genotypes representing the various seed coat colors were measured using the fiber optic photometer described in chapter three. Spectral curves have been presented to enable visual assessment of the interaction of the seed coats with different wavelengths of light in the UV-VIS-NIR region. A notable finding in this regard is that all seed coat types, except zero tannin, effectively absorbed or reflected (showed no detectable percentage transmission) shorter wavelength UV light (UVB and UVC; 250-415 nm). This wavelength range is a significant contributor to photochemical degradation, according to literature; the lack of transmission in this range suggests seed coats provide some protection against these effects. However, there was detectable light transmission in longer wavelength UV and visible regions; this necessitates studying the effect these wavelengths on lentil cotyledon color.

Based on an analysis of variance, it was concluded that there are real differences in UV, visible, and NIR transmission among seed coats of lentil market classes. Differences were found between classes based on the cumulative transmission in all three spectral ranges. Multiple comparisons showed that while differences do exist, not all of the samples studied separated along market class based on cumulative measures. This may be because the cumulative measures did not provide the spectral resolution to make color differentiation possible in all cases.

PROLOGUE TO CHAPTERS 5 & 6

The following two chapters involve the application of machine vision and color analytics to study the effect of light exposure on the cotyledon color of lentil seeds and the protective effect of seed coat.

This part of the thesis was presented virtually at the American Society of Agricultural and Biological Engineers conference, Omaha, Nebraska, United States (July 13th – 15th, 2020), titled: "**Application of Machine Vision & Color Analytics for Evaluating the Effect of Light on Lentil Quality**."

Chapter 5 : EFFECT OF LIGHT EXPOSURE ON COLOR OF LENTIL COTYLEDON

In the previous chapter, light transmission was detected through all the various lentil seed coat types. Except for zero tannin seed coats, no transmission of short-wavelength UVC and UVB radiation (250-315 nm)) was detected. However, all the seed coat types (except black and mottled black) transmitted some amounts of longer wavelength UVA, and all transmitted high amounts of visible light. Given that light is being transmitted through the seed coats, this chapter investigates the effect of light exposure in different wavebands on the color of lentil cotyledons. Although UVB and UVC light are known contributors to photodegradation (SCENIHR, 2012), they were not studied further due to lack of measurable transmission; the contributions of UVA and visible wavelengths on cotyledon color change remained unknown.

This study was designed to understand the influence of light in the UVA (315 – 400 nm) and visible (400 to 700 nm) wavebands on the color of red, green, and yellow lentil cotyledons. In addition to the full visible spectrum, blue, green, and red light effects were also considered individually. Each cotyledon color was treated as a class. The basis of comparison was color change before and after treatment, as measured by differences in the CIEL*a*b* color space.

The results from this study will be informative to breeding programs that focus on enhancing the cotyledon color of lentils. It will also be useful in making decisions regarding the de-hulling of lentils, and de-hulled lentil material handling.

5.1 Materials and Methods

Lentil samples with red (CDC Maxim), green (CDC QG-3), and yellow (Indianhead) cotyledons were obtained from Plant Sciences Field Laboratory, University of Saskatchewan. The seeds were harvested during the 2019 harvest season, stored in woven bags at normal room conditions, and this study was carried out in December 2019. The samples were de-hulled using a grain testing mill (TM05, Satake Engineering Co., Hiroshima, Japan). Square seed sample holders with partitions were designed and fabricated using a 3D printer. Each partition was equipped with pockets to hold individual seeds (See Figure 5.1). This arrangement made it possible to consider

the seeds on an individual basis by placing them at specific positions and in a particular order. The partitions allowed the separation of the three cotyledon types and flipping over to expose both sides of the seeds to light. The compact arrangement ensured that all seeds were exposed to equal intensities of light.

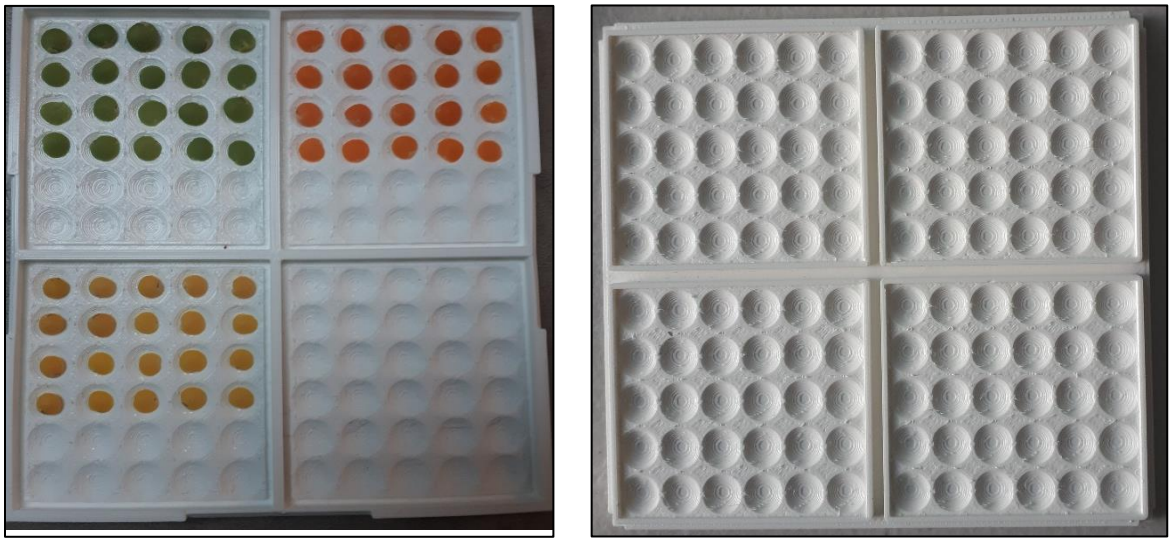

Figure 5.1: Lentil sample holders for light treatment. From left to right: the first open half for holding seeds, the second open half for turning over the seeds.

5.1.1 Experimental Design

The study involved one-factor experiments on each of the three colors of lentil cotyledon (red, green, and yellow). Light treatment was the factor at six levels, namely, ultraviolet, blue, green, red, full-range visible, and control (dark). The responses were the changes in L*, a*, and b* and overall color change (ΔE*) (equations 2.4-2.6). Twenty seeds from each of the three cotyledon color classes were subjected to the light treatments at room temperature (nominally 23°C).

5.1.2 Color Measurement

The color of the individual seeds was measured before and after each treatment. This gave a more specific assessment of the color change experienced by the treated and control seeds. Prior to light treatment, the color of individual seeds was measured using the BELT and phenoSEED computer vision described by Halcro *et al.* (2020). The seeds were placed on the equipment belt and made to pass through a camera that acquired their images. The image acquisition and storage protocols

were carried out using software written for that purpose (LentilSoftware) (Halcro, 2019 – personal communication). For this study, the seeds were tracked individually to facilitate pre- and post-analysis on a per-seed basis. The saved RGB images were then processed to obtain equivalent CIEL* a*b* values using the phenoSEED python code. The color values were obtained as comma-delimited (CSV) files for analysis. This procedure was repeated with post-treatment.

5.1.3 Light Treatment

For each cotyledon class, seed samples were exposed to five light treatment chambers, namely, UV (315-400 nm), full-spectrum visible (with flux density 30.12W/m^2), red (with flux density 21.08W/m^2), green (with flux density 9.04 W/m^2), and blue (with flux density 9.04 W/m^2). One sample group was kept as the control in the dark in a wooden cabinet under normal room conditions. Each side of the seeds was exposed to light for seven days.

5.1.4 Data Analysis

The before- and after-treatment data were reformatted and combined into one comma-delimited file. The file was then loaded to a script on R program for analysis. The color change on individual seeds was computed as changes in L*, a*, b* values, ΔL^*, Δa^* ,Δb^* , and the overall color difference ΔE^*. The R algorithms used for this computation were based on the color difference equations (equations 2.4 to 2.7) of section 2.6.3. Pre-treatment measurements were used as the reference measurements (subscript r), and post-treatment measurements were the new measurements (subscript n) in these calculations.

The color differences were treated as continuous response variables, while light exposure was treated as a categorical explanatory variable. For each cotyledon class, a GLM was fit to the data using the color changes (ΔL^*, Δa^*, Δb^* , and ΔE^*) as the response variables, and the treatment as categorical explanatory variables. The GLM allows for directly comparing means of one treatment level of interest (set as the control in this case by assigning the first letter of the alphabet to control) to the means the other treatment levels using t-tests. The means are estimated using the modern technique of maximum likelihood based on equation 5.5.

$$Y = \alpha + \beta_1 X_1 + \beta_2 X_2 \ldots \beta_n X_n + \varepsilon_i \qquad 5.5$$

The GLM algorithm recodes the categorical variables into dummy codes and estimates the parameters such that: α is the mean of the level whose initial is the earliest letter in the alphabet (in this case the control); $\alpha + \beta_n$ is the mean of treatment level n. The function $summary(model)$ is a model summary that produced t-test results, which allowed direct comparisons of the mean of each light treatment versus the control and the mean of control with zero. See Appendix E5 for the R script used for plotting and modeling the color data.

5.2 Results and Discussion

Figure 5.2 shows grouped bar plots revealing the mean changes in color coordinates and overall color change as a function of light treatment and cotyledon color. Generally, the effect sizes were largest for green-cotyledon lentils. The boxplots of Figures 5.3 to 5.5 indicate the statistical significance and will be used alongside the bar plot to discuss the significance and direction of the effect of the different light treatments. See Tables C1 – C12 (Appendix C) for the effect size estimates and the respective p-values. The statistical significance is based on the results of the t-test produced by the GLM summary. The diagnostic plots for all the GLM fit used in this test showed that the errors were fairly normally distributed, the variances were homogeneous, and there were no data points with undue leverage on the models.

In a GLM summary, the "estimate" of the control generally represents its mean (the effect (change) on the control), while the estimate of the other treatments represents the difference between their respective means and the mean of the control. The p-value of the control indicates if its mean is significantly different from zero (i.e. if the control has changed), while treatment p-values indicate if the mean is significantly different from control.

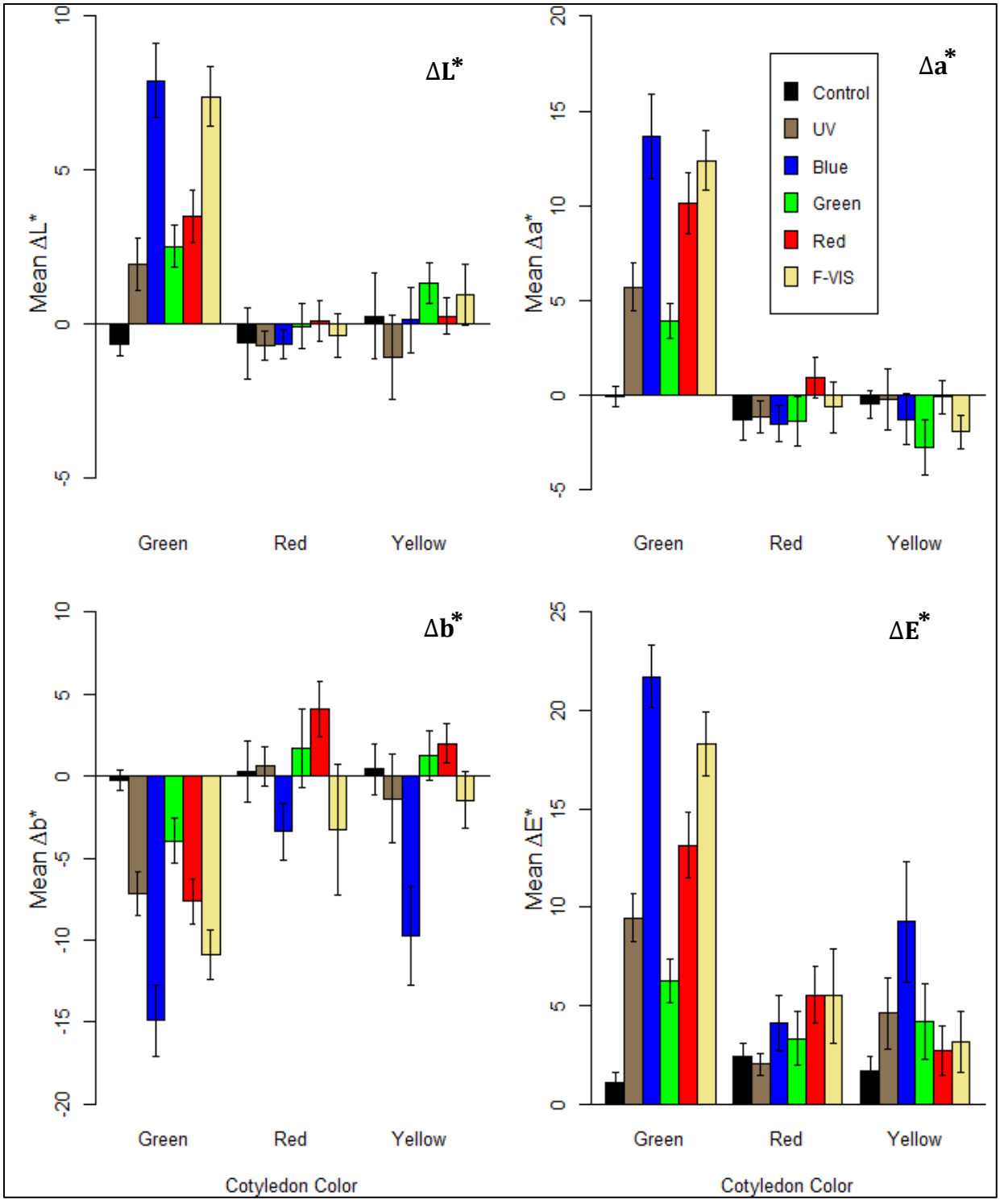

Figure 5.2: Mean changes in color values as a function of cotyledon color and light treatment: Error bars indicate ± 1 standard deviation, N= 20.

5.2.1 Effect of Light Treatment on Green Lentil Cotyledons

Figure 5.3 presents, for green lentils, the spread of changes in L*, a*, b* values, and the overall color change, $\Delta E*$, as functions of treatment. The figure also indicates data points were distributed symmetrically under most of the light treatments. The mean changes in color values are shown in Figure 5.2.

The effect sizes/mean values (Figure 5.2a) and indicated statistical significance (Figure 5.3a) show that the mean $\Delta L*$ of all treated green lentil cotyledons were significantly ($p<0.01$) higher than that of control. The effect size on the control seed was very small (-0.7 units) but significant ($p<0.01$), indicating that the control seed underwent minute L*-value changes; this might be due to environmental factors, such as heat and oxygen. The mean $\Delta a*$ and $\Delta b*$ of all treated green lentil cotyledons were all significantly ($p<0.01$) higher than the control. In a*- and b*-coordinates, the p-values of the controls indicated that they did not change significantly.

The overall color difference, $\Delta E*$ of all treated seeds were significantly higher than the control (Figure 5.3a). Considering the mean overall color differences (Figure 5.2a) and the minimum perceptible difference (MPD) threshold ($\Delta E* \approx 2.3$) (Mahy *et al.*, 1994), the treated green cotyledons were perceptually different from control in all cases. This was seen by looking at the seeds. The overall effect size on the control seed was very small (less than the MPD threshold) but significant ($p<0.01$); this indicates that the color changes in control seeds before and after the experiment were not perceptible by the human eye (consistent with personal observation).

The results show that green lentil cotyledons subjected to all light treatments experienced positive changes in L*-value, compared to the control, which was slightly negative. This indicates that seeds exposed to the light treatments turned lighter, the lightest being seeds exposed to full-visible light. The large positive change in a*-values for treated green lentils, compared to the control, indicates that the treated seeds turned redder (or less green) in the redness-greenness coordinate; this might be due to the breakdown in chlorophyll. Further, all light treatments resulted in high negative changes in b* -values of green lentils, showing that the seeds became more bluish in the yellowness-blueness coordinate; this would be consistent with a breakdown in carotenoids. The

overall color changes ΔE* revealed large significant and visually noticeable effect sizes due to all light treatments on green cotyledons.

All light treatments (UVA, blue, green, red, and full-visible) resulted in significant color changes in green lentil cotyledon. Thus, it was concluded that exposure of green lentil cotyledons to light results in photo-degradation, leading to color loss. This finding also contributes to the knowledge that it is not only shorter wavelength UV radiation that produces photochemical effects on biological materials; depending on the material longer wavelength UVA and visible light may cause color changes in materials.

5.2.2 Effect of Light Treatment on Red Lentil Cotyledons

Figure 5.4 shows the distribution of changes in L*, a*, b* values, and the overall color change, ΔE*, in red lentil cotyledons as functions of treatment. See Figure 5.2 for mean color changes. Generally, there was much less variation between the treatments and control, compared to green lentils discussed in section 5.2.1. Also, the red lentils show the most change in the yellowness-blueness index, and not the redness-greenness. This is probably due to carotenoid breakdown being the major driver of change.

Here, only red light treatments resulted in significant (Figure 5.4) ($p<0.01$) and higher (Figure 5.2) ΔL*-values of the lentil cotyledons. However, as Figure 5.2 shows, the effect sizes were small, compared to those experienced by green cotyledons. UV, green, blue light, and full-visible light treatments did not have significant effects on the L*-values of red lentil cotyledon. The L*-value changes on the control seeds were small (-0.64 units) but significant ($p<0.01$).

In the a* - coordinate, it was also only red light treatment that resulted in significantly higher Δa* ($p < 0.01$); however, the effect sizes were small. UVA, green, full-visible, and blue light treatment had no significant effect on the b*-values of red lentil cotyledon. The Δa* of control seeds was significantly different from zero ($p<0.01$). Red light significantly increased the b*-values ($p < 0.01$) of the lentil seeds. Conversely, blue and full-visible light treatments resulted in a significant reduction in b*-values ($p < 0.01$). UVA and green light had no significant effect on b*-values of red lentil cotyledons. There was no significant change in b*-values of the control seeds.

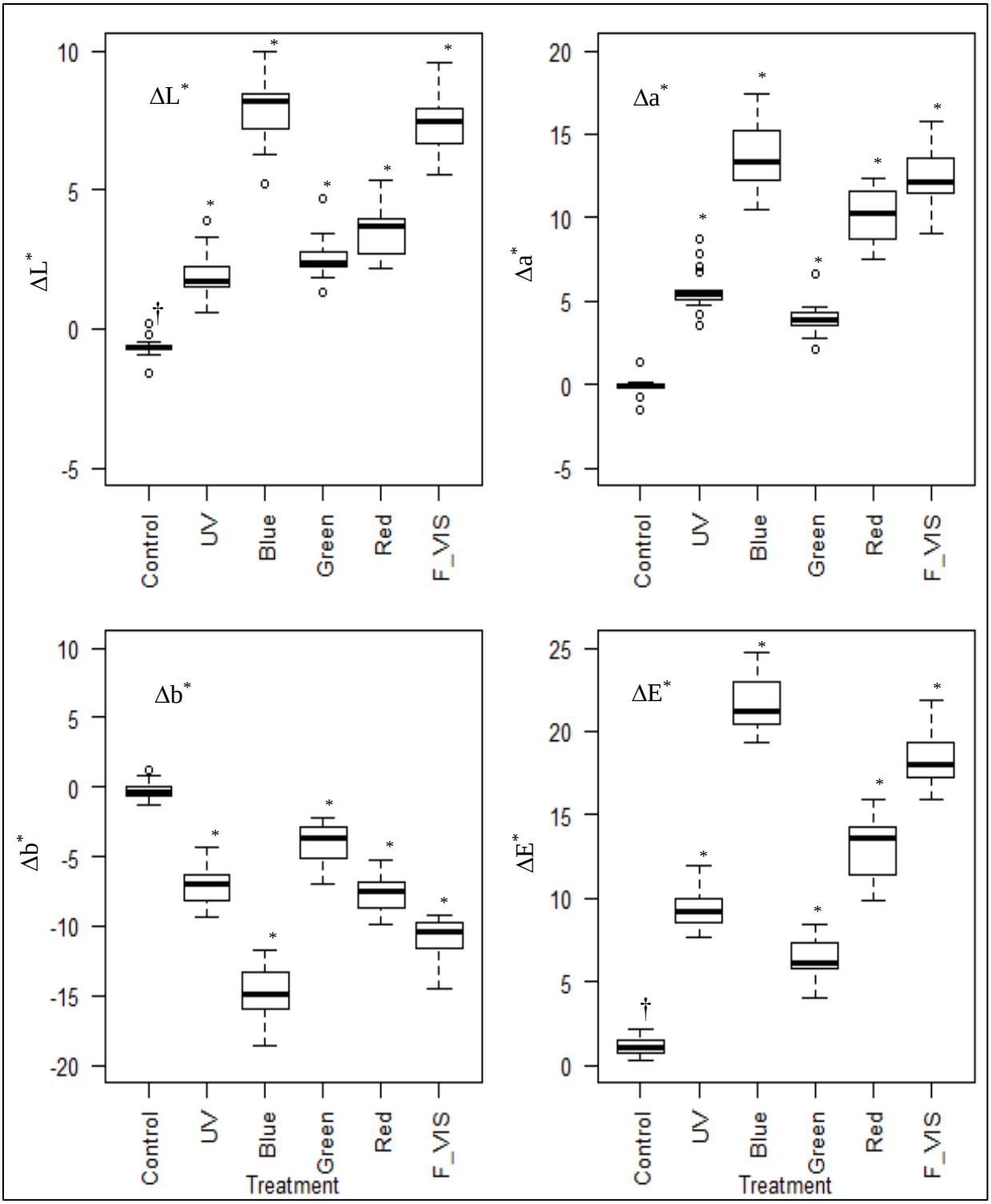

Figure 5.3: Spread in color change values of green lentil cotyledons as a function of light treatment (The symbol † indicates that the control is significantly different from zero; * indicates that treatment is significantly different from control (α=0.05); F_VIS = full visible light).

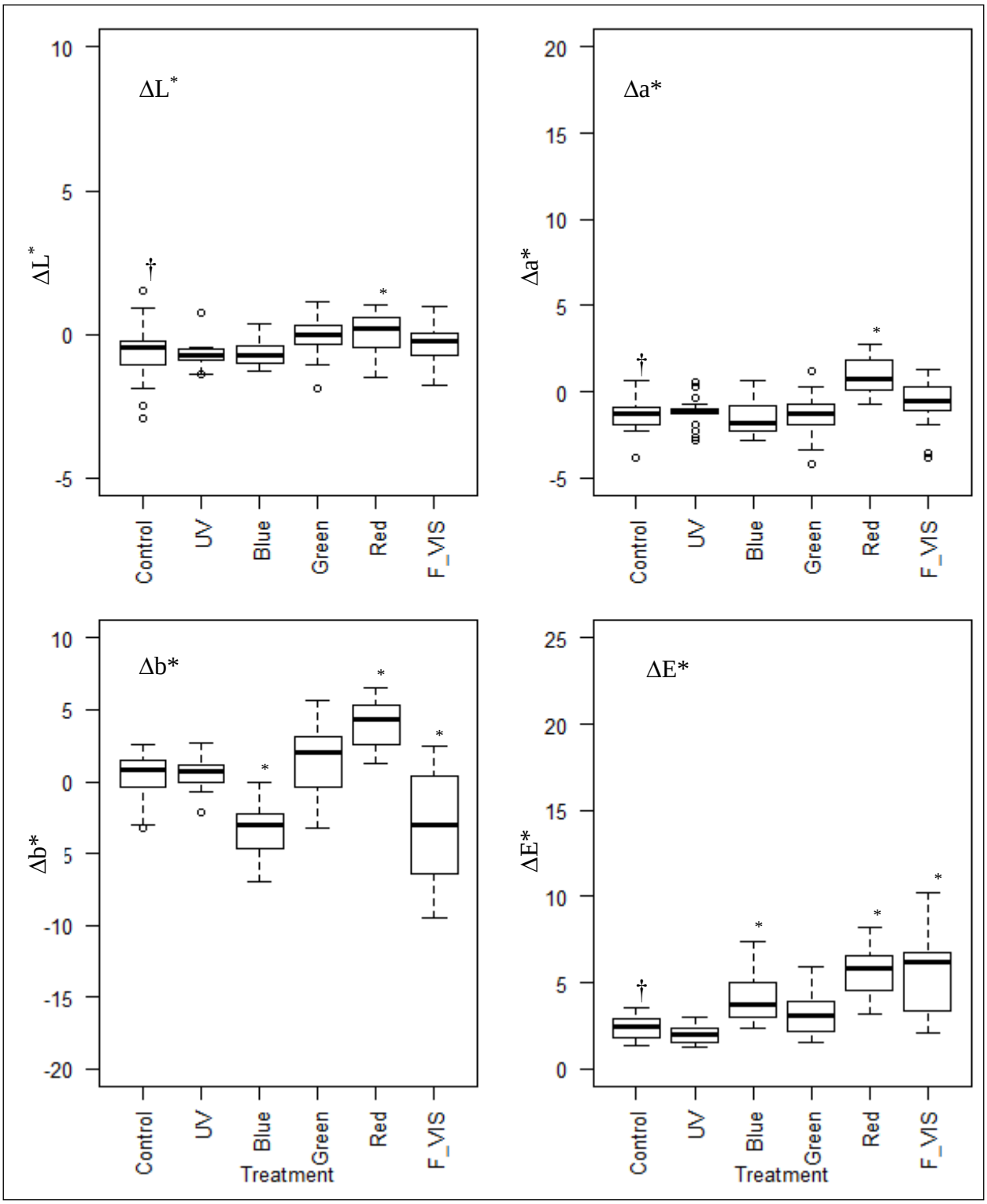

Figure 5.4: Spread in color change values of red lentil cotyledons as a function of light treatment (The symbol † indicates that the control is significantly different from zero; * indicates that treatment is significantly different from control (α=0.05); F_VIS = full visible light).

The overall color changes, ΔE*, in red lentil cotyledons due to blue, full-visible, and red light were significantly ($p < 0.01$) higher than control. Green light and UVB did not have significant overall effects on red lentil cotyledon. The control seeds underwent significant ($p<0.01$) overall color change. The mean overall color differences (Figure 5.2a) and the MPD threshold ($\Delta E^* \approx 2.3$) indicate that the color differences were visually perceptible only under red and full-visible light treatments; however, from personal observation, these differences are difficult to see.

The results show that red light treatments caused a slight increase in lightness of red lentil cotyledon, while UV, blue, green, and full-visible light did not affect the seeds. Interestingly, red lentils subjected to red light turned slightly redder to a significant degree. The mean/effect sizes shown in the bar plot of Figure 5.2 show that seeds exposed to red light experienced the highest positive difference from the control and red light was the only treatment with mean positive Δa*-value (which means that the seeds became redder in the redness-greenness color coordinate). In the b*-coordinate, red light treatment resulted in a significant yellowing effect on the red lentil cotyledon; blue and full-visible light treatments tended to cause the seeds to turn bluer.

Although red, blue, green, and full-visible lights significantly affected the color of the red lentil cotyledon in one or more color coordinate(s), the effect sizes were generally small. In the case of green lentils, the mean color changes in the control seeds were only significantly different from zero in the L* coordinate, whereas, in red lentils, there were some significant changes in the color values of control seeds in all coordinates. This suggests that red cotyledon lentils are more susceptible to color change and possible loss of market quality due to factors other than light treatment, such as heat and oxygen.

5.2.3 Effect of Light Treatment on Yellow Lentil Cotyledons

The boxplots of Figure 5.5 show the distribution of changes in L*, a*, b* values, and the overall color change, ΔE* for yellow lentil cotyledons as functions of treatment. See Figure 5.2 for mean changes in the color values in yellow lentils. Full-visible and green light treatments resulted in significant ($p < 0.01$) positive changes, while UVA treatment caused significant ($p < 0.01$) negative change in L*-values of yellow lentil cotyledons; the effects of blue and red lights were not significant (Figure 5.5a).

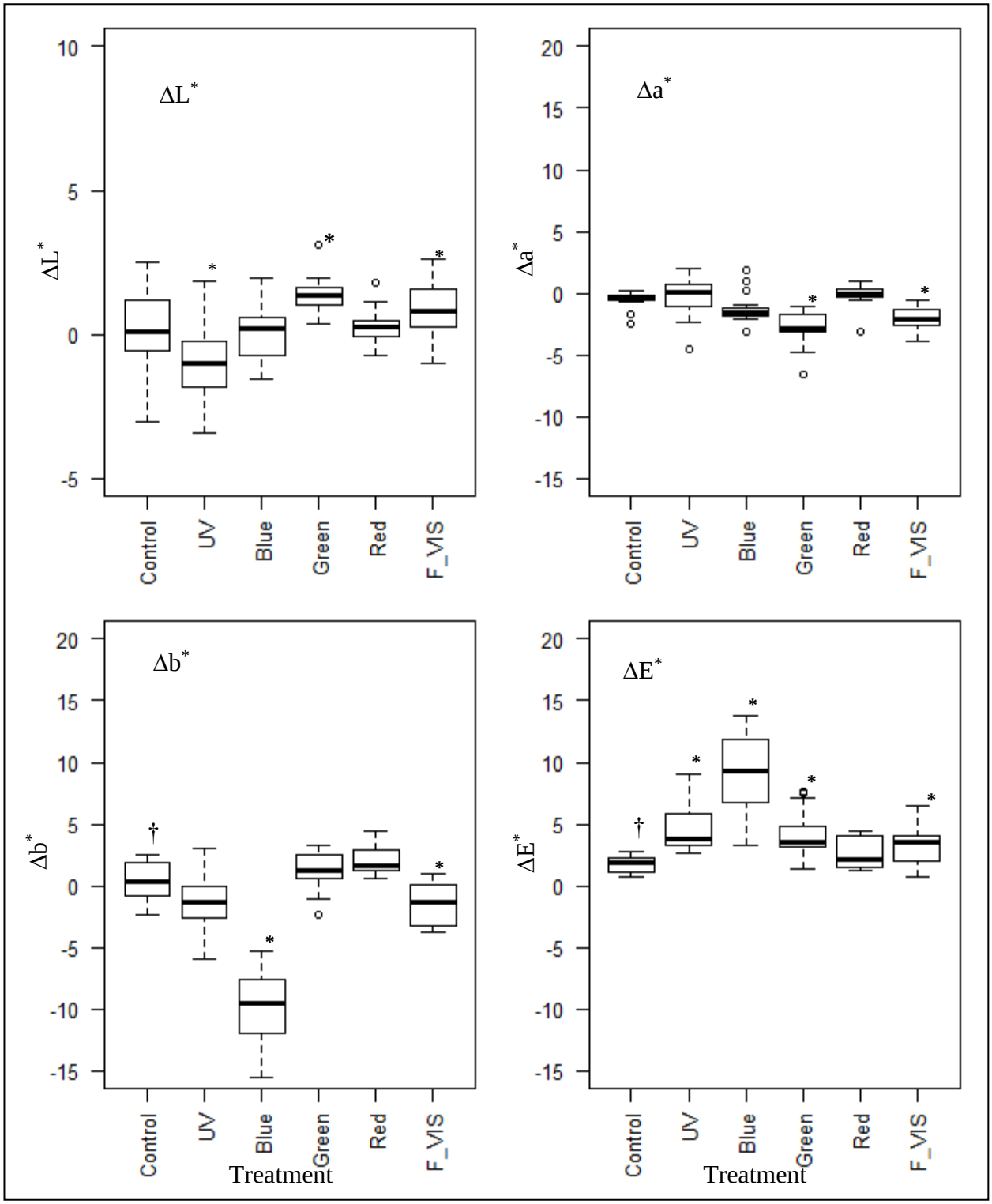

Figure 5.5: Spread in color change values of yellow lentil cotyledons as a function of light treatment (The symbol † indicates that the control is significantly different from zero; * indicates that treatment is significantly different from control (α=0.05); F_VIS = full visible light).

In the a*- coordinate (Figure 5.5b), the effects of UVA treatment, blue, and red light were not significant; blue, green, and full-visible light treatment had a significant ($p < 0.01$) but small effect on a*-values. Figure 5.5c shows that in b*- coordinate, blue, full-visible light, and UVA treatments resulted in significant ($p < 0.01$) reduction in b*-values; the effects of green and red-light treatments were not significant.

In terms of the overall color change ΔE^*(Figure 5.5d), all treatments, except red light had significant effects ($p < 0.01$) on the color of yellow lentil cotyledon. The color changes in the control yellow cotyledon seeds were significantly different from zero in the b*- coordinate; the overall color changes in the control, ΔE^* was also significant. Considering the mean overall color differences (Figure 5.2a) and the MPD threshold ($\Delta E^* \approx 2.3$), the color differences were visually perceptible only under blue light treatment; however, from personal observation, these differences were difficult to see.

The results show that full-visible and green light treatments caused the yellow lentil cotyledon to turn slightly lighter while UVA treatment had a darkening effect. Blue, green, and full-visible light treatments caused the seeds to turn greener in the greenness-redness (a*-) coordinate. Further, blue, full-visible light and UVA treatment caused yellow lentil cotyledon to slightly lose their yellowness and turn bluer in the yellowness-blueness (b*-) coordinate. Overall, the findings show that all the kinds of light treatment except red resulted in significant color changes in yellow lentil cotyledon; they significantly affected the overall color change and had effects on different color coordinates.

The effect sizes on yellow lentil cotyledons, like with red type, were generally small. However, their significance confirms that wavelengths of light other than short wavelength UV radiation may produce photochemical effects on biological materials.

5.3 Summary/General Discussion and Conclusion

This chapter was designed to answer the third research question in this thesis, does light exposure have a significant influence on color degradation of lentil cotyledons? Results showed that the

color changes (ΔL^*, Δa^*, Δb^*, and overall color change, ΔE^*) in green lentil cotyledons exposed to all light treatments were significantly different from color changes in control, and with large effect sizes. The color changes were also visually perceptible under all light treatments, both as indicated by the overall color change being much higher than the MPD threshold and from visual observation. Thus, it has been established that exposure of green lentil cotyledons to light results in photo-degradation, leading to color loss.

For red lentils the effect sizes were small, and the light treatments did not all significantly cause changes in all color coordinates, as experienced in the green category. However, red, blue, green, and full-visible lights significantly affected the color of the seeds in one or more coordinate(s).

The effect sizes on yellow lentil were also small, albeit with significant UVA, full-visible, and green light effects on L-value; blue, full-visible, and green light on a-value; blue, full-visible, and green light on b-value; and all treatments except red light on overall color change.

From the previous chapter, the question of whether the wavelength range of light at which there were detectable transmission (UVA and visible light) would have a degradative effect on the color of lentil cotyledons was raised. This chapter has shown that UVA and visible light can cause degradation in lentil cotyledon. This is notable because it is believed that UV radiation is the chief culprit for photochemical action in materials (SCENIHR, 2012). The findings call for a more extensive study to investigate the degradative effect that may occur on the cotyledon when whole lentil seeds are exposed to light, as well as differences in protective effects of different kinds of lentil seed coat.

Another important finding in this study is that red lentil cotyledons exposed to red light (with flux density 21.08W/m^2) for one week caused a slight increase in the redness of the seeds. Considering the fact that cotyledon redness is an important marketing criterion for Canadian lentils, this finding might be worth exploring further. It might be interesting to study the effect of higher intensity red light and longer exposure times on the color of red lentils.

Chapter 6 : INFLUENCE OF LIGHT ON COTYLEDON COLOR OF WHOLE LENTIL SEEDS

In the previous chapter, it was found that different wavelengths of radiation in the UVA-VIS region had some significant effect on the color of green, red, and yellow lentil cotyledons. In the seed coat transmission study, all kinds of lentil seed coat transfer detectable amounts of light in this wavelength range. It is therefore pertinent to investigate the effect of seed coat presence in mitigating the effect of light on underlying lentil cotyledons and how the different seed coat types differ in their protective ability.

In this chapter, experiments were designed to find out if cotyledon photo-degradation can occur when whole (non-dehulled) lentil seeds are exposed to light, and how much protection the seed coat offers.

6.1 Materials and Methods

Samples of green, red, and yellow cotyledon lentils were obtained from the Plant Sciences Field Laboratory, University of Saskatchewan. Samples with five seed coat classes of red and yellow cotyledon lentils (black, green, gray, colorless zero tannin, and gray zero tannin) and four seed coat classes of green cotyledon lentils (black, green, gray, and gray zero tannin) were obtained for the study. All the seeds were harvested in 2019 and stored in woven bags at normal room conditions. See Table 6.1 for the lentil varieties information. In each case, one set of samples were de-hulled using a grain testing mill (TM05, Satake Engineering Co., Hiroshima, Japan).

6.1.1 Experimental Design

Green cotyledon lentils with four seed coat classes (black, green, gray, and gray zero tannin respectively) and two conditions (dehulled and whole seed (non-dehulled)) were subjected to three treatments, namely, UVA, visible light and dark control. The factors were combined based on the questions of interest to form five experimental groups for each seed coat class, namely, whole seed-visible (non-dehulled seeds exposed to visible light), whole seed-control (non-dehulled seeds

kept under dark control), whole seed-UVA (non-dehulled seeds exposed to UVA light), dehulled-UVA (lentil cotyledons exposed to UVA light), and dehulled-visible (lentil cotyledons exposed to visible light). This was done in triplicates (a total of 60 samples). Each sample was made up of 10 seeds.

Table 6.1: Lentils used for the study.

Cotyledon	Seed Coat	Name
Green	Black	8627-1-H2-4
Green	Grey ZT	2019 F3 Bulk
Green	Normal Green	1267
Green	Normal Gray	No name
Red	Black	8023-1-H2-23
Red	Colorless Zero tannin	8122-H2-10
Red	Grey Zero Tannin	8122-H2-10
Red	Normal Green	1264-1
Red	Normal Gray	CDC Maxim
Yellow	Black	Indianhead
Yellow	Colorless Zero tannin	ZT-4
Yellow	Grey ZT	7060-2
Yellow	Normal Green	CDC Greenstar
Yellow	Normal Gray	6419-8

Red and yellow cotyledon lentils with five seed coat classes (black, green, gray, gray zero tannin, and colorless zero tannin) and two conditions (Dehulled and Whole seed (non-dehulled)) were subjected to three treatments, namely, UVA, visible light and dark control. The factor combinations resulted in five experimental groups, as in the first case. These were also done in triplicate (total of 150 samples. i.e., 75 samples each for red and yellow cotyledon lentils). Each sample was made up of 10 seeds. Treatment was a categorical explanatory variable, while changes in L*, a*, and b* values, and overall color change ΔE^* were continuous response variables.

6.1.2 Color Measurement

The initial color of the de-hulled group was measured using the computer vision lentil imaging and image processing system (BELT and phenoSEED) and processed as previously described (Chapter Five). For this experiment, it was assumed that the initial cotyledon colors of whole seed samples were the same as the initial colors of their de-hulled counterparts; this made it possible to

have estimates of the initial (before treatment) color values of the whole seed group (i.e., the initial colors of the de-hulled group were used as the reference). Color measurement was repeated after treatment on the dehulled groups, as well as on the whole seeds groups after de-hulling them. The need for mass-dehulling after treatment necessitated looking at the color of the seeds in aggregate, and not on an individual seed basis as in Chapter 5. Thus, each color data point represented the average for the group.

6.1.3 Light Treatment

The seeds were placed on sample holders specially designed to allow for flipping the seeds over for exposure on both sides. For green cotyledon lentils, one side of the seeds was exposed to UVA (315-400 nm) and visible light (flux density 30.12W/m^2) in separate chambers for seven days. The holders were then flipped to expose the opposite side for another seven days. For red and yellow cotyledons, a longer exposure time (ten days) was used, to show the effect.

6.1.4 Data Analysis

The cotyledon color datasets before and after treatment were subjected to initial reformatting and combined into one CSV data frame. The file was then loaded into an R program script for analysis. The cotyledon color changes on seed sample groups were computed in terms of changes in L*, a*, b* values (ΔL^*, Δa^* and Δb^*), as well as the overall color difference ΔE^* using R algorithms based on the color change equations 2.4 – 2.7. The color differences were plotted using a script written on Gnuplot (Appendix E6). For each cotyledon class (green, red, and yellow), GLM was fit to the data using the model in equation 5.5. GLM ANOVA and multiple comparisons (GLM Tukey test) were used to compare the cotyledon color changes in the experimental groups. See Appendix E7 for the R script used for plotting and modeling the color data.

6.2 Results and Discussion

This section presents selected multiple comparisons that are important to the questions of interest from the Tukey test results. It is important to note that each seed coat class represents a different lentil variety; thus, it was not appropriate to directly fit a model to compare them across seed coat classes. The approach used here was to compare each treatment group to its corresponding dark

control group. The effect size (magnitude of observed differences) and the statistical significance observed in each category could then be compared. Comparisons were made between (i) whole light treated seeds vs whole seed control group; (ii) dehulled light treated seeds vs whole light treated seeds; and (iii) dehulled light treated seeds vs whole seed control group. These are presented for both UVA and visible light treatments. The first and second comparisons reveal the seed coat effect. The third comparison shows the effect of light exposure on the dehulled cotyledon of that genotype; it provided insight into what happens if the seed coat were not present. Comparing the color values of the dehulled seeds after treatment to the control, and not to their initial values (before treatments) factored out the color changes that might be due to other factors.

Figures 6.1 – 6.12 are plots of the mean color changes against treatment, with whiskers representing ± one standard deviation. Each plot is divided into three sections showing control, UVA treatment, and visible light treatment, respectively; this allows for specific comparisons to be made. The treatments in the second section (UVA) are compared against each other, and the control. The same applies to the third section (visible). See Tables D1 – C24 (Appendix D) for the effect size estimates and the respective p-values.

6.2.1 Light and Color of Green Cotyledon Lentils

Figures 6.1 to 6.4 are the mean plots for green cotyledon lentils. Tables D1 to D8 (Appendix D) show the result of multiple comparisons of the experimental groups. Figure 6.1 shows that in all the green lentil genotypes used for this test, the ΔL^* in dehulled-visible (D_VIS) light treated seeds were significantly higher ($p<0.01$) than those of whole control seeds. This agrees with earlier findings (Chapter Five) that exposure to visible light lightens green lentil cotyledons. There were significant differences between whole seeds and dehulled seeds under visible-light treatment (W_VIS and D_VIS) in all cases, which indicated that the presence of the seed coat reduces the effect. Further, looking at the comparisons between whole seeds exposed to visible light (W_VIS) and whole seeds kept under control (Control), there was a significant increase in L^*-values ($p<0.01$) of cotyledons when whole green lentils with green and grey zero tannin seed coats were exposed to visible light, whereas there were no such differences in the case of grey and black seed coat.

The L^*-values changes in the control groups were large and unexpected (especially in the varieties with black, grey, and grey zero tannin seed coats), unlike the variety (CDC QG-3) used for the study in chapter 5, where the L^*-values changes were close to zero. This indicates that these other varieties were more susceptible to color changes due to factors other than light treatment.

Under UVA treatment (Figure 6.1), the ΔL^* in the treated dehulled groups were not significantly different from those of treated whole seeds for all the seed coat types. Further, only the lentil variety with black seed coat showed a significant ($p<0.05$) difference between the dehulled treated and the control seeds. The effect size was small and comparable to other varieties; it was probably significant due to the tight within-sample variation in the case of this variety. UVA light also did not affect the cotyledon of any of the whole green lentils. These indicate that the presence of a black seed coat protected the seeds against color loss.

Effects of light treatment on the redness-greenness index (a^*) are shown in Figure 6.2. For the visible light treatment, dehulled samples for all seed-coat genotypes had significantly higher ($p<0.01$) Δa^* values than both treated and control whole-seed counterparts. This shows that exposure to visible light resulted in a reduction in the greenness of green lentils. It further shows that the presence of the seed coat reduced this effect. The cotyledons of whole lentils with grey, green, and zero tannin seed coats experienced significant ($p<0.01$) reduction in greenness under visible light, while whole lentil seeds with black seed coat did not. Under UVA treatment, the genotype with black seed coat had a significantly higher Δa^*in the dehulled treated group ($p<0.01$) than in the whole UVA treated and control seeds, respectively. The variety with green seed coats only showed significant differences in Δa^* between the dehulled treated group and control. The dehulled treated group of varieties with grey and grey zero tannin seed coat were not affected by UVA. UVA treatment had no significant effect on the a^*-values of the cotyledon of any of the whole green lentils.

In the a* -coordinate, the control groups of varieties with grey and grey zero tannin seed coats changed widely, indicating that they were more susceptible to color changes due to factors other than light treatment.

In the b^* coordinate (Figure 6.3), the visible light treatment caused significant negative changes in all the tested green lentil genotypes. The comparisons between whole seeds exposed to visible light and whole seeds under control show that there were significant reductions in b^*- values of cotyledons when whole green and grey lentils were exposed to visible light, whereas there were no such differences in the case of grey zero tannin and black seed coat. The result here was unexpected because zero tannin seed coat transmits more light than the tannin-containing types; however, the overall effect ΔE^* did follow the expected trend. Under UVA, none of the tested whole seeds were affected, although the dehulled seeds were highly susceptible.

The b^*-values tended to change in a positive direction in the control groups, largely and unexpectedly in all the varieties, unlike the variety (CDC QG-3) used for the study in chapter 5, where the b^*-values changes were close to zero. Exposure to light tended to switch the color changes in the negative direction, meaning the seeds tended to turn bluer. This indicates that in the absence of light, these varieties may become yellower over time, while exposure to light turns them bluer.

The total color differences, ΔE^* are shown in Figure 6.4. Overall, there were significant color change differences between dehulled-visible light treated lentil seeds and whole seeds (both visible light-treated and control) for all the lentil varieties. Thus, as reported in Chapter Five, exposure to visible light causes significant overall changes in the color of green cotyledon lentils. The seed coat offers some significant protection to the seeds. When whole seeds were exposed to visible light, the cotyledons of lentils with grey, green, and zero tannin seed coats experienced significant overall color changes, while those with black seed coat did not. The overall color changes in the three varieties were larger than the MPD threshold ($\Delta E^* \approx 2.3$) and, thus, perceptible (Mahy *et al.*, 1994). UVA only affected the varieties with black and green seed coats when dehulled; the seed coats in the whole seed groups significantly reduced this effect and the cotyledon of whole seeds was not significantly affected by UVA.

The overall color changes on the control group (with reference to before and after treatment) were large and above the MPD threshold of perceptibility, unlike the variety (CDC QG-3) used for the study in chapter 5. Much of these changes were contributed to by the large positive changes in the

b^*-values, which was opposite to the negative changes due to light. The factors and phenomena underlying these observations are open to further exploration.

The results showed that the cotyledon color of all tested genotypes of green cotyledon lentils was affected by visible light; some varieties were susceptible to UVA, while others were not. This suggests that there may be a genotype effect on the susceptibility of lentil cotyledons to light, which may be important to explore further. The seed coat of green cotyledon lentils was found to offer some protection to the seeds against photo-degradation, especially from UVA radiation, which was the least transmitted (Chapter Four).

Of the four seed coat types used for this study, only the black seed coat offered complete protection, resulting in no significant color change in any of the metrics. Normal grey offered some protection that resulted in no significant change in the L^*-values of green cotyledon lentil; however, the other coordinates and the overall color change were affected. Overall, the order of protective effect of lentil seed coat from least to highest was found to be as follows: grey zero tannin, green, normal grey, and black. This agrees with the findings of Chapter Four (Figure 4.10), which showed that zero tannin seed coat transmitted the highest amount of light, followed by green, grey, and black, in that order. The black seed coat transmitted no UV and visible light up to 600 nm; this explains why it offers the best protection against photodegradation of green cotyledon lentils.

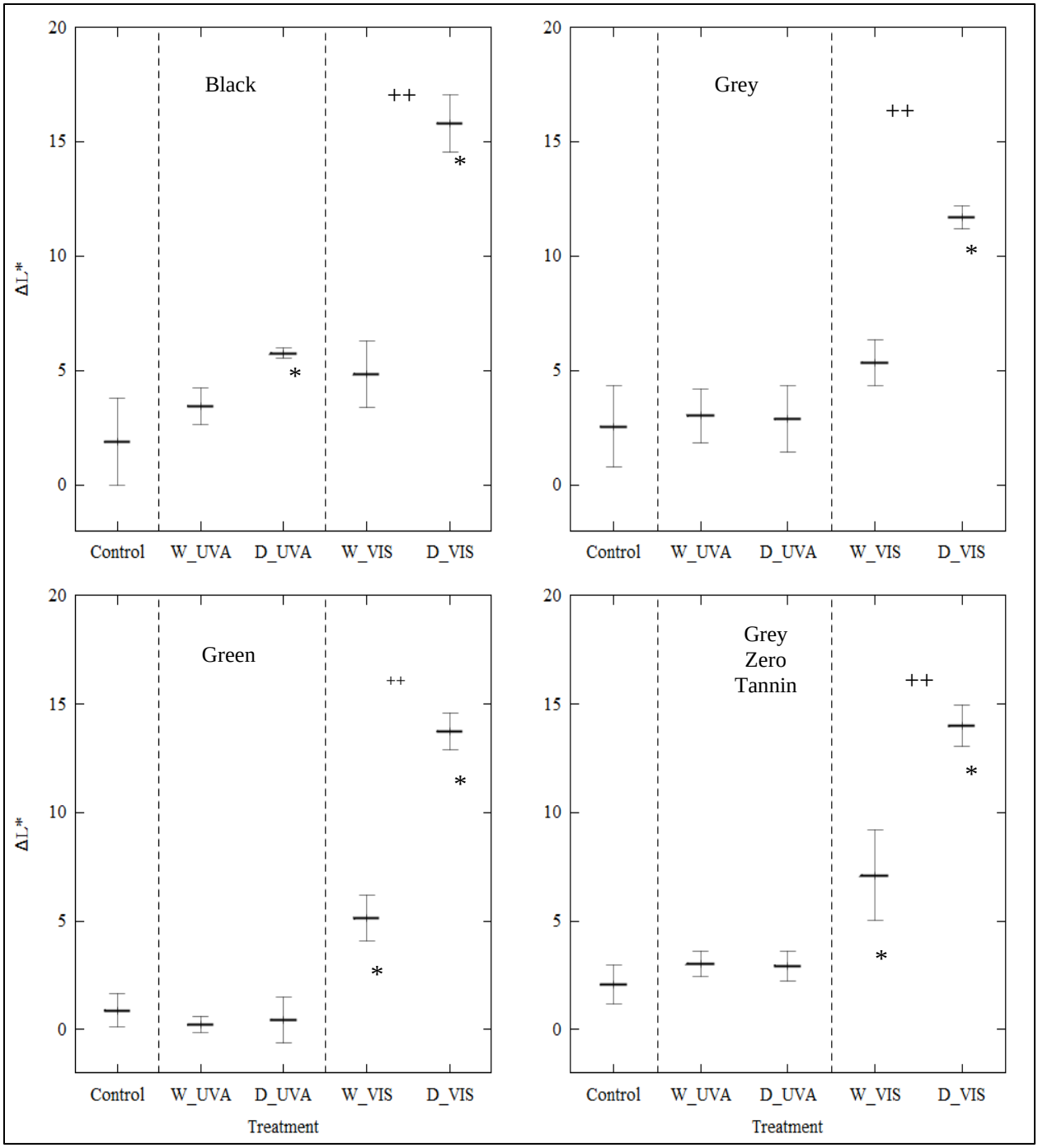

Figure 6.1: Changes in L^*-value in different seed coat classes and treatment groups (green lentils): The symbol "*" indicates that the treatment is significantly different from the whole-seed control, "**" above two UVA treatment groups indicate they are significantly different from each other, "++" above two visible light treatment groups indicate they are different from each other ($\boldsymbol{\alpha = 0.05}$) (x-axis labels: Control = whole seed – control; W_UVA = whole seed - UVA; D_UVA = dehulled -UVA; W_VIS = whole seed - visible; D_VIS = dehulled - visible).

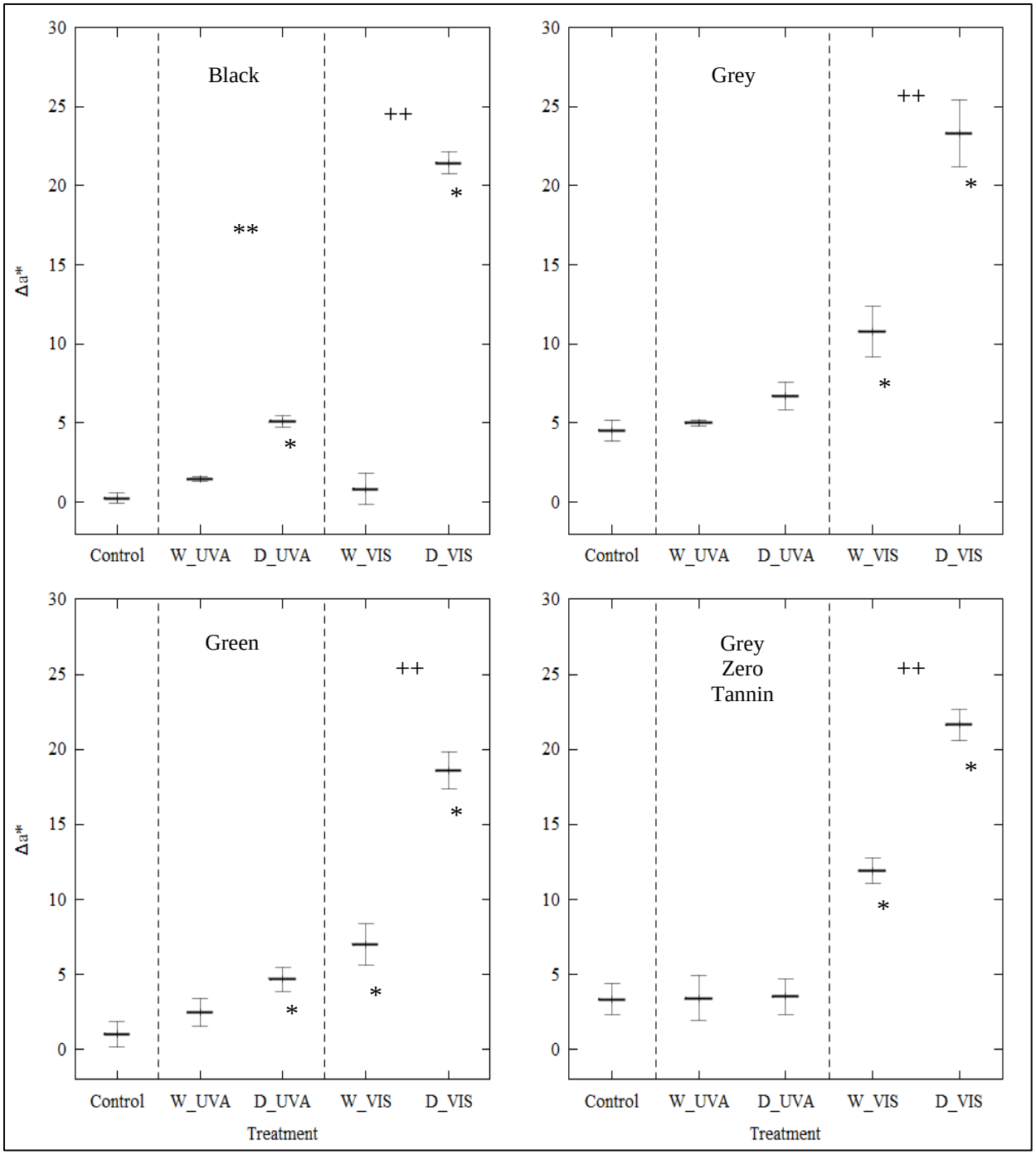

Figure 6.2: Changes in a^*-value in different seed coat classes and treatment groups (green Lentils): The symbol "*" indicates that the treatment is significantly different from control, "**" above two UVA treatment groups indicate they are significantly different from each other, "++" above two visible light treatment groups indicate they are different from each other ($\boldsymbol{\alpha = 0.05}$) (x-axis labels: Control = whole seed – control; W_UVA = whole seed - UVA; D_UVA = dehulled -UVA; W_VIS = whole seed - visible; D_VIS = dehulled - visible).

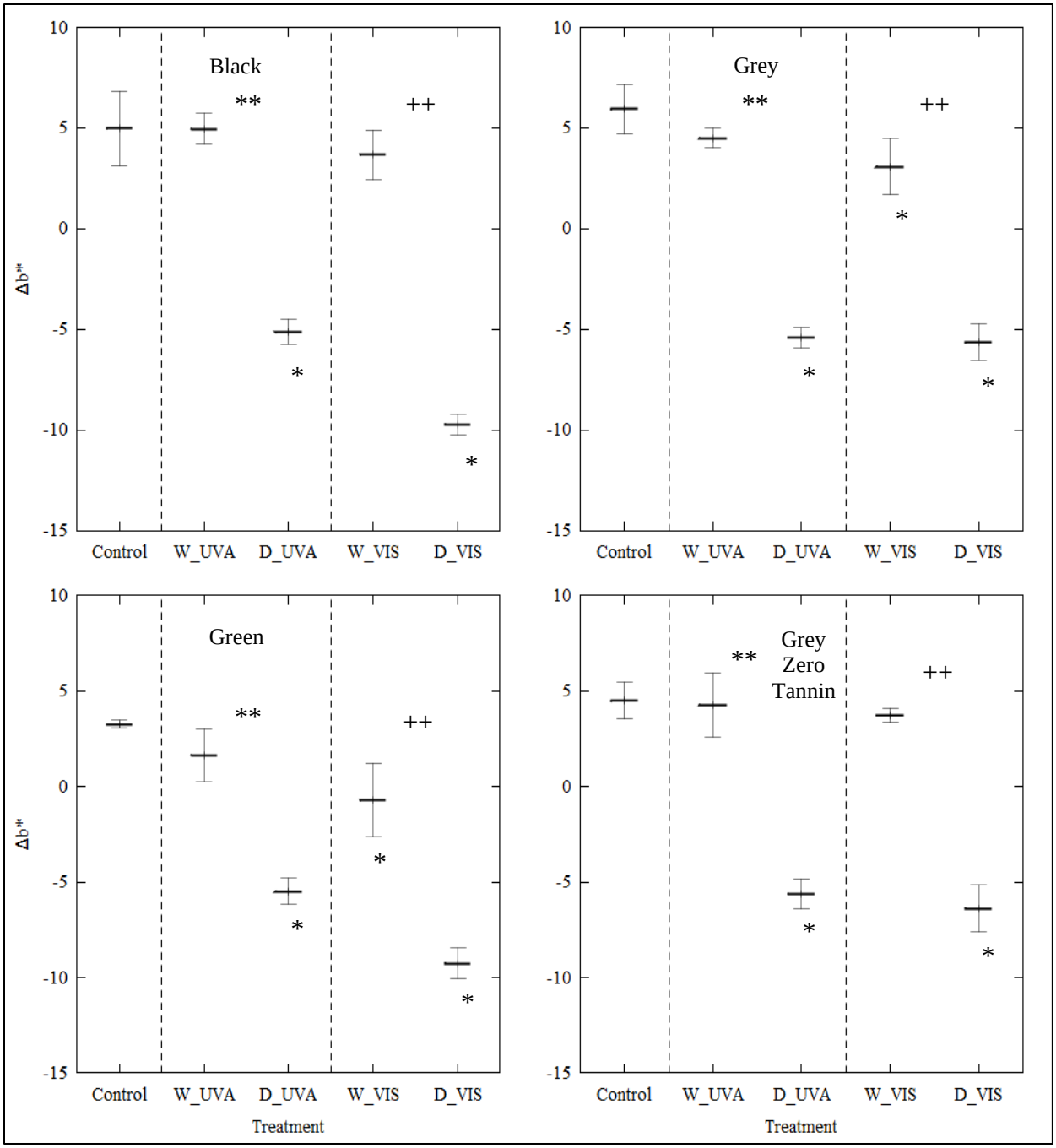

Figure 6.3: Changes in b^*-value in different seed coat classes and treatment groups (green lentils): The symbol "*" indicates that the treatment is significantly different from control; "**" above two UVA treatment groups indicates they are significantly different from each other; "++" above two visible light treatment groups indicates they are different from each other ($\boldsymbol{\alpha = 0.05}$) (Control = whole seed – control; W_UVA = whole seed - UVA; D_UVA = dehulled -UVA; W_VIS = whole seed - visible; D_VIS = dehulled - visible).

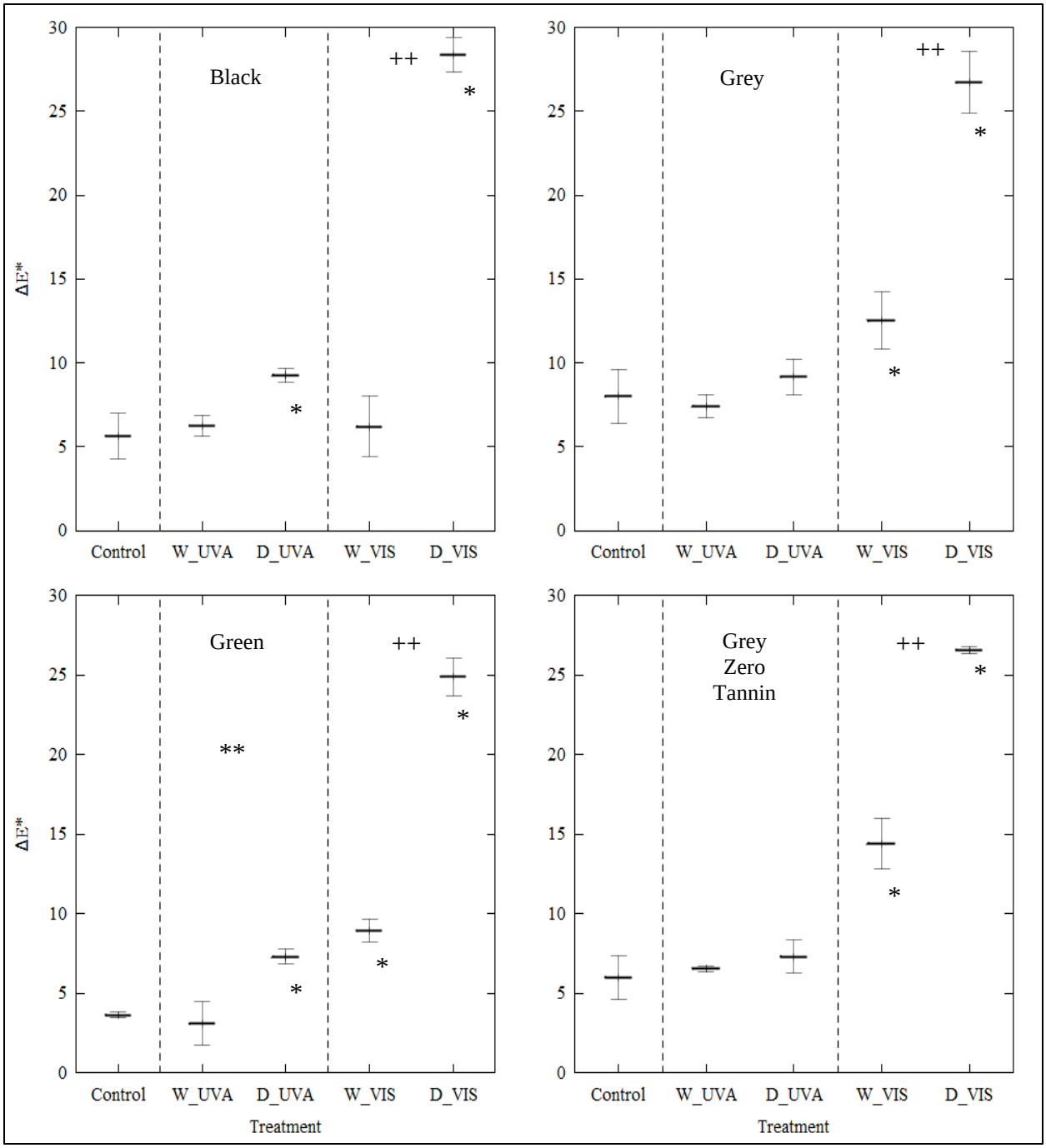

Figure 6.4: Changes in E^* in different seed coat classes and treatment groups (Green Lentils): The symbol "*" indicates that the treatment is significantly different from control, "**" above two UVA treatment groups indicate they are significantly different from each other, "++" above two visible light treatment groups indicate they are different from each other ($\boldsymbol{\alpha = 0.05}$) (x-axis labels: Control = whole seed – control; W_UVA = whole seed - UVA; D_UVA = dehulled -UVA; W_VIS = whole seed - visible; D_VIS = dehulled - visible).

6.2.2 Light and Color of Red Cotyledon Lentils

Figures 6.5 to 6.8 show the changes in color coordinates (ΔL^*, Δa^* and Δb^*) and the overall color difference ΔE^* experienced by the different experimental groups of red cotyledon lentils. The results of multiple comparisons (from GLM Tukey tests) of the experimental groups are shown in Tables D9 to D16 (Appendix D). Figure 6.5 shows that in their dehulled form the lightness, L^* − values of red lentils from varieties that had black, grey, and zero tannin seed coats were not affected by visible light; however, those from green and grey zero tannin seed coat classes were slightly (with small effect sizes) ($p<0.05$) affected. For the two varieties whose dehulled seeds (cotyledon) were slightly affected by visible light (with green and grey zero tannin seed coat), a comparison of whole treated and control seeds shows that there were no significant L^*-values changes in the cotyledon of whole seeds due to the visible light treatment. This means that the presence of the seed coat effectively removed the slight effect of visible light on red lentils.

The L^* −values of dehulled red lentil varieties with black, green and grey zero tannin seed coats were slightly (with minute effect sizes, as indicated by the estimates) affected ($p<0.05$) by UVA treatment, while those with grey and colorless zero tannin seed coats were not (Figure 6.5). A comparison of whole treated and control seeds shows that there were no significant L^* − values changes in the cotyledon of whole seeds due to the UVA treatment.

In the a^*-coordinate, visible light and UVA treatment had no significant effect on the red cotyledon lentils (Figure 6.6). With no significant effect of light on the $a*$-values of red lentils, there is no gain giving any consideration to the effect of seed coat in this coordinate.

Figure 6.7 shows that the b^*-values of red lentils from all the varieties (having black, grey, green, grey zero tannin and colorless zero tannin seed coats) were affected ($p<0.05$) by visible light and UVA treatment. The comparison of whole treated and control seeds shows that only colorless zero tannin seed coat (which was found to have the highest transmission properties (Chapter 4) allowed significant b^*-values changes in the cotyledon of whole seeds under visible light. For the UVA treatment, none of the observed differences between whole treated seed and control were statistically significant, meaning that all seed coat types, including colorless zero tannin, effectively protected against UVA.

The total color changes, ΔE*, in the experimental groups of red lentils are shown in Figure 6.8. Overall, there were significant ($p<0.05$) color changes between dehulled visible light treated lentil seeds and whole seeds (control) for red lentil varieties with green, grey, and grey zero tannin seed coats; however, the effect sizes were small. The genotypes with black and colorless zero tannin seed coats were, in their dehulled form, not significantly affected by visible light. Further, in terms of the overall color change, there were no significant differences between treated whole seeds and control in any of the tested genotypes. Dehulled UVA treated seeds did not show any significant color changes compared to whole seeds under UVA and control, meaning UVA did not have any effect in the overall color of red lentil cotyledons.

These results agree with the findings of Chapter Five, which showed that red cotyledon lentils generally have a high level of colorfastness when exposed to light, unlike green lentils. In some color coordinates, and, in terms of overall color change, some of the dehulled samples experienced statistically significant effects. However, the effect sizes were mostly too small to raise any concern; they were lower than the MPD threshold ($\Delta E^* \approx 2.3$) and, thus, visually not perceptible (Mahy *et al.*, 1994), It is important to note that statistical significance alone does not determine whether we should be interested in an effect; only a notably large effect size that is statistically significant is of interest. Moreover, with the presence of the seed coat, these small effects were no longer observed on the cotyledon; none of the whole seeds treated with either UVA or full-visible light experienced an overall color changes that were higher than the MPD threshold ($\Delta E^* \approx 2.3$) and, thus, the color changes were perceptible (both as indicated by the MPD and by visual observation.

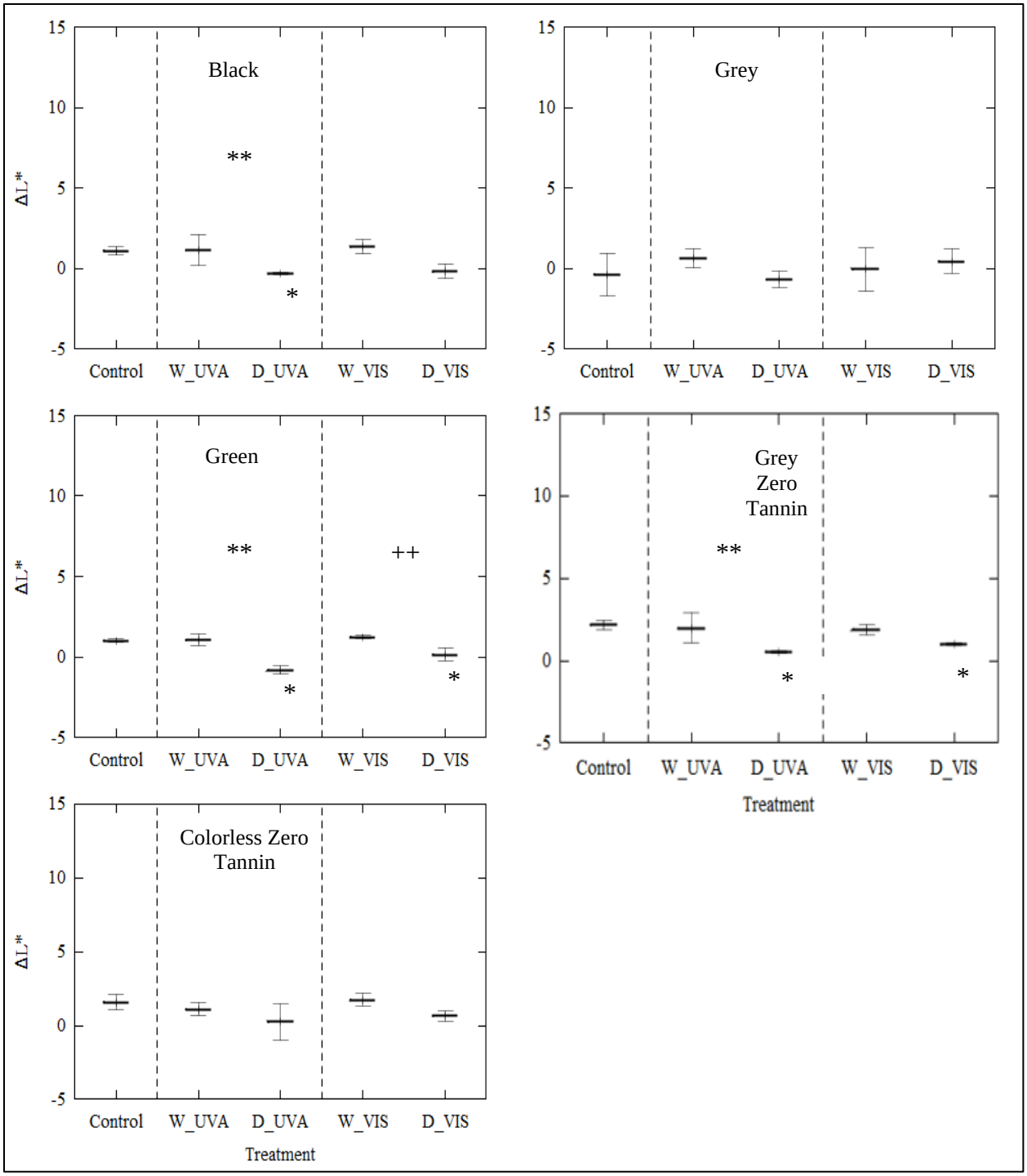

Figure 6.5: Changes in L^*-values in different seed coat classes and treatment groups (red lentils): The symbol "*" indicates that the treatment is significantly different from control, "**" above two UVA treatment groups indicates they are significantly different from each other, "++" above two visible light treatment groups indicates they are different ($\boldsymbol{\alpha = 0.05}$).

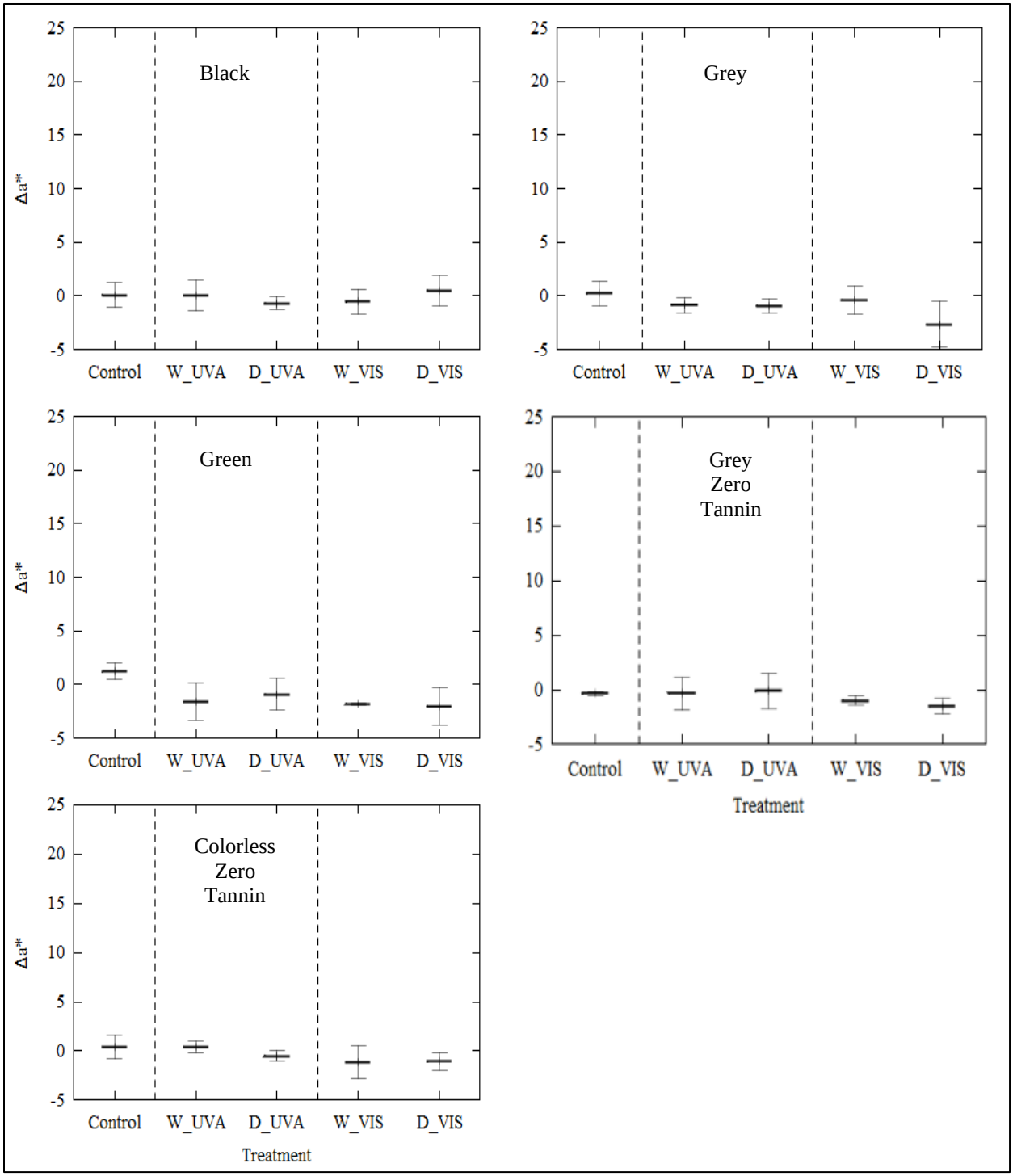

Figure 6.6: Changes in a^*-values in different seed coat classes and treatment groups (red lentils): The symbol "*" indicates that the treatment is significantly different from control, "**" above two UVA treatment groups indicates they are significantly different from each other, "++" above two visible light treatment groups indicates they are different ($\boldsymbol{\alpha = 0.05}$).

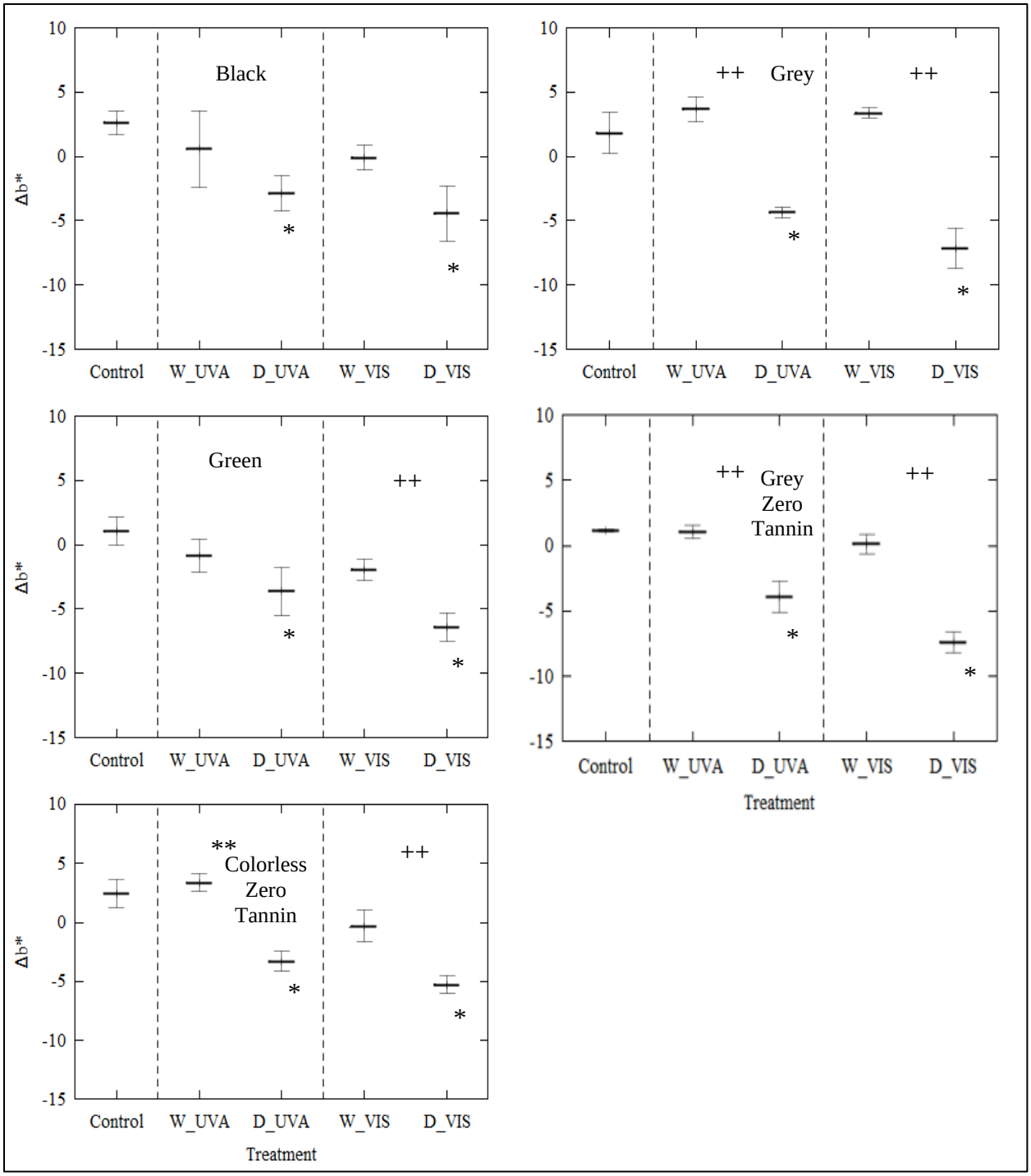

Figure 6.7: Changes in b^*-values in different seed coat classes and treatment groups (red lentils): The symbol "*" indicates that the treatment is significantly different from control, "**" above two UVA treatment groups indicates they are significantly different from each other, "++" above two visible light treatment groups indicates they are different ($\boldsymbol{\alpha = 0.05}$).

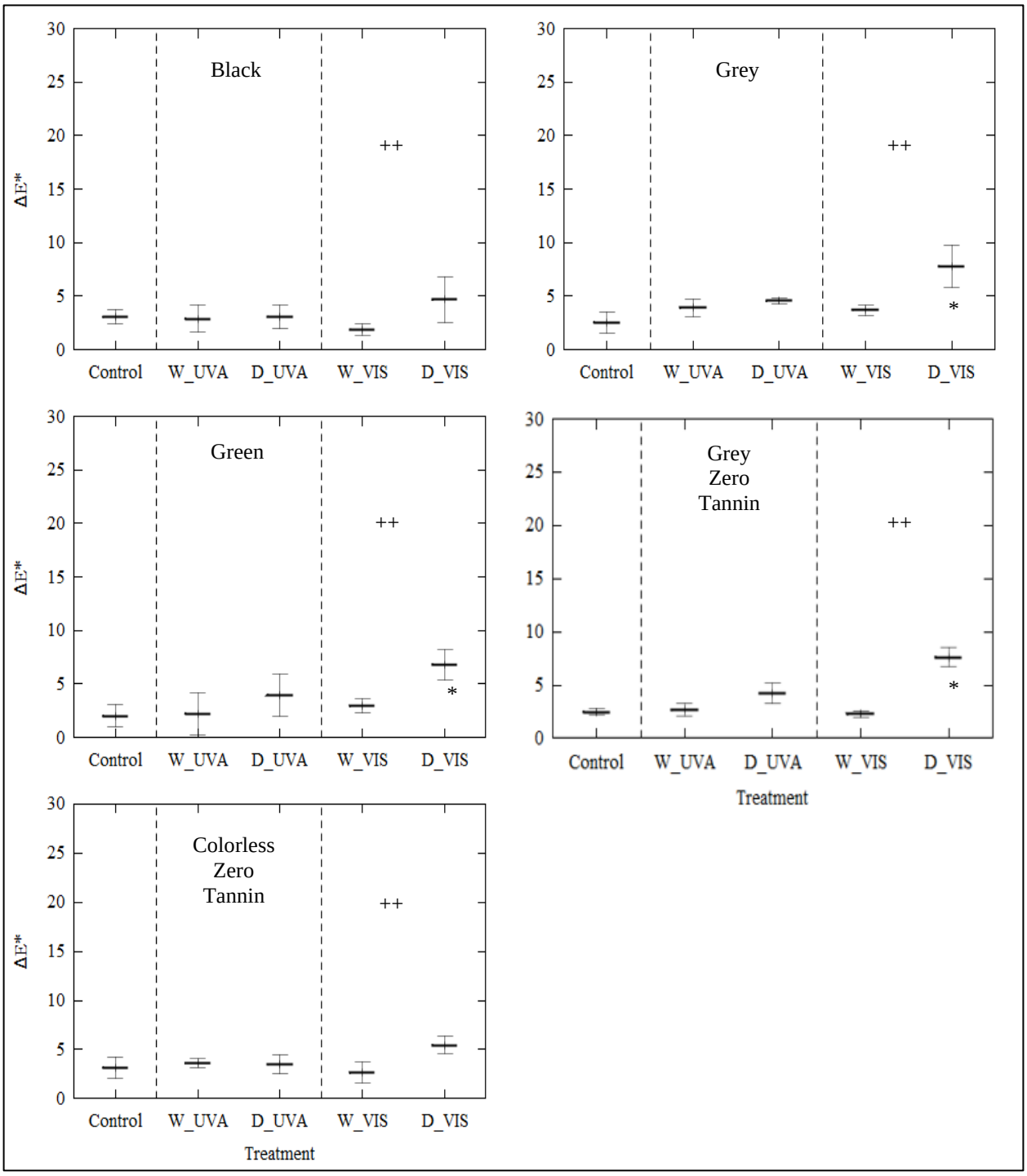

Figure 6.8: Changes in E^* in different seed coat classes and treatment groups (red lentils): The symbol "*" indicates that the treatment is significantly different from control, "**" above two UVA treatment groups indicates they are significantly different from each other, "++" above two visible light treatment groups indicates they are different ($\boldsymbol{\alpha = 0.05}$).

6.2.3 Light and Color of Yellow Cotyledon Lentils

Figures 6.9 – 6.12 show the color changes ΔL^*, Δa^* and Δb, and the overall color difference ΔE^* experienced by the different experimental groups (whole seed - visible, whole seed - control, whole seed - UVA, dehulled - UVA, and dehulled - visible) of yellow cotyledon lentils. Tables D17 to D24 (Appendix D) show the results of multiple comparisons (from GLM Tukey tests) of the experimental groups. Figure 6.9 reveals that, in the dehulled form, the lightness, L^* – values of yellow lentils from only varieties with grey and grey zero tannin seed coat classes were significantly ($p<0.05$) affected by visible light. These effects were slight, and a comparison of whole treated and control seeds indicated no significant L^*-values changes in the cotyledon of whole seeds.

Dehulled seeds from varieties that had black, green, and colorless zero tannin seed coats were significantly affected by UVA ($p<0.05$); however, there were no significant L^*-values changes in the cotyledon of the whole seeds. The presence of the seed coats effectively removed the slight lightening effect of visible light and UVA on yellow cotyledon lentils. In all seed coat classes, there were no significant differences in lightness values of whole seeds and dehulled seeds under visible light and UVA.

In the a^*-coordinate (Figure 6.10), under visible light treatment, the indicated slight differences between dehulled seeds and their controls were statistically significant for varieties with grey and grey zero tannin seed coat, but not significant for those with black, green and colorless zero tannin seed coat. Under UVA treatment, differences between dehulled seeds and their controls were statistically significant for varieties with green and colorless zero tannin seed coat, but not significant for those with black, grey, and grey zero tannin seed coat. Further, there were no significant differences between the treated whole seeds from the affected classes and their control, which means that the slight effect of light on $a*$-values were contained by seed coat presence.

Figure 6.11 shows that the yellowness (b^*-values) of yellow cotyledon lentils from all tested genotypes were significantly affected by both visible light and UVA treatments. In all cases, the changes were negative, indicating a significant reduction in yellowness. When whole treated and control seeds were compared, there was a significant reduction in yellowness ($p<0.01$) in the

colorless zero-tannin seed coat genotype due to visible light, but not in others. Thus, the effect of light exposure on b^*-values were effectively contained by seed coat presence in all cases, except colorless zero tannin (which, according to Chapter 4 has the highest light transmission properties).

Figure 6.12 shows that, in terms of the overall color difference, ΔE^*, there were significant color changes between dehulled treated lentil seeds and whole seeds (control) due to visible light for all the tested genotypes. Unlike in the case of red lentils, the effect sizes were higher. Under UVA treatment, there were significant ($p<0.05$) color changes between dehulled, visible light treated lentil seeds and whole seeds (control) for yellow lentil varieties with green, grey, and grey zero tannin seed coat. In terms of the overall color change, all the seed coat types tested offer significant protection to the seeds, as there were no significant differences between treated whole seeds and control.

The results show that the colorfastness of yellow cotyledon lentils is generally higher than that of green cotyledon lentils, but lower than red. In some color coordinates, and overall color change, some of the dehulled samples experienced statistically significant effects; the effect sizes were considerable in the b^*-coordinate.

Notably, with the presence of the seed coat, these effects were largely contained. However, whole seeds with colorless zero tannin seed coat experienced a significant reduction in yellowness (tended to become more bluish) due to UVA and visible light treatment. These results also serve as a confirmation of the findings of Chapter Five, which showed that de-hulled yellow lentils were not as susceptible to light as green lentils. The effect sizes observed in that chapter were also considerable, but small compared to green lentil cotyledons, although some of the observations were statistically significant.

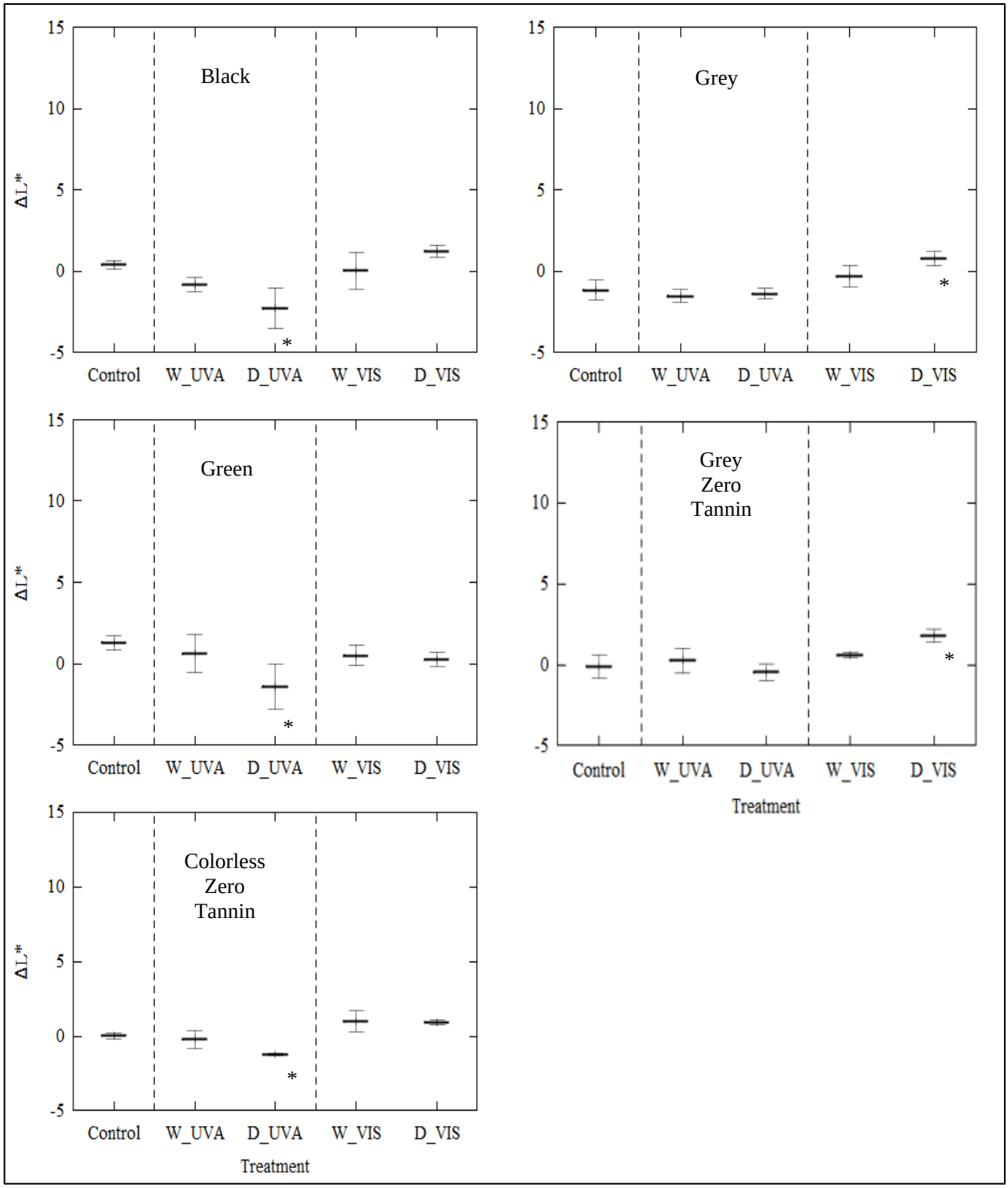

Figure 6.9: Changes in L*-values in different seed coat classes and treatment groups (yellow lentils): The symbol "*" indicates that the treatment is significantly different from control, "**" above two UVA treatment groups indicates they are significantly different from each other, "++" above two visible light treatment groups indicates they are different ($\boldsymbol{\alpha = 0.05}$).

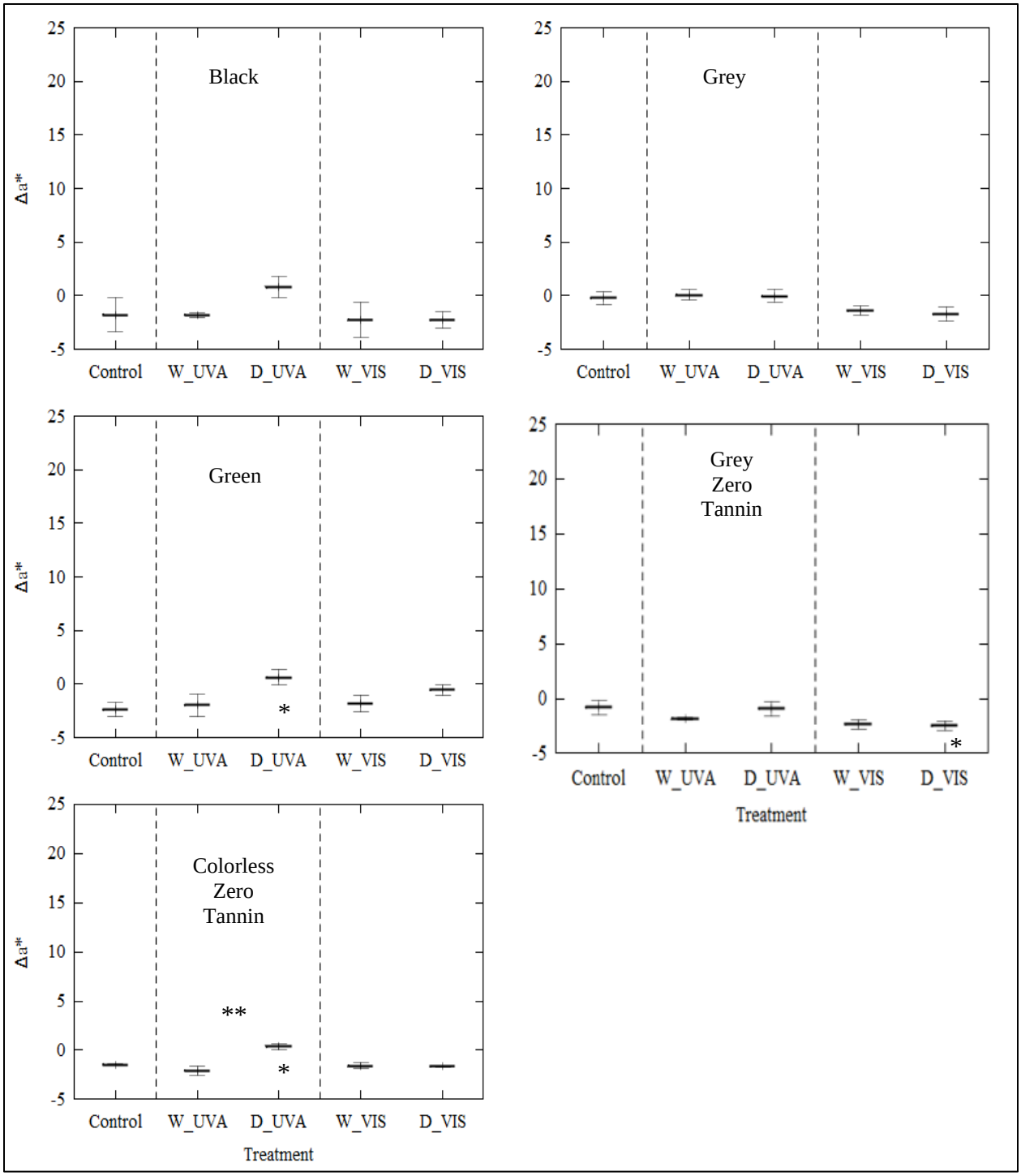

Figure 6.10: Changes in a^*-values in different seed coat classes and treatment groups (yellow lentils): The symbol "*" indicates that the treatment is significantly different from control, "**" above two UVA treatment groups indicates they are significantly different from each other, "++" above two visible light treatment groups indicates they are different ($\boldsymbol{\alpha = 0.05}$).

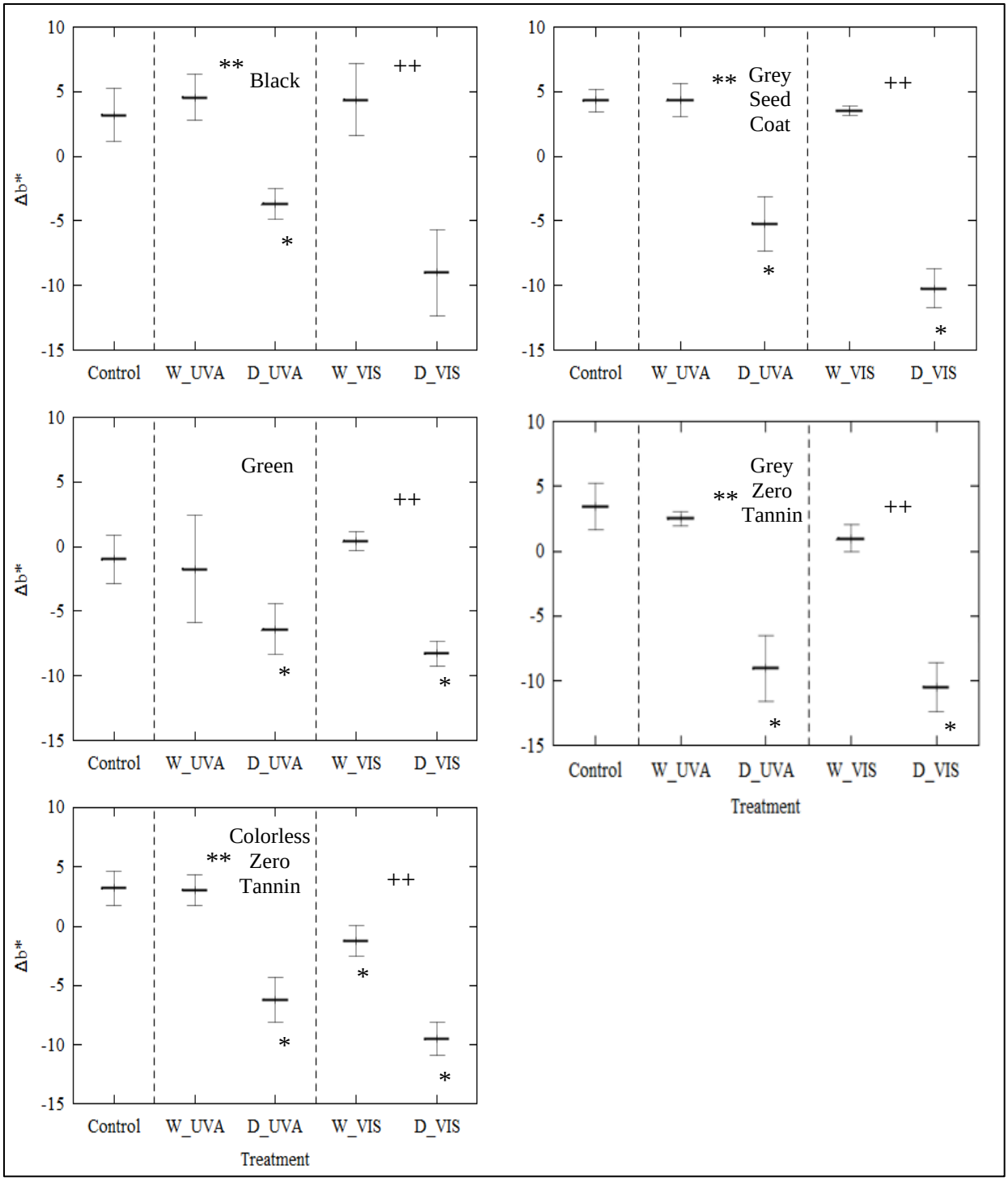

Figure 6.11: Changes in b^*-values in different seed coat classes and treatment groups (yellow lentils): The symbol "*" indicates that the treatment is significantly different from control, "**" above two UVA treatment groups indicates they are significantly different from each other, "++" above two visible light treatment groups indicates they are different ($\boldsymbol{\alpha = 0.05}$).

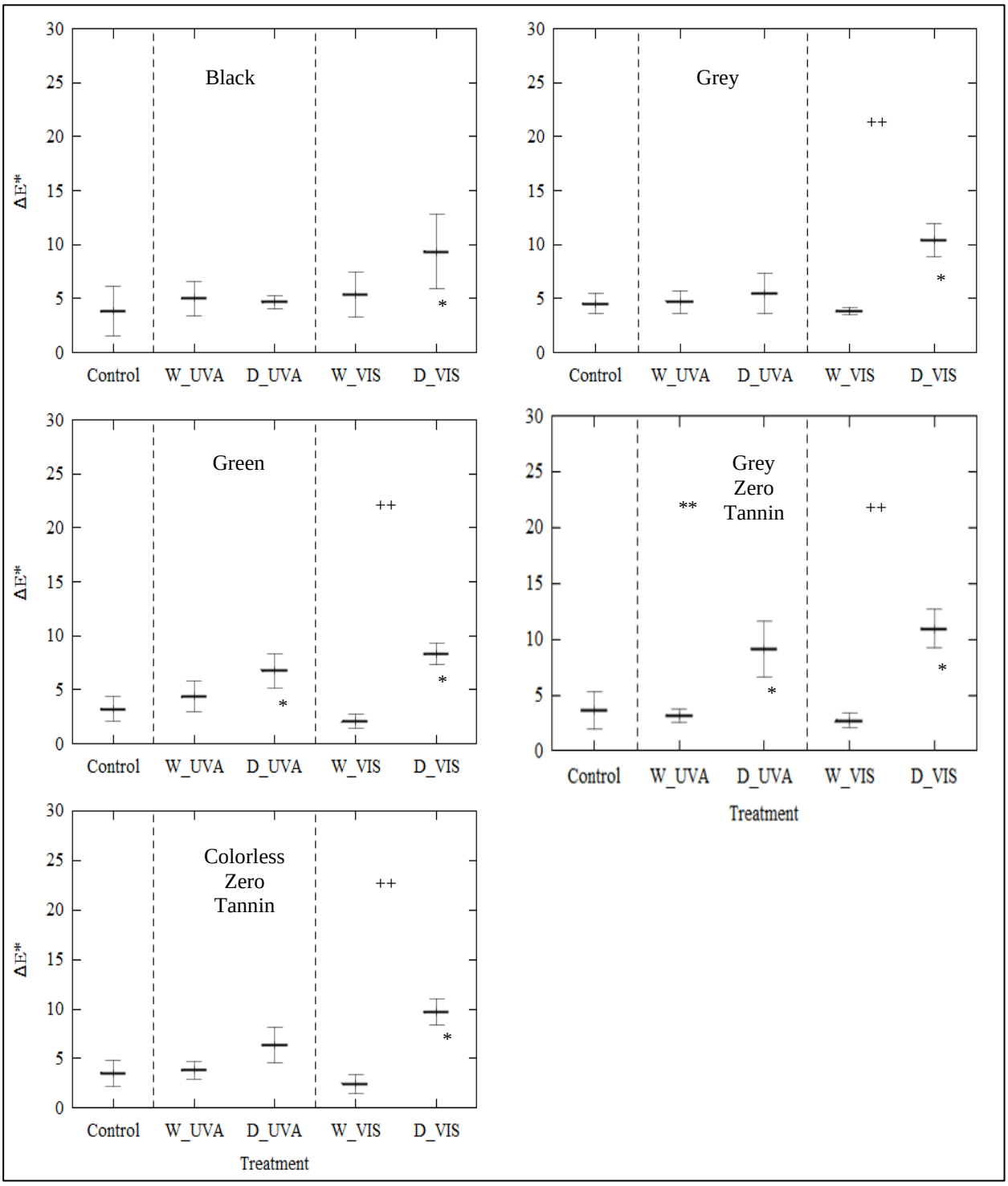

Figure 6.12: Changes in E^* in different seed coat classes (yellow lentils): The symbol "*" indicates that the treatment is significantly different from control; "**" above two UVA treatment groups indicates they are significantly different from each other; "++" above two visible light treatment groups indicates they are different ($\boldsymbol{\alpha = 0.05}$).

6.3 Summary/General Discussion and Conclusion

This chapter answers the fourth research question: what influence does seed coat have on cotyledon color retention, and which seed coat types have significant protective effects? It was not possible to obtain samples of the same genotype with different seed coat types, and some varietal differences in the response of dehulled lentils were observed. Therefore, direct comparisons of color changes between genotypes could not be made using ANOVA/GLM. The approach was to carry out multiple comparisons of dehulled seeds treated with light versus whole seeds kept under dark control, dehulled seeds treated with light versus whole seeds treated with light, and whole seeds treated with light versus whole seeds kept under dark control.

For the green cotyledon class, significant color changes (L*, a*, b*, and overall color change) were found in dehulled seeds (cotyledons) under visible light (with large effect sizes) and UVA (with smaller effect sizes). It was found that the seed coat of green lentils offers some protection to the seeds against photo-degradation, especially from UVA radiation. However, out of the four seed coat types used for the study (black, green, normal grey, and grey zero tannin), only the black seed coat offered complete protection, which resulted in no significant color change in any of the coordinates, or the overall color change. Overall, the black seed coat offered the best protection, followed by grey, green, and colorless zero tannin, in that order.

The red cotyledon class generally has a high level of colorfastness when exposed to light, unlike green lentils. Some of the dehulled samples experienced statistically significant effects in some coordinates and/or overall color change. However, the effect sizes were generally too small to raise any concern. Moreover, the slight effects were not observed with the presence of seed coat in cases of black, green, and normal grey, and grey zero tannin seed coat types. Under visible light, whole red lentils with colorless zero tannin seed coat were affected in the b^* - coordinate only.

Finally, the yellow cotyledon class proved to be more susceptible to light exposure than red, but less susceptible compared to green. In some color coordinates, as well as in terms of overall color change, some of the dehulled samples experienced statistically significant effects. However, with the presence of the seed coat, these effects were no longer observed in most cases. The exception was the colorless zero-tannin genotype, which was affected in the b*-coordinate only.

Chapter 7 : GENERAL DISCUSSION, CONCLUSIONS, AND FUTURE RESEARCH

For Canada to maintain its market share as the world's largest exporter of lentils, there is a need to ensure that the product is of top quality. The influence of light on the quality of the Canadian lentils is of concern, especially during the period after maturation, when the crop is swathed or desiccated with chemicals and allowed to remain in the field to dry. During this period, there may be a loss of quality due to light exposure, which is referred to as photodegradation. In the red lentil market, cotyledon color is one of the most important market criteria. Although the concern about cotyledon color is mostly associated with red lentils (which is the most dehulled class of lentils), it was also important to consider the influence of light exposure on the green and yellow cotyledon classes. This is because, regardless of type, color correlates well with other quality attributes of a commodity; the loss of color may indicate a loss in nutrients and secondary metabolites.

The foregoing would be of concern if lentil cotyledon is susceptible to photodegradation and if a high amount of light penetrates the seed coat. Furthermore, the seed coat's ability to offer protection to the underlying cotyledon would depend on its optical properties. For this reason, an investigation of the optical properties of the seed coat of different lentil genotypes was undertaken. Moreover, optical properties information might find applications in many areas, such as pattern recognition and classification of materials, disease detection, quality determination, etc.

7.1 Discussion

This thesis represents a research effort to characterize the different kinds of lentil seed coats in terms of their light transmission, study color degradation in lentil seeds exposed to different wavelengths of light, study the effect of light exposure of whole lentil seeds, and the influence of seed coat presence and type on the amount of color loss in the cotyledon.

The first part of the study involved developing a suitable instrumentation system for measuring the optical properties of the lentil seed coats. The constraints associated with the small size and brittleness of lentil seed coats made them unamenable for measurement using conventional

spectrophotometers. An optical fiber photometer was set up using available and fabricated optics and spectroscopy components and a method validation procedure found the system satisfactory for the study.

In the second part of the study, light transmission and reflectivity properties of seed coats from 20 lentil genotypes, representing the various seed coat colors, were measured using the fiber optic system (from 250 to 850 nm). It was found that all the tested seed coat types, except colorless zero tannin, showed no detectable percentage transmission of shorter wavelength UV light (UVB and UVC; 250-415 nm). Published literature reported that this is the wavelength range most responsible for photochemical effect in materials. The focus of the remaining work was therefore directed toward what, if any, photodegradation resulted from the UVA and visible spectra, and the potential protective effects of the seed coat in these ranges. Black seed coats transmitted only visible light (from 650 nm) and NIR. Longer wavelength UVA and visible light were transmitted by the rest of the seed coat types. Further, the transmission properties of selected seed coat types were compared using ANOVA via GLM and a post-hoc test. Real overall differences in UV, VIS, and NIR transmission among seed coats of lentil market classes were found. Multiple comparisons showed that some of the phenotypes were optically different from each other, while others were not.

The third part of the thesis investigated the effect of light in the UVA and visible ranges on lentil cotyledons. It was established that exposure of green lentil cotyledons to all forms of light (UVA, blue, green, red, and full visible spectrum) resulted in photodegradation, with large effect sizes. For the red and yellow lentil classes, there were some effect in certain color coordinates/overall color change, but the effect sizes were small. Notably, exposure to red light caused an increase in the redness of red lentil cotyledon in the genotype tested.

Based on the MPD threshold ($\Delta E \approx 2.3$), the light-treated green cotyledons were perceptually different from control in all cases. In the case of red lentils, there were visually noticeable differences between treated seeds and control under red and full-visible light treatments, in the case of yellow lentils, only seeds exposed to blue light were perceptually different from control.

These visually noticeable differences underscore the need to store dehulled lentil seeds away from light.

The final part of the thesis investigated whether the light transmitted through the various seed coat types would affect the underlying cotyledon color of whole lentils. It was found that light exposure significantly affects the color of the underlying cotyledon of green lentils. Of the four seed coat types tested (black, green, normal grey, and grey zero tannin), only the black seed coat protected the cotyledon such that no significant color changes were observed when the seeds were subsequently dehulled and their color measured. Overall, the black seed coat offered the best protection, followed by grey, green, and colorless zero tannin, in that order. This pattern agreed with the transmission properties of the seed coat types; the lower the transmission properties of the seed coat type, the lower the amount of color loss experienced by the underlying cotyledon when exposed to light and vice versa.

In the case of red cotyledon class, the effect sizes on dehulled seeds were generally too small to raise serious concern, and there were no significant effects with the presence of seed coats in cases of black, green, grey, and normal grey seed coat types. However, whole red lentils with colorless zero tannin seed coat exposed to visible light showed a statistically significant color difference from control in the b^*-coordinate only. The yellow cotyledon class were more susceptible to light exposure than red, but less susceptible compared to green. However, the presence of the seed coat, in most cases, effectively removed any effect of light on the cotyledon. Given these observations with red and yellow lentils, the best way to compare the light protecting effect of different kinds of seed coat is by using the case of green lentils, where the effect sizes were large and consistent.

7.2 Conclusions

The optical properties of single lentil seed coats (or seeds) are best obtained using a fiber optics spectrometer adapted for that purpose. This helps overcome constraints such as the small size of the sample and its brittleness. The specially designed sample holder allows the material to sit horizontally without cracking/breaking, while the thin fiber directs a narrow beam of light on it. Light transmission and reflectivity of the lentil seed coat were successfully obtained using this method. Further, the different seed coat types of lentils differ in the way they transmit light. More

so, real patterns exist in the light reflectivity properties of the lentil seed coat, and this may be useful in lentil market class identification, disease detection, and quality prediction in lentil seeds.

Furthermore, exposure to light has some significant effect on the cotyledon of green, red, and yellow lentils. The effect sizes are considerably high in green lentils. Yellow lentils experience smaller effect sizes, while red lentils experience the least.

Some whole (non-dehulled) green cotyledon lentils experience color loss in the underlying cotyledon when they are exposed to light. The amount of color loss depended on the seed coat type and the pattern agreed with the light transmission properties of the seed coat. The black seed coat, which has minimal light transmission in the UV-VIS region, offered protection that resulted in no significant color loss. The amount of color changes in the remaining seed coat classes were in the order of their light transmission. Thus, breeding programs that aim to protect the quality of lentil cotyledon can make the selection of seed coat type based on their light transmission properties.

Red and yellow lentil classes have high levels of colorfastness, and their seed coats can successfully protect the cotyledon from these minimal effects. Thus, breeding for seed coat protection may not improve the cotyledon color of Canadian red lentils (the most de-hulled market class).

7.3 Future Research

Based on the findings of this research, the following future studies are recommended:

- Application of spectroscopy and machine learning for lentil market class classification. This work may lead to the development of a fast method/tools of determining the market class of a lentil variety; for example, objectively determining if a sample belongs to zero tannin seed coat class or not.
- Application of spectroscopy and machine learning for detection of diseases (such as anthracnose or stemphylium blight) in lentil seeds, as well as for prediction of milling/de-hulling quality of lentil seeds. This work may lead to the development of tools for lentil quality testing.

- Effect of light exposure on biochemical quality (such as polyphenol profiles) of lentil seeds by liquid chromatography-mass spectrometry (LC-MS). It may be interesting to see how exposure of whole lentils to light affects the biochemistry/polyphenol profiles of the cotyledon. This may guide decisions on breeding for seed coat protection.
- Effect of high intensity, long-time red light exposure on quality of red lentil cotyledon.
- Effect of NIR radiation on the quality of lentil cotyledon.

REFERENCES

Adascan. (2017). Canadian Green and Red Lentils Exporter & Supplier - Adascan Grain Corporation. Online at: *http://www.adascan.ca/products/pulses-crops/lentils/.* Accessed: October 9, 2018.

Amarowicz, R., Estrella, I., Hernández, T., Dueñas, M., Troszyńska, A., Kosińska, A., & Pegg, R. B. (2009). Antioxidant activity of a red lentil extract and its fractions. *International Journal of Molecular Sciences*, *10*(12), 5513–5527. DOI: https://doi.org/10.3390/ijms10125513.

Asim, M. U., & Kasi, R. (2018). The effects of ultraviolet B (UVB) irradiation on color quality and decay rate of Capia pepper during postharvest storage. *Food Science and Technology*, *38*(2), 363-368. DOI: https://doi.org/https://doi.org/10.1590/1678-457x.05817.

Auguie, B. (2017). gridExtra: functions in Grid graphics. R Package Version 2.3. *CRAN PROJECT*.

B&W Tek. (2019). Spectrometer Knowledge - Part 8: Fiber Optic Probes. Online at: https://bwtek.com/spectrometer-part-8-fiber-optic-probes/. Accessed: April 8, 2019.

Boye, J. I. (2015). Lentil. The Canadian Encyclopedia. Online at: https://www.thecanadianencyclopedia.ca/en/article/lentil. Accessed: December 4, 2018.

Büchert, A. M., Gómez Lobato, M. E., Villarreal, N. M., Civello, P. M., & Martínez, G. A. (2011). Effect of visible light treatments on postharvest senescence of broccoli (Brassica oleracea L.). *Journal of the Science of Food and Agriculture*, 91 (2), 355-361. DOI: https://doi.org/10.1002/jsfa.4193.

CFIA. (n.d.). Varieties of Crop Kinds Registered in Canada Lookup Results - Canadian Food Inspection Agency. Online at: https://www.inspection.gc.ca/active/netapp/regvar/regvar_resultse.aspx?lang=e&Reg=&Kind=Lentil&SubKind=&Name=&PNTRadio=All&Rep=&Status=&startDate=&endDate=&btn_submit=Submit. Accessed: May 8, 2020.

Cleland, T. M. (1937). A practical description of the Munsell color system : with suggestions for its use. Online at: https://www.worldcat.org/title/practical-description-of-the-munsell-color-system-with-suggestions-for-its-use/oclc/10527942. Accessed: November 10, 2019.

Davey, B. F. (2007). Green Seed Coat Color Retention in Lentil (M.Sc. Thesis). University of Saskatchewan, Saskatoon, Canada.

Delwiche, S. R., & Norris, K. H. (1993). Classification of Hard Red Wheat By Near-Infrared Diffuse Reflectance Spectroscopy. *Cereal Chemistry*, 70 (1), 29-35.

Diffey, B. L. (2002). Sources and measurement of ultraviolet radiation. *Methods*. 28(1):4-13.

doi: 10.1016/s1046-2023(02)00204-9.

Donskikh, A. O., Minakov, D. A., Sirota, A. A., & Shulgin, V. A. (2017). Methods of analysis and classification of the components of grain mixtures based on measuring the reflection and transmission spectra. *Scientific Study and Research: Chemistry and Chemical Engineering, Biotechnology, Food Industry*, 18 (3), 291-302.

Duncan, S. E., & Chang, H. (2012). Implications of Light Energy on Food Quality and Packaging Selection. In *Advances in Food and Nutrition Research* (pp. 25–49). Elsevier Inc.

Durán, L., & Calvo. (2004). Optical Properties of Foods. In *Encyclopedia of Life Support Systems (EOLSS)*. Food Engineering – Vol. I. United Nations Educational Scientific and Cultural Organization.

Emami, M., & Sharma, B. (1996). Digenic Control of Cotyledon Colour in Lentil (Lens culinaris). *Indian Journal of Genetics, 56*(3), 357–361.

Engineering Toolbox. (2014). Saturated Salt Solutions and Air Humidity. Online at: *https://www.engineeringtoolbox.com/salt-humidity-d_1887.html.* Accessed: July 1, 2020.

Erdoğan, C. (2015). Genetic characterization and cotyledon color in lentil. *Chilean Journal of Agricultural Research,*18 (3), 291-302.

Eu, M. T. (1997). Reflectance characteristics of bulk grains using a spectrophotometer (Master of Science Thesis). University of Manitoba, Winnipeg, Canada.

El-Mesery, H., Mao, H., & Abomohra, A. (2019). Applications of Non-destructive Technologies for Agricultural and Food Products Quality Inspection. *Sensors*, *19*(4), 846-869. https://doi.org/https://doi.org/10.3390/s19040846.

Elessawy, F., Bazghaleh, N., Vandenberg, A., Purves, R. 2019. Polyphenol profile comparisons of seed coats of five pulse crops using a semi-quantitative liquid chromatography-mass spectrometric method. Phytochemical Analysis. 2019;1–14.

Fritsch, S., Guenther, F., & Wright, M. (2019). neuralnet: Training of Neural Networks. R package version 1.44.2. https://cran.r-project.org/package=neuralnet.

Gaberščik, A., Jones, A., & Jansen, M. (n.d.). All you wanted to know about UV radiation and plants. The International Association for Plant UV Research. Online at: https://www.uv4plants.org/wp-content/uploads/2014/10/UV-web-opt.pdf. Accessed: March 29, 2020.

Gallo, C. (2014). Artificial Neural Networks Tutorial. In *Encyclopedia of Information Science and Technology, Third Edition*, 179-189. Information Resources Management Association, USA. EISBN13: 9781522522560.

Ghosh, S., Mishra, P., Mohamad, S. N. H., de Santos, R. M., Iglesias, B. D., & Elorza, P. B. (2016). Discrimination of peanuts from bulk cereals and nuts by near-infrared reflectance spectroscopy. *Biosystems Engineering*, 151, 178-186.

Gómez, P. L., Salvatori, D. M., García-Loredo, A., & Alzamora, S. M. (2012). Pulsed Light Treatment of Cut Apple: Dose Effect on Color, Structure, and Microbiological Stability. *Food and Bioprocess Technology,* 5 (6), 2311-2322.

Grisanti, E., Totska, M., Huber, S., Calderon, C. K., Hohmann, M., Lingenfelser, D., & Otto, M. (2018). Dynamic localized SNV, Peak SNV, and partial peak SNV: Novel standardization methods for preprocessing of spectroscopic data used in predictive modeling. *Journal of Spectroscopy*,2018, 1-14.

Halcro, K., McNabb, K., Lockinger, A., Socquet-Juglard, D., Bett, K. E., & Noble, S. D. (2020). The BELT and phenoSEED platforms: shape and color phenotyping of seed samples. *Plant Methods*, *16*(49). https://doi.org/https://doi.org/10.1186/s13007-020-00591-8.

Hamner, B., & Frasco, M. (2018). Metrics: Evaluation Metrics for Machine Learning version 0.1.4 from CRAN. https://rdrr.io/cran/Metrics/.

Haralick, R. M., & Shapiro, L. G. (1992). Computer and Robot Vision, Volume II. In *Computer Vision Technology for Food Quality Assurance. Trends in Food Science and Technology 1996 (7), 245-246.*

Helmenstine. A. M. (2017). Spectroscopy Definition and Difference vs Spectrometry. Online at: https://www.thoughtco.com/definition-of-spectroscopy-605676. Accessed: October 9, 2018.

Hofmann, A. (2010). Spectroscopic Techniques: I Spectrophotometric Techniques. In *Principles and Techniques of Biochemistry and Molecular Biology* (pp. 477–519). Cambridge University Press. ISBN-13:9780521731676.

Huang, H., Liu, L., & Ngadi, M. O. (2014). Recent developments in hyperspectral imaging for the assessment of food quality and safety. In *Sensors*, 14 (4), 7248-7276.

Hunt, R. W. G., & Pointer, M. R. (2011). Measuring Colour: Fourth Edition. John Wiley and Sons Ltd, West Sussex, United Kingdom.

Hunterlab. (2012). Measuring Color using Hunter L, a, b versus CIE 1976 L*a*b*. Online at: https://support.hunterlab.com/hc/en-us/articles/204137825-Measuring-Color-using-Hunter-L-a-b-versus-CIE-1976-L-a-b-AN-1005b. Accessed: November 27, 2019.

ITACA. (2018). The Sun As A Source Of Energy. Online at: https://www.itacanet.org/the-sun-as-a-source-of-energy/. Accessed: November 27, 2019.

Johnson, G. (2015). Heat Effects on Vegetable and Fruit Crops | Weekly Crop Update. Online at: https://sites.udel.edu/weeklycropupdate/?p=8354. Accessed: January 28, 2019.

Kim, A., Kim, H., & Park, S. (2011). Measuring of the Perceptibility and Acceptability in Various Color Quality Measures. *Journal of the Optical Society of Korea*, *15*(3), 310–317.

Kucheryavskiy, S. (2019). mdatools: Multivariate Data Analysis for Chemometrics. R package version 0.9.4. https://cran.r-project.org/package=mdatools.

Kumar, Y., Kumar, J., & Chaturvedi, S. (2018). Genetics of Cotyledon Colour in Lentil (Lens

culinaris Medik.). *The Bioscan, 13*(1), 55–69.

Lentils.org. (2020). Lentil Production. Online at: https://www.lentils.org/about-lentils/lentil-production/. Accessed: May 5, 2020.

Mahy, M., Van, E. L., & Oosterlinck, A. (1994). Evaluation of uniform color spaces developed after the adoption of CIELAB and CIELUV. *Color Research and Application*, *19*(2), 105–121.

Mahyar, F., Cheung, V., & Westland, S. (2009). Different transformation methods between CIELAB coordinates and Munsell hue. *Society of Dyers and Colourists, Color Technology, 126 (1)*, 31–36.

Marcus, R. (1998). The Measurement of Color. In K. Nassau (Ed.), *Color for science, art, and technology.* (Ist Edition), 31-96. Elsevier Science, Amsterdam, The Netherlands.

Martinelli, F., Scalenghe, R., Davino, S., Panno, S., Scuderi, G., Ruisi, P., Villa, P., Stroppiana, D., Boschetti, M., Goulart, L. R., Davis, C. E., & Dandekar, A. M. (2015). Advanced methods of plant disease detection. A review. Agronomy for Sustainable Development. 35 (1), 1–25. https://doi.org/10.1007/s13593-014-0246-1.

McVicar, R., McCall, P., Brenzil, C., Hartley, S., Panchuk, K., Mooleke, P., Vandenberg, A., & Banniza, S. (2017). *Lentils in Saskatchewan*. Online at: http://publications.gov.sk.ca/documents/20/86381-LentilsinSaskatchewan.pdf. Accessed: February 29, 2019.

Mendoza, F., Kelly, J., & Cichy, K. (2017). Automated prediction of sensory scores for color and appearance in canned black beans (*Phaseolus vulgaris L*.) using machine vision. *International Journal of Food Properties*, *20*(1), 83–99. https://doi.org/10.1080/10942912.2015.1136939.

Mevik, B., Wehrens, R., & Liland, K. (2019). pls: Partial Least Squares and Principal Component Regression. R package version 2.7-1. https://cran.r-project.org/package=pls.

Mirali, M., Purves, R. W., Stonehouse, R., Song, R., Bett, K., & Vandenberg, A. (2016). Genetics and Biochemistry of Zero-Tannin Lentils. *PLoS ONE*, *11*(10), 1–16. https://doi.org/doi:10.1371/journal. pone.0164624.

Mirali, M., Purves, R.W. & Vandenberg, A. (2016). Phenolic profiling of green lentil (*Lens culinaris* Medic.) seeds subjected to long-term storage. *European Food Resource Technology*, 242, 2161–2170. https://doi.org/10.1007/s00217-016-2713-1.

Mirali, M., Purves, R., & Vandenberg, A. (2017). Profiling the Phenolic Compounds of the Four Major Seed Coat Types and Their Relation to Color Genes in Lentil. *Journal of Natural Products, 80(5)*, 1310−1317.

Moomkesh, S., Mireei, S. A., Sadeghi, M., & Nazeri, M. (2017). Early detection of freezing damage in sweet lemons using Vis/SWNIR spectroscopy. *Biosystems Engineering, 164*, 157–170. https://doi.org/10.1016/j.biosystemseng.2017.10.009.

Muehlbauer, F., & Sarker, A. (2011). Tannin free lentils: A promising development for specialty use and increased value. *Grain Legumes*, 57, 27-28.

Nature Education. (2014). *allele*. Online at: *https://www.nature.com/scitable/definition/allele-48/.* Accessed: July 1, 2020.

OceanOptics. (2018). Perform a Reflectance Spectroscopy Measurement. Online at: https://spectroscopytv.com/perform-a-reflectance-spectroscopy-measurement/. Accessed: June 5, 2020.

Osborne, B. G. (2000). Near-Infrared Spectroscopy in Food Analysis. In *Encyclopedia of Analytical Chemistry*. https://doi.org/10.1002/9780470027318.a1018. John Wiley & Sons, Inc.

Palmer, J. (1995). Chapter 25: The measurement of transmission, absorption, emission, and reflection. In *Handbook of optics*: *Devices, Measurements, and Properties*, 2, 1-25.

Peters, R., & Noble, S. (2014). Spectrographic measurement of plant pigments from 300 to 800 nm. *Remote Sensing of Environment*, *148*, 119–123.

Porep, J. U., Kammerer, D. R., & Carle, R. (2015). On-line application of near-infrared (NIR) spectroscopy in food production. *Trends in Food Science and Technology*, 46(2):211–230. https://doi.org/10.1016/j.tifs.2015.10.002.

Posudin, Y. (2007). Practical Spectroscopy in Agriculture and Food Science. Science Publishers, Enfield, NH, USA.

R Development Core Team (2011). R: A Language and Environment for Statistical Computing. In *R Foundation for Statistical Computing*. https://doi.org/10.1007/978-3-540-74686-7.

Rinnan, A., Vandenberg, F., & Engelsen, S. (2009). Review of the most common pre-processing techniques for near-infrared spectra. *Trends in Analytical Chemistry*, *28*(10), 1201–1222.

Robinson, D., & Hayes, A. (2019). *broom:* Convert Statistical Analysis Objects into Tidy Tibbles. R package version 0.5.3. https://cran.r-project.org/package=broom.

Russel, R. (2007). The Multispectral Sun - Windows to the Universe. Online at: https://www.windows2universe.org/sun/spectrum/multispectral_sun_overview.html. Accessed: January 26, 2019.

Sahin, S., & Sumnu, S. G. (2006). Electromagnetic Properties. In *Physical Properties of Foods* (pp. 157–173). Springer Science+Business Media, LLC.

Salasnich, L. (2014). Quantum Physics of Light and Matter: A Modern Introduction to Photons, Atoms, and Many-Body Systems. *UNITEXT for Physics*. Springer Cham Heidelberg New York Dordrecht London. https://doi.org/10.1007/978-3-319-05179-6.

Saldaña, E., Siche, R., Huamán, R., Luján, M., Castro, W., & Quevedo, R. (2013). Computer vision system in real-time for color determination on flat surface food. *Scientia Agropecuaria*, 4(1):55-63. https://doi.org/10.17268/sci.agropecu.2013.01.06.

Sanderson, L.-A., Caron, C., Tan, R., Shen, Y., Liu, R., & Bett, K. (2019). A Web-Resource Focused on Diversity Data for Pulse Crop Improvement. Front. Plant Sci.10:965. https://doi.org/doi: 10.3389/fpls.2019.00965. "The genetics of lentil color - inside & out." Accessed: February 10, 2020. https://knowpulse.usask.ca/project/The-genetics-of-lentil-color---inside-%26-out.

Soares, J. (2014). Introduction to Optical Characterization of Materials. In *Practical Materials Characterization* (pp. 43–92). Springer New York Heidelberg Dordrecht London. https://doi.org/10.1007/978-1-4614-9281-8.

Sarkar, D. (2008). Lattice - Multivariate Data Visualization with R. https://www.springer.com/gp/book/9780387759685.

Saskatchewan Pulse Growers (2020). Harvest. Online at: https://saskpulse.com/growing-pulses/lentils/harvest/. Accessed March 26, 2020.

SCENIHR (2012). Health effects of artificial light. Report. Scientific Committee on Emerging and Newly Identified Health Risks. Directorate-General for Health and Food Safety (European Commission). DOI: https://doi.org/10.2772/8624.

Singh, C. B., Paliwal, J., Jayas, D. S., White, N. D. G., & Alberta, E. (2006). Near-infrared spectroscopy: Applications in the grain industry. Paper No. 06-189. Presentated at the CSBE/SCGAB 2006 Annual Conference, edmonton, Alberta, Canada, July 16-19, 2006.

Statistics Canada. (2019). Production of principal field crops. Online at: https://www150.statcan.gc.ca/n1/en/daily-quotidien/191206/dq191206b-eng.pdf?st=I3zA5ZBd. Accessed: December 6, 2019.

Statistics Canada. (2015). Pulses in Canada. Online at: https://www150.statcan.gc.ca/n1/pub/96-325-x/2014001/article/14041-eng.htm Accessed: September 15, 2020.

Steidle Neto, A. J., Lopes, D. C., Toledo, J. V., Zolnier, S., & Silva, T. G. F. (2018). Classification of sugarcane varieties using visible/near-infrared spectral reflectance of stalks and multivariate methods. *Journal of Agricultural Science*,156(4),537-546.

Subedi, M., Tabil, L. G., & Vandenberg, A. (2018). Influence of Seed Coat Color Genes on Milling Qualities of Red Lentil (Lens culinaris Medik.). *Journal of Agricultural Science*, 10 (10), 88-99.

Sun, L., Hsiung, C., & Smith, V. (2019). Investigation of Direct Model Transferability Using Miniature Near-Infrared Spectrometers. *Molecules*, *24*(1997), 1–19. https://doi.org/doi:10.3390/molecules24101997.

Thomas, T. (2016). Understanding the Genetic Basis of Carotenoid Concentration in Lentil (*Lens culinaris* Medik.) Seeds (M.Sc. Thesis). University of Saskatchewan, Saskatoon, Canada.

UNEP. (1998). Environmental Effects of Ozone Depletion: 1998 Assessment. Report. United Nations Environment Program. Online at: http://hdl.handle.net/20.500.11822/8236. Accessed: November 6, 2019.

Vaillancourt, R. E., & Slinkard, A. E. (1992). Inheritance of new genetic markers in lentil. *Euphytica*, *64*, 227–236.

Vandenberg, A., & Slinkard, A. (1990). Genetics of seed coat color and pattern in lentil. *Journal of Heredity*, *81*(6), 484–8.

Venables, W. N., & Ripley, B. D. (2002). Modern Applied Statistics with S. New York: Springer. *Http://www.Stats.Ox.Ac.Uk/Pub/MASS4*.

Vo. K. (2019). Spectrophotometry - Chemistry LibreTexts. Online at: https://chem.libretexts.org/Bookshelves/Physical_and_Theoretical_Chemistry_Textbook_Maps/Supplemental_Modules_(Physical_and_Theoretical_Chemistry)/Kinetics/Reaction_Rates/Experimental_Determination_of_Kinetcs/Spectrophotometry. Accessed: January 5, 2020.

Vyawahare, A., Rao, K. J., & Pagote, C. N. (2013). Computer Vision System for Colour Measurement - Fundamentals and Applications in Food Industry : A Review. *Research and Reviews : Journal of Food and Dairy Technology*, 1(2), 22–31.

Wickham, H. (2018). Package 'scales' - Scale Functions for Visualization. In *CRAN Repository*.

Woodall, G. S., & Stewart, G. R. (1998). Do anthocyanins play a role in UV protection of the red juvenile leaves of Syzygium? *Journal of Experimental Botany*, 49(325), 1447–1450.

Xu, F., Shi, L., Chen, W., Cao, S., Su, X., & Yang, Z. (2014). Effect of blue light treatment on fruit quality, antioxidant enzymes, and radical-scavenging activity in strawberry fruit. *Scientia Horticulturae*, 175: 181-188. https://doi.org/10.1016/j.scienta.2014.06.012.

X-rite (nd). A Guide to Understanding Color | X-Rite Color Management Whitepaper. Online at: *https://www.xrite.com/learning-color-education/whitepapers/a-guide-to-understanding-color.* Accessed: March 29, 2020.

Zapotoczny, P., & Majewska, K. (2010). A Comparative Analysis of Colour Measurements of The Seed Coat and Endosperm of Wheat Kernels Performed by Various Techniques. *International Journal of Food Properties*, 13 (1): 75–89. https://doi.org/10.1080/10942910802180174.

Zhanga, B., Penga, H., Denga, Z., & Tsao, R. (2018). Phytochemicals of lentil (Lens culinaris) and their antioxidant and anti-inflammatory effects. *Journal of Food Bioactives*, 1 (1), 93–103.

Zhou, C., Han, L., Pislariu, C., Nakashima, J., Fu, C., Jiang, Q., Quan, L., Blancaflor, E.B., Tang, Y., Bouton, J. H., Udvardi, M., Xia, G., & Z. Wang. (2011). From model to crop: functional analysis of a stay-green gene in the model legume Medicago truncatula and effective use of the gene for alfalfa improvement. *Plant Physiology*, 157: 1483– 1496.

Zwinkels, J. C. (2015). Light, Electromagnetic Spectrum. In *Encyclopedia of Color Science and Technology*. Springer Science+Business Media New York. https://doi.org/10.1007/978-3-642-27851-8.

APPENDIX A: ANOVA TABLES FOR LIGHT TRANSMISSION PROPERTIES OF LENTIL SEED COAT

Table A.1: ANOVA for Cumulative UV Transmission

	DF	Deviance	Resid. Df	Resid. Dev	F	p-value
			197	20892.3		
Genotype	9	19615	188	1277.3	320.79	2.2e-16 ***

Table A.2: ANOVA for Cumulative VIS Transmission

	DF	Deviance	Resid. Df	Resid. Dev	F	p-value
			197	13935295		
Genotype	9	13440480	188	494815	567.4	2.2e-16 ***

Table A.3: ANOVA for Cumulative NIR Transmission

	DF	Deviance	Resid. Df	Resid. Dev	F	p-value
			194	2416054		
Genotype	9	2056369	185	359685	117.52	2.2e-16 ***

Table A.4: Multiple Comparisons for Seed Coat Light Transmission

	Cumulative UV Transmission		Cumulative VIS Transmission		Cumulative NIR Transmission	
Comparison	Estimate	Adj.p-value	Estimate	Adj.p-value	Estimate	Adj.p-value
7312g_M Black)-73111_Black	24.1202	0.7771	1.6700	0.5819	24.1202	0.7771
CDC QG3_Green-73111_Black	229.7490	0.0000	5.9741	0.0000	229.7490	0.0000
CDC Marble _M Green-73111_Black	49.2786	0.0181	6.8114	0.0000	49.2786	0.0181
CDC QG4_ M Green-73111_Black	168.7024	0.0000	1.7891	0.4807	168.7024	0.0000
CDC Robin_Brown-73111_Black	116.3515	0.0000	0.6629	0.9985	116.3515	0.0000
CDC Rosebud_Tan-73111_Black	35.7228	0.2435	3.4312	0.0024	35.7228	0.2435
Indianhead _Black-73111_Black	-71.2210	0.0001	0.0000	1.0000	-71.2210	0.0001
SB4IBC929_Grey-73111_Black	-37.0868	0.1983	3.3629	0.0026	-37.0868	0.1983
ZT4_Zero tannin-73111_Black	243.8743	0.0000	34.8120	0.0000	243.8743	0.0000
CDC QG3_Green-7312g_M Black)	205.6289	0.0000	4.3042	0.0000	205.6289	0.0000
CDC Marble _M grey-7312g_M Black)	25.1584	0.7318	5.1414	0.0000	25.1584	0.7318
CDC QG4_ M Green-7312g_M Black)	144.5822	0.0000	0.1191	1.0000	144.5822	0.0000
CDC Robin_Brown-7312g_M Black)	92.2313	0.0000	-1.0070	0.9681	92.2313	0.0000
CDC Rosebud_Tan-7312g_M Black)	11.6026	0.9980	1.7612	0.5234	11.6026	0.9980
Indianhead _Black-7312g_M Black)	-95.3412	0.0000	-1.6700	0.5819	-95.3412	0.0000
SB4IBC929_Grey-7312g_M Black)	-61.2070	0.0008	1.6929	0.5623	-61.2070	0.0008
ZT4_Zero tannin-7312g_M Black)	219.7541	0.0000	33.1421	0.0000	219.7541	0.0000
CDC Marble _M Green-CDC QG3_Green	-180.4705	0.0000	0.8372	0.9918	-180.4705	0.0000
CDC QG4_ M Green-CDC QG3_Green	-61.0467	0.0008	-4.1851	0.0000	-61.0467	0.0008
CDC Robin_Brown-CDC QG3_Green	-113.3975	0.0000	-5.3112	0.0000	-113.3975	0.0000
CDC Rosebud_Tan-CDC QG3_Green	-194.0262	0.0000	-2.5429	0.0774	-194.0262	0.0000
Indianhead _Black-CDC QG3_Green	-300.9700	0.0000	-5.9741	0.0000	-300.9700	0.0000
SB4IBC929_Grey-CDC QG3_Green	-266.8359	0.0000	-2.6113	0.0551	-266.8359	0.0000
ZT4_Zero tannin-CDC QG3_Green	14.1253	0.9912	28.8379	0.0000	14.1253	0.9912
CDC QG4_ M Green-CDC Marble _M Green	119.4238	0.0000	-5.0223	0.0000	119.4238	0.0000
CDC Robin_Brown-CDC Marble _M Green	67.0730	0.0002	-6.1485	0.0000	67.0730	0.0002
CDC Rosebud_Tan-CDC Marble _M Green	-13.5557	0.9935	-3.3802	0.0036	-13.5557	0.9935
Indianhead _Black-CDC Marble _M Green	-120.4995	0.0000	-6.8114	0.0000	-120.4995	0.0000
SB4IBC929_Grey-CDC Marble _M Green	-86.3654	0.0000	-3.4485	0.0022	-86.3654	0.0000
ZT4_Zero tannin-CDC Marble _M Green	194.5958	0.0000	28.0007	0.0000	194.5958	0.0000
CDC Robin_Brown-CDC QG4_ M Green	-52.3509	0.0102	-1.1262	0.9359	-52.3509	0.0102
CDC Rosebud_Tan-CDC QG4_ M Green	-132.9796	0.0000	1.6421	0.6235	-132.9796	0.0000
Indianhead _Black-CDC QG4_ M Green	-239.9234	0.0000	-1.7891	0.4807	-239.9234	0.0000
SB4IBC929_Grey-CDC QG4_ M Green	-205.7892	0.0000	1.5738	0.6627	-205.7892	0.0000
ZT4_Zero tannin-CDC QG4_ M Green	75.1719	0.0000	33.0230	0.0000	75.1719	0.0000
CDC Rosebud_Tan-CDC Robin_Brown	-80.6287	0.0000	2.7683	0.0358	-80.6287	0.0000
Indianhead _Black-CDC Robin_Brown	-187.5725	0.0000	-0.6629	0.9985	-187.5725	0.0000
SB4IBC929_Grey-CDC Robin_Brown	-153.4384	0.0000	2.6999	0.0403	-153.4384	0.0000
ZT4_Zero tannin-CDC Robin_Brown	127.5228	0.0000	34.1491	0.0000	127.5228	0.0000
Indianhead _Black-CDC Rosebud_Tan	-106.9438	0.0000	-3.4312	0.0024	-106.9438	0.0000
SB4IBC929_Grey-CDC Rosebud_Tan	-72.8097	0.0000	-0.0683	1.0000	-72.8097	0.0000
ZT4_Zero tannin-CDC Rosebud_Tan	208.1515	0.0000	31.3808	0.0000	208.1515	0.0000
SB4IBC929_Grey-Indianhead _Black	34.1341	0.3889	3.3629	0.0026	34.1341	0.3889
ZT4_Zero tannin-Indianhead _Black	315.0953	0.0000	34.8120	0.0000	315.0953	0.0000
ZT4_Zero tannin-SB4IBC929_Grey	280.9611	0.0000	31.4492	0.0000	280.9611	0.0000

PROLOGUE TO APPENDIX B

The following Appendix involves the application of machine learning to classify lentil genotypes using their seed coat light reflectivity data.

This part of the thesis was presented at the Plant Phenotyping and Imaging Research Symposium, Saskatoon, Oct. 24, 2019, titled: "**Machine Learning Models for Discriminating Lentil Genotypes using Seed Coat Reflectivity**."

APPENDIX B: MACHINE LEARNING MODELS FOR PREDICTING LENTIL GENOTYPES USING SEED COAT REFLECTIVITY

Machine learning tools were used to investigate if there is a recognizable pattern in light reflectivity of lentil seed coat, which might be useful in market class discrimination, quality prediction, and disease detection in the seeds. Such pattern would be demonstrated in the ability of classifier algorithms to correctly predict lentil genotypes using light reflectivity data. This will act as additional prove on the reliability of the optical fiber instrument in capturing real variations in the optical properties of the materials. The reflectivity data collected in section 4.1.1 were used for this study. Three machine learning techniques for the classification of 20 lentil genotypes were considered; the techniques include the following: Linear Discriminant Analysis (LDA), Artificial Neural Network (ANN), and Partial Least Square Discriminant Analysis (PLS-DA).

B.1 Signal Preprocessing

Common spectral preprocessing tools include Multiplicative Scatter Correction and Standard Normal Variate (SNV). These tools are, in theory, used to improve the predictive power of a model fit from the data. The reflectivity data were preprocessed using SNV from R package "mdatools" Kucheryavskiy (2019) to normalize the data and eliminate baseline and scatter effects. SNV serves to remove the offset in data points (that may be due to sample geometry or baseline factors) when samples from the same class are replicated. This is done by subtracting the mean values and bringing all spectra to the same scale by subsequent division by the standard deviation (Grisanti *et al.*, 2018).

SNV preprocessing was based on the principle that each spectrum vector with *m* measured data points and a form such as equation B.1 is transformed into the standardized form, such as in equation B.2 (Grisanti *et al.*, 2018).

$$x = (x_1, x_2, x_3, \ldots x_k) \quad \text{B.1}$$

$$z = (z_1, z_2, z_3, \ldots z_k) \quad \text{B.2}$$

$$z_i = \frac{x_i - \overline{x}}{\sqrt{\sum_1^m (x_i - \overline{x})/m}} \quad \text{B.3}$$

$$\overline{x} = \frac{1}{m} \sum_1^m x \quad \text{B.4}$$

This is done by bringing the spectra to zero mean and unit variance, based on equations B.3 and B.4, where the mean spectrum x is subtracted from each data point x_i and divided by the standard deviation (Grisanti *et al.*, 2018).

Figure B.1(i) shows the reflectivity signals of the samples before SNV preprocessing, while Figure B.1(ii) represents the signal after SNV, which removes the baseline and scatter effects to further compress the data.

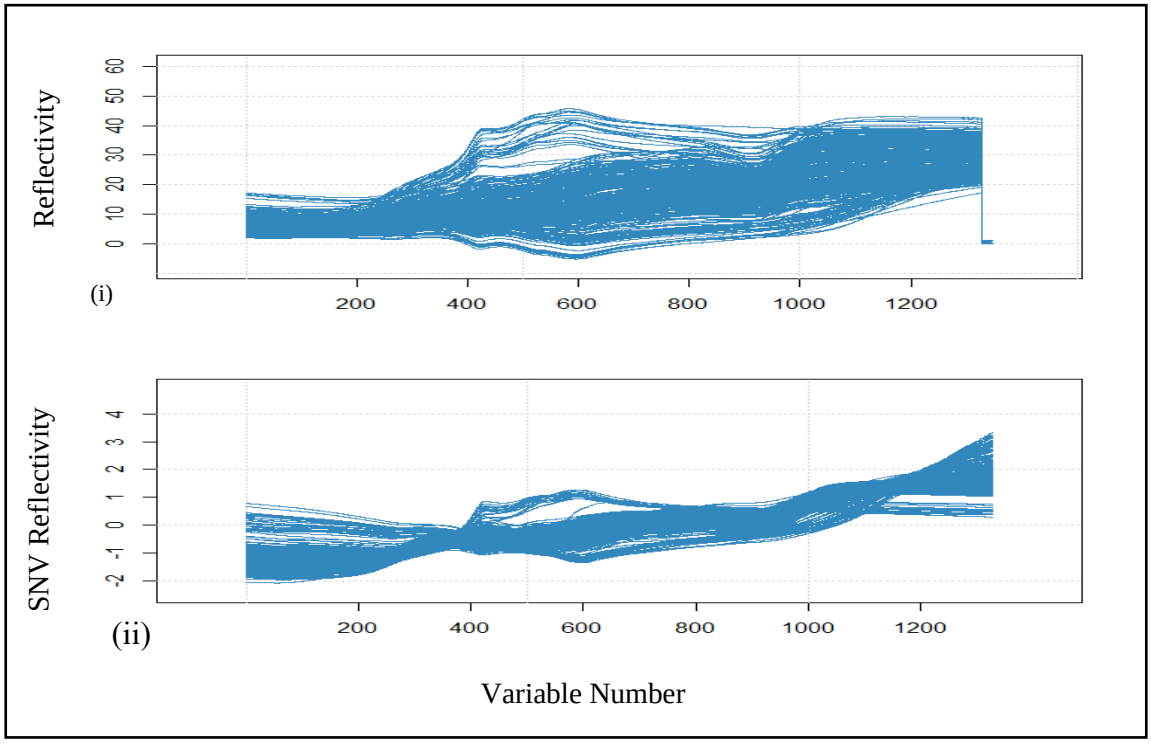

Figure B.1: Reflectivity spectra of seed coat; (a) before pre-processing; (b) after pre-processing.

B.2 Data Modeling

To make model building and validation on separate datasets possible, a random sampling algorithm was used to partition data into 80% training and 20% testing sets, using the same seed

value to ensure comparability across models. This was repeated for all the models. In each case, the training and testing data were stored in separate objects for future use.

ANN, LDA, and PLS-DA algorithms were fit to the data using 80% of the data (training set). The models use a supervised learning approach, with the lentil genotype class as the categorical response variable and the light reflectivity or normalized light reflectivity as multivariate predictor variables.

The general function governing all the models is shown in equation B.5:

$$f\,(R\,(\%)\,) \;=\; Genotype \tag{B.5}$$

Where R (%) is a vector of raw, SNV transformed or normalized percentage light reflectivity on lentils seed coat with 400 data points; and Genotype is the class of lentils with the reflectivity information, such that;

$$\begin{bmatrix} X_{11} & X_{12} & X_{13} & \cdots & X_{1n} \\ X_{21} & X_{22} & X_{23} & \cdots & X_{2n} \\ X_{31} & X_{32} & X_{33} & \cdots & X_{3n} \\ \vdots & \vdots & \vdots & \cdots & \vdots \\ X_{m1} & X_{m2} & X_{m3} & \cdots & X_{mn} \end{bmatrix} = \begin{bmatrix} G_1 \\ G_2 \\ G_3 \\ \vdots \\ G_m \end{bmatrix} \tag{B.6}$$

The left-hand side matrix represents light reflectivity with n dimensions and m replications, while the right-hand side represents the Genotypes with m examples.

The LDA model from the "MASS" library (Venables & Ripley, 2002) was trained using raw spectral data. An LDA model is a data reduction algorithm that finds a linear combination of variables that maximizes the separation between classes. Generally, the multidimensional sample space is reduced to a feature space by maximizing the between-sample variation and minimizing the within-sample variation. The reduced feature space is then automatically used for the classification. At first, the training was done using separate bands of the spectrum, i.e., UV, VIS, and NIR. It was then repeated with the full spectrum, making a total of four models. The procedure was repeated using SNV transformed data. For each model, performance plots were generated (considering the version with the highest accuracy; raw or SNV transformed) using functionalities in "scales" (Wickham, 2018), "gridExtra" (Auguie, 2017), and ggplot2 libraries.

PLS-DA, which works due to functionalities available on R packages “mdatools”, “pls” (Mevik *et al.*, 2019), “MASS”, and “lattice” (Sarkar, 2008) was also trained using raw spectral data and SNV transformed data. A PLS-DA model is a version of partial-least square regression applied to categorical or binary response variables (as opposed to normal partial-least square, which is applied to continuous response variables). PLS-DA also reduces the variables by projecting them to a plane of maximum variance between classes, and automatically uses the reduced feature space for classification.

The SNV transformed data was used to fit a base PLS-DA model and the accuracy was assessed using the “Metrics” library. In PLS-DA the number of components to be used for model calibration is explicitly specified in the model function; thus, the effect of the number of components on prediction accuracy was tested by simulating with different number of components. The optimum number of components for both raw and SNV transformed model was 200.

Variable selection was carried out using VIP (Variable Important to Projection) scores approach. The main objective of variable selection was to optimize the PLS-DA model in terms of run time (the full spectrum models took an average of 20 minutes to run). VIP selection involves passing the base model as an argument to a function, which ranks the various variables based on their contribution to the model accuracy. From the calculated VIP scores, variables with values greater than 1.1 were selected for further modeling. This resulted in five variables in the UV region (designated as VIP1), 28 variables in the VIS region (VIP2), and 17 variables in the NIR region (VIP3). New models were then fit using the VIP1, VIP2 and VIP3 variables. Further, the three groups of variables were combined to form VIP-full and another model was fit to the data.

The next pattern recognition algorithm fit to the data was Artificial Neural Network (ANN). This was done using R package “neuralnet” (Fritsch *et al.*, 2019). Artificial neural networks are information processing structures, which find the pattern that links input data to output (providing the connection between input and output data) using an approach inspired by the physiological structure and functioning of human brain structures (Gallo, 2014). Two modeling approaches were employed. First, the data were normalized using min-max centering. Second, feature reduction was carried out on the data using principal components analysis (PCA).

Four different configurations of fully connected ANN were trained using both the centered data and PCA loadings/principal components, with one, two, three, and four hidden layers of perceptron. The response variable (Genotype) was encoded as a "one-hot vector" multi-label data. The network layers were activated using the "logistic" function and the model was run using "resilient backpropagation" and "sum of square error" function. Using resilient backpropagation, the network "learned from experience" by iteratively comparing the response (lentil genotype class) to the prediction obtained using applied "weights" and readjusting the weights until a point of convergence is reached, where output matches the true value.

B.3 Model Validation

Model validation was carried out by predicting genotype classes using "unseen" data, the remaining 20% of the data (testing set) from the data partitioning algorithm. This involved supplying the input variables and allowing LDA, PLS-DA, and ANN to predict the genotype class the seeds belong to. Confusion matrices were produced, which displayed the number of correct and wrong classification in tables. The metric used to assess the performance of the models was accuracy from the "Metrics" package (Hamner & Frasco, 2018). The "accuracy" function is defined as shown in equation B.7.

$$\text{Accuracy} = \frac{N_c}{N_T} \times 100\% \qquad \text{B.7}$$

Where; $N_c = \text{number of correctly classified samples}$; and $N_T = \text{Total number of samples}$.

B.4 Results and Discussion

The classification accuracies of LDA models fit to the reflectivity data are shown in Table B.1. The model using reflectivity data in the UV region predicted lentil Genotypes to accuracy of 66%; however, after SNV transformation the accuracy reduced to 53.7%. A reduction in accuracy after SNV transformation also occurred in NIR reflectivity. On the contrary, the classification accuracies of models fit using VIS spectra and the full spectrum (250-850 nm) improved in accuracy when SNV transformation was applied to the spectra.

Table B.1: Classification accuracies of LDA models.

LDA Model	Accuracy (%) - Before SNV	Accuracy (%) - after SNV
UV Region	66.3	53.7
VIS Region	72.5	98.7
NIR Region	97.5	85.0
UV-VIS-NIR	92.5	98.7

Figure B.2 shows the performance plots of the best performing models fit to UV, VIS, NIR, and full-spectrum (the plots represent before SNV model for UV and NIR region and after SNV for NIR and UV-VIS-NIR region). The figures provide a visual view of the discrimination of lentil genotypes achieved by each model using seed coat reflectivity data.

The results indicate that most of the real variations in light reflectivity among the lentil genotypes occurred in the visible region of the spectrum. This finding is valid because, based on common theoretical knowledge, the color of a material is a function of the spectral components of visible light it reflects. Thus, while some pigments may also absorb in the UV region, most of the real variations in light absorption is due to visible light-absorbing pigments. Consequently, for future studies on lentil market class (major seed coat classes) discrimination, it may be reasonable to focus on the visible region.

Table B.2 shows the classification accuracies of six versions of PLS-DA classifiers. The first two models were fit using the full spectra as predictors: one with raw spectra and the second with SNV-transformed spectra. SNV transformation helped improve the model accuracy by 9%. However, the highly multidimensional nature of the predictors caused the PLS-DA models to be too slow (average of 20 minutes running time each).

Variable selection using the VIP scores approach reduced the calibration time of the models to a few seconds each. It also enables understanding of which portion of the spectrum contributes most to the overall model accuracy, hence revealing the region which accounts for most variation in light reflectivity of seed coats of the different lentil genotypes. The calculated VIP scores showed

the highest proportion of high scores in the VIS region (i.e., when the threshold of 1.1 was selected the VIP region had the highest number of remaining variables).

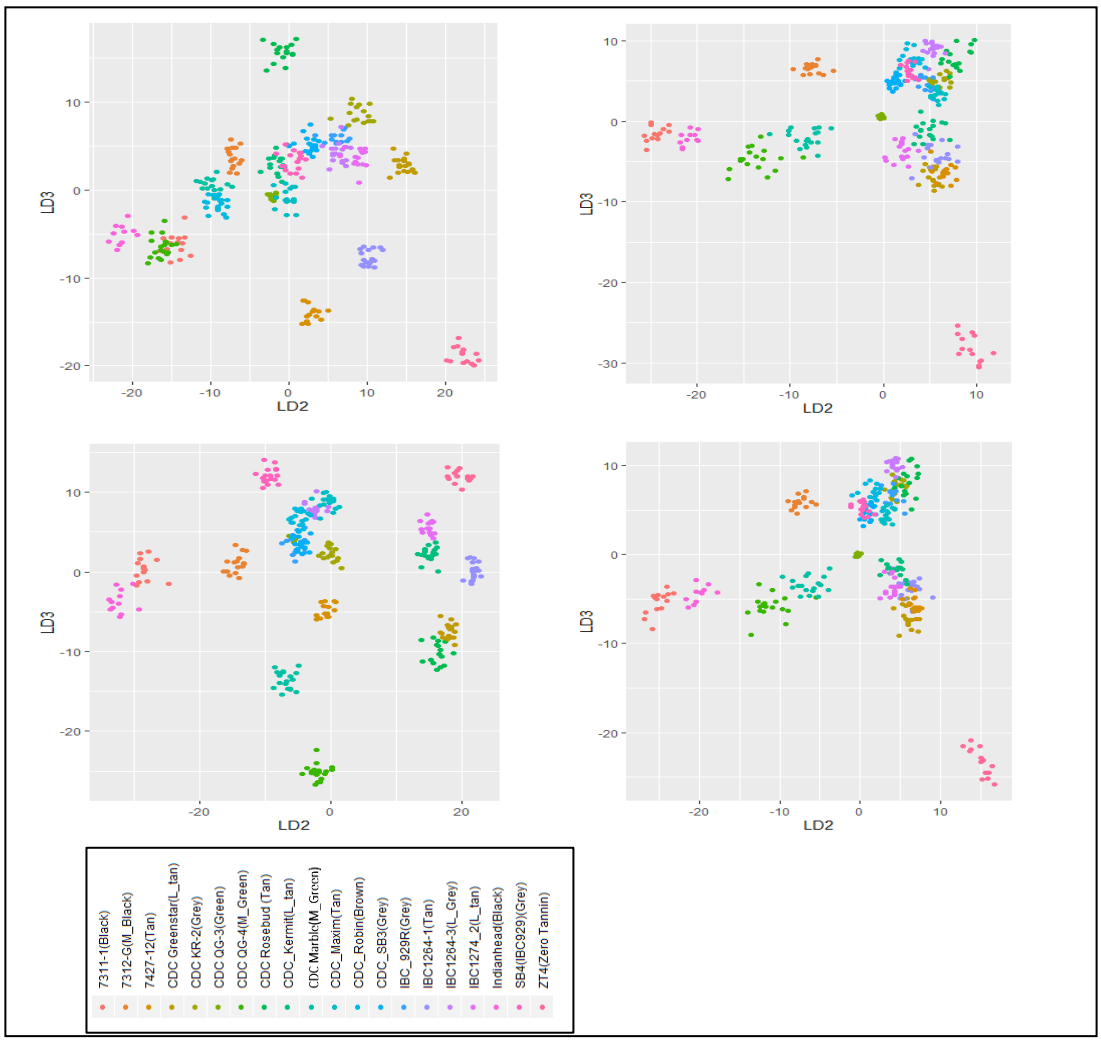

Figure B.2: Performance Plots for LDA Models: (a) UV; (b) VIS; (c) NIR; (d) UV-VIS-NIR.

Further, as shown in Table B.2, the variables selected in the VIS region resulted in the highest classification accuracy. However, the results show that selecting the particular set of variables resulted in sacrificing accuracy for time, as the overall model accuracy reduced from 85.5% to 70.9%, while the calibration time reduced from 20 minutes to a few seconds. Variable selection by the VIP score method is thus a good calibration time optimizing technique, but a lot of work may be involved in picking variables that would not sacrifice prediction accuracy.

Table B.2: Classification accuracies of the PLS-DA models.

PLS-DA Model	Accuracy (%)
Full Spectrum (Before SNV)	76.5
Full Spectrum (After SNV)	85.5
VIP1 (UV Region)	6.0
VIP2 (467 to 558 nm)	51.0
VIP3 (700 to 850 nm)	29.0
Combined VIP	70.9

The findings above also agree with the results of LDA models; the greatest variation in optical properties of the different seed coats were captured in the visible portion of their light reflectivity.

Table B.3 shows the classification accuracies on the testing set, of four configurations of neural networks trained using min-max centered reflectivity data (without PCA). The numbers in brackets are the number of neurons in the respective layers. The result shows that a single layer perceptron with 50 neurons resulted in the highest classification accuracy (87.3%) on the testing set. It may seem ironical that more complex architectures resulted in lower classification accuracies; however, due to the high dimensionality of the data, more complex architectures might result in high degrees of model overfitting.

After PCA (Table B.4), the model with four layers sharply increased in accuracy from 75% to 82.5% while the one with one layer experienced a slight increase, from 87.3% to 88.8%. However, when ANN with two and three layers and the same number of neurons in each layer as before were trained using PCA transformed data, there were sharp drop in prediction accuracy. Re-tuning the neuron numbers yielded the classification accuracies shown.

The ANN accuracies presented are the results of the modeling and tuning effort using the seed coat reflectivity data with 400 data points. It might be possible to improve the prediction by collecting more data, applying a more robust feature reduction approach, and/or carrying out more robust tuning of model hyperparameters.

Table B.3: Classification accuracies of neural networks (before PCA).

Architecture	Accuracy (%)
1 Layer (50)	87.3
2 Layers (100,100)	86.3
3 Layers (43,50,125)	82.5
4 Layers (50,75,125,130)	75.0

Table B.4: Classification accuracies of neural networks (after PCA)

Architecture	Accuracy (%) Before PCA
1 Layer (50)	88.8
2 Layers (20,10)	85.0
3 Layers (50,13,25)	82.5
4 Layers (50,75,125,130)	82.5

B.5 Conclusion

This study was designed to answer the question, “Is it possible to find a computer-recognizable pattern in light reflectivity of lentil seed coat?” This was addressed by fitting the reflectivity data to three widely recognized machine learning algorithms. All the algorithms successfully found patterns in the reflectivity properties of the lentil genotypes and performed classifications, albeit with varying levels of success. This shows that the data contained real information about the seeds and that fiber optics spectroscopy and pattern recognition tools may be useful for quality prediction, disease detection, and market class discrimination in lentil seeds and other crops.

APPENDIX C: ANOVA TABLES FOR EFFECT OF LIGHT TREATMENT ON LENTIL COTYLEDON

Table C.1: GLM model summary for green lentil (ΔL*-value).[1]

Treatment	Estimate	Pr(>|t|)
Control	-0.66	0.00186 **
Ultraviolet	2.62	2.96e-14 ***
Red light	4.15	< 2e-16 ***
Green light	3.18	< 2e-16 ***
Blue light	8.57	< 2e-16 ***
Full-Visible	8.06	< 2e-16 ***

Table C.2: GLM model summary for green lentil (Δa*-value).

Treatment	Estimate	Pr(>|t|)
Control	-0.11	0.771
Ultraviolet	5.80	< 2e-16 ***
Red light	10.21	< 2e-16 ***
Green light	4.01	9.8e-13***
Blue light	13.79	< 2e-16 ***
Full-Visible	12.47	< 2e-16 ***

Table C.3: GLM model summary for green lentil (Δb*-value).

Treatment	Estimate	P-value (>|t|)
Control	-0.24	0.474
Ultraviolet	-6.92	< 2e-16 ***
Red light	-7.39	< 2e-16 ***
Green light	-3.72	3e-12 ***
Blue light	-14.66	< 2e-16 ***
Full-Visible	-10.66	< 2e-16 ***

Table C.4: GLM model summary for green lentil (ΔE).

Treatment	Estimate	P-value (>|t|)
Control	1.11	0.00072 ***
Ultraviolet	8.54	< 2e-16 ***
Red light	12.06	< 2e-16 ***
Green light	5.18	< 2e-16 ***
Blue light	20.61	< 2e-16 ***
Full-Visible	17.22	< 2e-16 ***

[1] The symbol "*" indicates statistical significance; the number of symbols indicates the degree of significance.

Table C.5: GLM model summary for red lentil (ΔL*-value).

Treatment	Estimate	P-value (>|t|)
Control	-0.64	0.0009 **
Ultraviolet	-0.06	0.8053
Red light	0.73	0.0059 **
Green light	0.55	0.0633
Blue light	-0.01	0.4408
Full-Visible	0.27	0.2919

Table C.6: GLM model summary for red lentil (Δa*-value).

Treatment	Estimate	P-value (>|t|)
Control	-1.37	7.22e-06 ***
Ultraviolet	0.18	0.6506
Red light	2.26	1.71e-07 ***
Green light	-0.04	0.9244
Blue light	-0.18	0.6466
Full-Visible	0.70	0.0723

Table C.7: GLM model summary for red lentil (Δb*-value).

Treatment	Estimate	P-value (>|t|)
Control	0.3219	0.6030
Ultraviolet	0.2777	0.7400
Red light	3.77	2.32e-05***
Green light	1.39	0.1040
Blue light	-3.69	2.56e-05***
Full-Visible	-3.60	4.91e-05***

Table C.8: GLM model summary for red lentil (ΔE).

Treatment	Estimate	P-value (>|t|)
Control	2.42	5.39e-08 ***
Ultraviolet	-0.38	0.4844
Red light	3.13	2.12e-07 ***
Green light	0.90	0.1019
Blue light	1.67	0.00267 **
Full-Visible	3.09	0.0001***

Table C.9: GLM model summary for yellow lentil (ΔL*-value).

Treatment	Estimate	Pr(>|t|)
Control	-0.22	0.3613
Ultraviolet	-0.87	0.0117*
Red light	0.48	0.1579
Green light	1.56	1.36e-05 ***
Blue light	0.34	0.3179
Full-Visible	1.16	0.00109 **

Table C.10: GLM model summary for yellow lentil (Δa*-value).

Treatment	Estimate	Pr(>|t|)
Control	-0.51	0.1002
Ultraviolet	0.24	0.5798
Red light	0.37	0.3743
Green light	-2.28	7.09e-07 ***
Blue light	-0.80	0..0658
Full-Visible	-1.47	0.0009 ***

Table C.11: GLM model summary for yellow lentil (Δb*-value).

Treatment	Estimate	Pr(>|t|)
Control	0.42	0.04171*
Ultraviolet	-1.78	0.0155*
Red light	1.59	0.0329
Green light	0.85	0.2486
Blue light	-10.16	<2e-16 ***
Full-Visible	-1.88	0.0117*

Table C.12: GLM model summary for yellow lentil (ΔE*-value).

Treatment	Estimate	Pr(>|t|)
Control	1.72	0.000390 ***
Ultraviolet	2.91	2.77e-05 ***
Red light	0.97	0.1377
Green light	2.66	0.001316 **
Blue light	7.57	2e-16 ***
Full-Visible	1.45	0.029956 *

APPENDIX D: ANOVA TABLES FOR EFFECT OF LIGHT TREATMENT ON WHOLE LENTILS

Table D.1: Multiple Comparison of ΔL^*-values of green cotyledon lentil under visible light.

Seed Coat Type	Comparison	Estimate	Adj.p-value
Black	(c) Whole seed-Visible – (a) Whole seed-Control	2.97	0.09623
	(e) De-hulled-Visible – (a) Whole seed-Control	13.92	7.76E-07
	(e) De-hulled-Visible – (c) Whole seed- Visible	10.95	7.34E-06
Grey	(c) Whole seed-Visible – (a) Whole seed-Control	2.80	0.11835
	(e) De-hulled-Visible – (a) Whole seed-Control	9.15	3.46E-05
	(e) De-hulled-Visible – (c) Whole seed- Visible	6.35	0.00076
Green	(c) Whole seed-Visible – (a) Whole seed-Control	4.24	0.00084
	(e) De-hulled-Visible – (a) Whole seed-Control	12.86	3.83E-08
	(e) De-hulled-Visible – (c) Whole seed- Visible	8.62	1.63E-06
Grey Zero tannin	(c) Whole seed-Visible – (a) Whole seed-Control	5.04	0.00262
	(e) De-hulled-Visible – (a) Whole seed-Control	11.92	1.60E-06
	(e) De-hulled-Visible – (c) Whole seed- Visible	6.88	0.00022

Table D.2: Multiple Comparison of ΔL^*-values of green cotyledon lentil under UVA.

Seed Coat Type	Comparison	Estimate	Adj.p-value
Black	(b) Whole seed-UVA – (a)Whole seed-Control	1.56	0.57967
	(d) De-hulled-UVA – (a) Whole seed-Control	3.88	0.02475
	(d) De-hulled-UVA– (b) Whole seed-UVA	2.31	0.24235
Grey	(b) Whole seed-UVA – (a)Whole seed-Control	0.48	0.98868
	(d) De-hulled-UVA – (a) Whole seed-Control	0.34	0.99704
	(d) De-hulled-UVA– (b) Whole seed-UVA	-0.14	0.99989
Green	(b) Whole seed-UVA – (a)Whole seed-Control	-0.66	0.87087
	(d) De-hulled-UVA – (a) Whole seed-Control	-0.44	0.96605
	(d) De-hulled-UVA– (b) Whole seed-UVA	0.22	0.99742
Grey Zero tannin	(b) Whole seed-UVA – (a)Whole seed-Control	0.97	0.84648
	(d) De-hulled-UVA – (a) Whole seed-Control	0.87	0.88691
	(d) De-hulled-UVA– (b) Whole seed-UVA	-0.09	0.99997

Table D.3: Multiple Comparison of Δa^*-values of green cotyledon lentil under visible light.

Seed Coat Type	Comparison	Estimate	Adj.p-value
Black	c) Whole seed-Visible – (a) Whole seed-Control	0.59	0.73751
	(e) De-hulled-Visible – (a) Whole seed-Control	21.18	1.70E-11
	(e) De-hulled-Visible – (c) Whole seed- Visible	20.59	2.26E-11
Grey	c) Whole seed-Visible – (a) Whole seed-Control	6.25	0.00103
	(e) De-hulled-Visible – (a) Whole seed-Control	18.77	5.54E-08
	(e) De-hulled-Visible – (c) Whole seed- Visible	12.51	2.44E-06
Green	c) Whole seed-Visible – (a) Whole seed-Control	5.95	0.00030
	(e) De-hulled-Visible – (a) Whole seed-Control	17.54	1.36E-08
	(e) De-hulled-Visible – (c) Whole seed- Visible	11.59	7.54E-07
Grey Zero tannin	c) Whole seed-Visible – (a) Whole seed-Control	8.58	2.43E-05
	(e) De-hulled-Visible – (a) Whole seed-Control	18.29	1.94E-08
	(e) De-hulled-Visible – (c) Whole seed- Visible	9.71	7.83E-06

Table D.4: Multiple Comparison of Δa^*-values of green cotyledon lentil under UVA.

Seed Coat Type	Comparison	Estimate	Adj.p-value
Black	b) Whole seed-UVA – (a)Whole seed-Control	1.20	0.17201
	(d) De-hulled-UVA – (a) Whole seed-Control	4.88	1.13E-05
	(d) De-hulled-UVA– (b) Whole seed-UVA	3.68	0.00013
Grey	b) Whole seed-UVA – (a)Whole seed-Control	0.46	0.99133
	(d) De-hulled-UVA – (a) Whole seed-Control	2.17	0.30519
	(d) De-hulled-UVA– (b) Whole seed-UVA	1.71	0.51326
Green	b) Whole seed-UVA – (a)Whole seed-Control	1.44	0.48978
	(d) De-hulled-UVA – (a) Whole seed-Control	3.64	0.01174
	(d) De-hulled-UVA– (b) Whole seed-UVA	2.20	0.15244
Grey Zero tannin	b) Whole seed-UVA – (a)Whole seed-Control	0.08	0.99998
	(d) De-hulled-UVA – (a) Whole seed-Control	0.18	0.99965
	(d) De-hulled-UVA– (b) Whole seed-UVA	0.09	0.99997

Table D.5: Multiple Comparison of Δb^*-values of green cotyledon lentil under visible light.

Seed Coat Type	Comparison	Estimate	Adj.p-value
Black	(c) Whole seed-Visible – (a) Whole seed-Control	-1.30	0.62113
	(e) De-hulled-Visible – (a) Whole seed-Control	-14.70	1.39E-07
	(e) De-hulled-Visible – (c) Whole seed- Visible	-13.39	3.26E-07
Grey	(c) Whole seed-Visible – (a) Whole seed-Control	-2.86	0.03175
	(e) De-hulled-Visible – (a) Whole seed-Control	-11.59	0.00003
	(e) De-hulled-Visible – (c) Whole seed- Visible	-8.73	0.00005
Green	(c) Whole seed-Visible – (a) Whole seed-Control	-3.97	0.01253
	(e) De-hulled-Visible – (a) Whole seed-Control	-12.51	9.23E-07
	(e) De-hulled-Visible – (c) Whole seed- Visible	-8.54	3.14E-05
Grey Zero tannin	(c) Whole seed-Visible – (a) Whole seed-Control	-0.75	0.91198
	(e) De-hulled-Visible – (a) Whole seed-Control	-10.86	2.04E-06
	(e) De-hulled-Visible – (c) Whole seed- Visible	-10.11	3.99E-06

Table D.6: Multiple Comparison of Δb^*-values of green cotyledon lentil under UVA.

Seed Coat Type	Comparison	Estimate	Adj.p-value
Black	(b) Whole seed-UVA – (a)Whole seed-Control	-0.02	0.99999
	(d) De-hulled-UVA – (a) Whole seed-Control	-10.12	4.53E-06
	(d) De-hulled-UVA– (b) Whole seed-UVA	-10.10	4.61E-06
Grey	(b) Whole seed-UVA – (a)Whole seed-Control	-1.44	0.42324
	(d) De-hulled-UVA – (a) Whole seed-Control	-11.35	0.000004
	(d) De-hulled-UVA– (b) Whole seed-UVA	-9.91	0.000002
Green	(b) Whole seed-UVA – (a)Whole seed-Control	-1.61	0.477841
	(d) De-hulled-UVA – (a) Whole seed-Control	-8.74	2.55E-05
	(d) De-hulled-UVA– (b) Whole seed-UVA	-7.13	0.000150
Grey Zero tannin	(b) Whole seed-UVA – (a)Whole seed-Control	-0.20	0.999358
	(d) De-hulled-UVA – (a) Whole seed-Control	-10.10	4.04E-06
	(d) De-hulled-UVA– (b) Whole seed-UVA	-9.90	4.86E-06

Table D.7: Multiple Comparison of ΔE^*-values of green cotyledon lentil under visible light.

Seed Coat Type	Comparison	Estimate	Adj.p-value
Black	(c) Whole seed-Visible – (a) Whole seed-Control	0.57	0.97372
	(e) De-hulled-Visible – (a) Whole seed-Control	22.72	2.19E-09
	(e) De-hulled-Visible – (c) Whole seed- Visible	22.15	3.02E-09
Grey	(c) Whole seed-Visible – (a) Whole seed-Control	4.50	0.02220
	(e) De-hulled-Visible – (a) Whole seed-Control	18.71	1.67 E-07
	(e) De-hulled-Visible – (c) Whole seed- Visible	14.21	2.18 E-06
Green	(c) Whole seed-Visible – (a) Whole seed-Control	5.29	0.000237
	(e) De-hulled-Visible – (a) Whole seed-Control	21.27	3.40E-10
	(e) De-hulled-Visible – (c) Whole seed- Visible	15.99	7.01E-09
Grey Zero tannin	(c) Whole seed-Visible – (a) Whole seed-Control	8.42	1.36E-05
	(e) De-hulled-Visible – (a) Whole seed-Control	20.57	1.68E-09
	(e) De-hulled-Visible – (c) Whole seed- Visible	12.15	4.41E-07

Table D.8: Multiple Comparison of ΔE^*-values of green lentil cotyledon under UVA.

Seed Coat Type	Comparison	Estimate	Adj.p-value
Black	(b) Whole seed-UVA – (a)Whole seed-Control	0.61	0.96579
	(d) De-hulled-UVA – (a) Whole seed-Control	3.64	0.02300
	(d) De-hulled-UVA– (b) Whole seed-UVA	3.03	0.06150
Grey	(b) Whole seed-UVA – (a)Whole seed-Control	-0.58	0.98661
	(d) De-hulled-UVA – (a) Whole seed-Control	1.16	0.85629
	(d) De-hulled-UVA– (b) Whole seed-UVA	1.74	0.59921
Green	(b) Whole seed-UVA – (a)Whole seed-Control	-0.55	0.94092
	(d) De-hulled-UVA – (a) Whole seed-Control	3.67	0.00407
	(d) De-hulled-UVA– (b) Whole seed-UVA	4.22	0.00144
Grey Zero tannin	(b) Whole seed-UVA – (a)Whole seed-Control	0.53	0.96834
	(d) De-hulled-UVA – (a) Whole seed-Control	1.30	0.56917
	(d) De-hulled-UVA– (b) Whole seed-UVA	0.77	0.88794

Table D.9: Multiple Comparison of ΔL^*-values of red cotyledon lentil under visible light.

Seed Coat Type	Comparison	Estimate	Adj.p-value
Black	(c) Whole seed-Visible—(a) Whole seed-Control	-0.64	0.96147
	(e) De-hulled-Visible — (a) Whole seed-Control	0.41	0.99227
	(e) De-hulled-Visible — (c) Whole seed- Visible	1.05	0.81333
Grey	(c) Whole seed-Visible—(a) Whole seed-Control	-0.61	0.99375
	(e) De-hulled-Visible — (a) Whole seed-Control	-2.90	0.37102
	(e) De-hulled-Visible — (c) Whole seed- Visible	-2.29	0.57821
Green	(c) Whole seed-Visible—(a) Whole seed-Control	-2.99	0.11553
	(e) De-hulled-Visible — (a) Whole seed-Control	-3.22	0.08385
	(e) De-hulled-Visible — (c) Whole seed- Visible	-0.22	0.99948
Grey Zero tannin	(c) Whole seed-Visible—(a) Whole seed-Control	-0.65	0.93941
	(e) De-hulled-Visible — (a) Whole seed-Control	-1.16	0.68345
	(e) De-hulled-Visible — (c) Whole seed- Visible	-0.50	0.97578
Colorless Zero tannin	(c) Whole seed-Visible—(a) Whole seed-Control	-1.56	0.44173
	(e) De-hulled-Visible — (a) Whole seed-Control	-1.47	0.49273
	(e) De-hulled-Visible — (c) Whole seed- Visible	0.08	0.99997

Table D.10: Multiple Comparison of ΔL^*-values of red cotyledon lentil under UVA.

Seed Coat Type	Comparison	Estimate	Adj.p-value
Black	(b) Whole seed-UVA — (a)Whole seed-Control	0.03	0.99998
	(d) De-hulled-UVA — (a) Whole seed-Control	-1.43	0.03881
	(d) De-hulled-UVA— (b) Whole seed-UVA	-1.46	0.03433
Grey	(b) Whole seed-UVA — (a)Whole seed-Control	0.99	0.72156
	(d) De-hulled-UVA — (a) Whole seed-Control	-0.32	0.99334
	(d) De-hulled-UVA— (b) Whole seed-UVA	-1.32	0.49517
Green	(b) Whole seed-UVA — (a)Whole seed-Control	0.04	0.99980
	(d) De-hulled-UVA — (a) Whole seed-Control	-1.82	7.1E-05
	(d) De-hulled-UVA— (b) Whole seed-UVA	-1.86	6.6E-05
Grey Zero tannin	(b) Whole seed-UVA — (a)Whole seed-Control	-0.20	0.97817
	(d) De-hulled-UVA — (a) Whole seed-Control	-1.63	0.00855
	(d) De-hulled-UVA— (b) Whole seed-UVA	-1.42	0.01996
Colorless Zero tannin	(b) Whole seed-UVA — (a)Whole seed-Control	-0.49	0.88756
	(d) De-hulled-UVA — (a) Whole seed-Control	-1.35	0.16665
	(d) De-hulled-UVA— (b) Whole seed-UVA	-0.86	0.53371

Table D.11: Multiple Comparison of Δa^*-values of red cotyledon lentil under visible light.

Seed Coat Type	Comparison	Estimate	Adj.p-value
Black	(c) Whole seed-Visible—(a) Whole seed-Control	-0.64	0.96147
	(e) De-hulled-Visible — (a) Whole seed-Control	0.41	0.99227
	(e) De-hulled-Visible — (c) Whole seed- Visible	1.05	0.81333
Grey	(c) Whole seed-Visible—(a) Whole seed-Control	-0.61	0.99375
	(e) De-hulled-Visible — (a) Whole seed-Control	-2.90	0.37102
	(e) De-hulled-Visible — (c) Whole seed- Visible	-2.29	0.57821
Green	(c) Whole seed-Visible—(a) Whole seed-Control	-2.99	0.11553
	(e) De-hulled-Visible — (a) Whole seed-Control	-3.22	0.08385
	(e) De-hulled-Visible — (c) Whole seed- Visible	-0.22	0.99948
Grey Zero tannin	(c) Whole seed-Visible—(a) Whole seed-Control	-0.65	0.93941
	(e) De-hulled-Visible — (a) Whole seed-Control	-1.16	0.68345
	(e) De-hulled-Visible — (c) Whole seed- Visible	-0.50	0.97578
Colorless Zero tannin	(c) Whole seed-Visible—(a) Whole seed-Control	-1.56	0.44173
	(e) De-hulled-Visible — (a) Whole seed-Control	-1.47	0.49273
	(e) De-hulled-Visible — (c) Whole seed- Visible	0.08	0.99997

Table D.12: Multiple Comparison of Δa^*-values of red cotyledon lentil under UVA.

Seed Coat Type	Comparison	Estimate	Adj.p-value
Black	(b) Whole seed-UVA — (a)Whole seed-Control	-0.05	0.99999
	(d) De-hulled-UVA — (a) Whole seed-Control	-0.79	0.92110
	(d) De-hulled-UVA— (b) Whole seed-UVA	-0.74	0.93522
Grey	(b) Whole seed-UVA — (a)Whole seed-Control	-1.05	0.95323
	(d) De-hulled-UVA — (a) Whole seed-Control	-1.14	0.93840
	(d) De-hulled-UVA— (b) Whole seed-UVA	-0.09	0.99999
Green	(b) Whole seed-UVA — (a)Whole seed-Control	-2.81	0.14984
	(d) De-hulled-UVA — (a) Whole seed-Control	-2.12	0.35607
	(d) De-hulled-UVA— (b) Whole seed-UVA	0.69	0.96702
Grey Zero tannin	(b) Whole seed-UVA — (a)Whole seed-Control	0.02	0.99999
	(d) De-hulled-UVA — (a) Whole seed-Control	0.22	0.99901
	(d) De-hulled-UVA— (b) Whole seed-UVA	0.19	0.99937
Colorless Zero tannin	(b) Whole seed-UVA — (a)Whole seed-Control	-0.003	1
	(d) De-hulled-UVA — (a) Whole seed-Control	-0.92	0.83040
	(d) De-hulled-UVA— (b) Whole seed-UVA	-0.92	0.83234

Table D.13: Multiple Comparison of Δb^*-values of red cotyledon lentil under visible light.

Seed Coat Type	Comparison	Estimate	Adj.p-value
Black	(c) Whole seed-Visible—(a) Whole seed-Control	-2.72	0.42182
	(e) De-hulled-Visible – (a) Whole seed-Control	-7.09	0.00584
	(e) De-hulled-Visible – (c) Whole seed- Visible	-4.37	0.09178
Grey	(c) Whole seed-Visible—(a) Whole seed-Control	1.55	0.45926
	(e) De-hulled-Visible – (a) Whole seed-Control	-8.98	1.19E-05
	(e) De-hulled-Visible – (c) Whole seed- Visible	-10.53	2.73E-06
Green	(c) Whole seed-Visible—(a) Whole seed-Control	-2.96	0.10229
	(e) De-hulled-Visible – (a) Whole seed-Control	-7.43	0.00024
	(e) De-hulled-Visible – (c) Whole seed- Visible	-4.48	0.01097
Grey Zero tannin	(c) Whole seed-Visible—(a) Whole seed-Control	-1.02	0.50136
	(e) De-hulled-Visible – (a) Whole seed-Control	-8.54	5.84E-07
	(e) De-hulled-Visible – (c) Whole seed- Visible	-7.53	1.94E-06
Colorless Zero tannin	(c) Whole seed-Visible—(a) Whole seed-Control	-2.77	0.041549
	(e) De-hulled-Visible – (a) Whole seed-Control	-7.71	2.41E-05
	(e) De-hulled-Visible – (c) Whole seed- Visible	-4.94	0.001044

Table D.14: Multiple Comparison of Δb^*-values of red cotyledon lentil under UVA.

Seed Coat Type	Comparison	Estimate	Adj.p-value
Black	(b) Whole seed-UVA – (a)Whole seed-Control	-2.06	0.66034
	(d) De-hulled-UVA – (a) Whole seed-Control	-5.52	0.02823
	(d) De-hulled-UVA– (b) Whole seed-UVA	-3.46	0.22369
Grey	(b) Whole seed-UVA – (a)Whole seed-Control	1.83	0.31487
	(d) De-hulled-UVA – (a) Whole seed-Control	-6.18	0.00031
	(d) De-hulled-UVA– (b) Whole seed-UVA	-8.01	3.3E-05
Green	(b) Whole seed-UVA – (a)Whole seed-Control	-1.89	0.41954
	(d) De-hulled-UVA – (a) Whole seed-Control	-4.64	0.00861
	(d) De-hulled-UVA– (b) Whole seed-UVA	-2.75	0.13743
Grey Zero tannin	(b) Whole seed-UVA – (a)Whole seed-Control	-0.09	0.99986
	(d) De-hulled-UVA – (a) Whole seed-Control	-5.07	6.9E-05
	(d) De-hulled-UVA– (b) Whole seed-UVA	-4.98	8.1E-05
Colorless Zero tannin	(b) Whole seed-UVA – (a)Whole seed-Control	0.91	0.80581
	(d) De-hulled-UVA – (a) Whole seed-Control	-5.75	0.00030
	(d) De-hulled-UVA– (b) Whole seed-UVA	-6.66	8.7E-05

Table D.15: Multiple Comparison of ΔE^*-values of red cotyledon lentil under visible light.

Seed Coat Type	Comparison	Estimate	Adj.p-value
Black	(c) Whole seed-Visible—(a) Whole seed-Control	-1.18	0.78036
	(e) De-hulled-Visible – (a) Whole seed-Control	1.60	0.55082
	(e) De-hulled-Visible – (c) Whole seed- Visible	2.78	0.12278
Grey	(c) Whole seed-Visible—(a) Whole seed-Control	1.15	0.70747
	(e) De-hulled-Visible – (a) Whole seed-Control	5.23	0.00120
	(e) De-hulled-Visible – (c) Whole seed- Visible	4.08	0.00731
Green	(c) Whole seed-Visible—(a) Whole seed-Control	0.92	0.93798
	(e) De-hulled-Visible – (a) Whole seed-Control	4.82	0.01832
	(e) De-hulled-Visible – (c) Whole seed- Visible	3.89	0.05890
Grey Zero tannin	(c) Whole seed-Visible—(a) Whole seed-Control	-0.23	0.99301
	(e) De-hulled-Visible – (a) Whole seed-Control	5.14	2.3E-05
	(e) De-hulled-Visible – (c) Whole seed- Visible	5.37	1.5E-05
Colorless Zero tannin	(c) Whole seed-Visible—(a) Whole seed-Control	-0.54	0.94933
	(e) De-hulled-Visible – (a) Whole seed-Control	2.27	0.07797
	(e) De-hulled-Visible – (c) Whole seed- Visible	2.82	0.02592

Table D.16: Multiple Comparison of ΔE^*-values of red cotyledon lentil under UVA.

Seed Coat Type	Comparison	Estimate	Adj.p-value
Black	(b) Whole seed-UVA – (a)Whole seed-Control	-0.16	0.99985
	(d) De-hulled-UVA – (a) Whole seed-Control	0.03	0.99999
	(d) De-hulled-UVA– (b) Whole seed-UVA	0.18	0.99973
Grey	(b) Whole seed-UVA – (a)Whole seed-Control	1.33	0.59161
	(d) De-hulled-UVA – (a) Whole seed-Control	1.99	0.24598
	(d) De-hulled-UVA– (b) Whole seed-UVA	0.66	0.94261
Green	(b) Whole seed-UVA – (a)Whole seed-Control	0.23	0.99969
	(d) De-hulled-UVA – (a) Whole seed-Control	1.97	0.52472
	(d) De-hulled-UVA– (b) Whole seed-UVA	1.74	0.62817
Grey Zero tannin	(b) Whole seed-UVA – (a)Whole seed-Control	0.18	0.99706
	(d) De-hulled-UVA – (a) Whole seed-Control	1.74	0.06289
	(d) De-hulled-UVA– (b) Whole seed-UVA	1.56	0.10405
Colorless Zero tannin	(b) Whole seed-UVA – (a)Whole seed-Control	0.44	0.97413
	(d) De-hulled-UVA – (a) Whole seed-Control	0.32	0.99190
	(d) De-hulled-UVA– (b) Whole seed-UVA	-0.12	0.99983

Table D.17: Multiple Comparison of ΔL^*-values of yellow cotyledon lentil under visible light.

Seed Coat Type	Comparison	Estimate	Adj.p-value
Black	(c) Whole seed-Visible—(a) Whole seed-Control	-0.36	0.97861
	(e) De-hulled-Visible — (a) Whole seed-Control	0.84	0.70339
	(e) De-hulled-Visible — (c) Whole seed- Visible	1.19	0.40180
Grey	(c) Whole seed-Visible—(a) Whole seed-Control	0.83	0.32842
	(e) De-hulled-Visible — (a) Whole seed-Control	1.94	0.00608
	(e) De-hulled-Visible — (c) Whole seed- Visible	1.10	0.13019
Green	(c) Whole seed-Visible—(a) Whole seed-Control	-0.81	0.80595
	(e) De-hulled-Visible — (a) Whole seed-Control	-1.06	0.62024
	(e) De-hulled-Visible — (c) Whole seed- Visible	-0.25	0.99651
Grey Zero tannin	(c) Whole seed-Visible—(a) Whole seed-Control	0.69	0.56235
	(e) De-hulled-Visible — (a) Whole seed-Control	1.89	0.01211
	(e) De-hulled-Visible — (c) Whole seed- Visible	1.19	0.12914
Colorless zero tannin	(c) Whole seed-Visible—(a) Whole seed-Control	0.95	0.13265
	(e) De-hulled-Visible — (a) Whole seed-Control	0.89	0.16103
	(e) De-hulled-Visible — (c) Whole seed- Visible	-0.05	0.99992

Table D.18: Multiple Comparison of ΔL^*-values of yellow cotyledon lentil under UVA.

Seed Coat Type	Comparison	Estimate	Adj.p-value
Black	(b) Whole seed-UVA — (a)Whole seed-Control	-1.23	0.38070
	(d) De-hulled-UVA — (a) Whole seed-Control	-2.71	0.01302
	(d) De-hulled-UVA— (b) Whole seed-UVA	-1.48	0.22973
Grey	(b) Whole seed-UVA — (a)Whole seed-Control	-0.36	0.90137
	(d) De-hulled-UVA — (a) Whole seed-Control	-0.24	0.97672
	(d) De-hulled-UVA— (b) Whole seed-UVA	0.12	0.99789
Green	(b) Whole seed-UVA — (a)Whole seed-Control	-0.71	0.86681
	(d) De-hulled-UVA — (a) Whole seed-Control	-2.70	0.02766
	(d) De-hulled-UVA— (b) Whole seed-UVA	-1.99	0.12142
Grey Zero tannin	(b) Whole seed-UVA — (a)Whole seed-Control	0.38	0.90931
	(d) De-hulled-UVA — (a) Whole seed-Control	-0.35	0.92848
	(d) De-hulled-UVA— (b) Whole seed-UVA	-0.73	0.50956
Colorless zero tannin	(b) Whole seed-UVA — (a)Whole seed-Control	-0.25	0.95200
	(d) De-hulled-UVA — (a) Whole seed-Control	-1.27	0.03267
	(d) De-hulled-UVA— (b) Whole seed-UVA	-1.02	0.09634

Table D.19: Multiple Comparison of Δa^*-values of yellow cotyledon lentil under visible light.

Seed Coat Type	Comparison	Estimate	Adj.p-value
Black	(c) Whole seed-Visible—(a) Whole seed-Control	-0.45	0.98764
	(e) De-hulled-Visible – (a) Whole seed-Control	-0.49	0.98246
	(e) De-hulled-Visible – (c) Whole seed- Visible	-0.05	0.99999
Grey	(c) Whole seed-Visible—(a) Whole seed-Control	-1.18	0.13225
	(e) De-hulled-Visible – (a) Whole seed-Control	-1.49	0.04495
	(e) De-hulled-Visible – (c) Whole seed- Visible	-0.31	0.95094
Green	(c) Whole seed-Visible—(a) Whole seed-Control	0.58	0.86679
	(e) De-hulled-Visible – (a) Whole seed-Control	1.85	0.07092
	(e) De-hulled-Visible – (c) Whole seed- Visible	1.27	0.28906
Grey Zero tannin	(c) Whole seed-Visible—(a) Whole seed-Control	-1.53	0.02463
	(e) De-hulled-Visible – (a) Whole seed-Control	-1.68	0.01465
	(e) De-hulled-Visible – (c) Whole seed- Visible	-0.13	0.99668
Colorless zero tannin	(c) Whole seed-Visible—(a) Whole seed-Control	-0.12	0.98795
	(e) De-hulled-Visible – (a) Whole seed-Control	-0.19	0.94141
	(e) De-hulled-Visible – (c) Whole seed- Visible	-0.07	0.99869

Table D.20: Multiple Comparison of Δa^*-values of yellow cotyledon lentil under UVA.

Seed Coat Type	Comparison	Estimate	Adj.p-value
Black	(b) Whole seed-UVA – (a)Whole seed-Control	-0.02	0.99999
	(d) De-hulled-UVA – (a) Whole seed-Control	2.54	0.12778
	(d) De-hulled-UVA– (b) Whole seed-UVA	2.55	0.12432
Grey	(b) Whole seed-UVA – (a)Whole seed-Control	0.31	0.95151
	(d) De-hulled-UVA – (a) Whole seed-Control	0.18	0.99356
	(d) De-hulled-UVA– (b) Whole seed-UVA	-0.13	0.99795
Green	(b) Whole seed-UVA – (a)Whole seed-Control	0.44	0.94516
	(d) De-hulled-UVA – (a) Whole seed-Control	3.01	0.00390
	(d) De-hulled-UVA– (b) Whole seed-UVA	2.57	0.01138
Grey Zero tannin	(b) Whole seed-UVA – (a)Whole seed-Control	-1.01	0.17378
	(d) De-hulled-UVA – (a) Whole seed-Control	-0.10	0.99888
	(d) De-hulled-UVA– (b) Whole seed-UVA	0.91	0.24938
Colorless zero tannin	(b) Whole seed-UVA – (a)Whole seed-Control	-0.62	0.19611
	(d) De-hulled-UVA – (a) Whole seed-Control	1.81	0.00028
	(d) De-hulled-UVA– (b) Whole seed-UVA	2.43	2.21E-05

Table D.21: Multiple Comparison of Δb^*-values of yellow cotyledon lentil under visible light.

Seed Coat Type	Comparison	Estimate	Adj.p-value
Black	(c) Whole seed-Visible—(a) Whole seed-Control	1.18	0.96923
	(e) De-hulled-Visible — (a) Whole seed-Control	-12.21	0.00061
	(e) De-hulled-Visible — (c) Whole seed- Visible	-11.22	0.00029
Grey	(c) Whole seed-Visible—(a) Whole seed-Control	-0.78	0.94825
	(e) De-hulled-Visible — (a) Whole seed-Control	-14.61	0.00000
	(e) De-hulled-Visible — (c) Whole seed- Visible	-13.76	0.00000
Green	(c) Whole seed-Visible—(a) Whole seed-Control	1.43	0.93369
	(e) De-hulled-Visible — (a) Whole seed-Control	-7.29	0.01892
	(e) De-hulled-Visible — (c) Whole seed- Visible	-8.72	0.00595
Grey zero tannin	(c) Whole seed-Visible—(a) Whole seed-Control	-2.45	0.44163
	(e) De-hulled-Visible — (a) Whole seed-Control	-13.90	0.00000
	(e) De-hulled-Visible — (c) Whole seed- Visible	-11.45	0.00006
Colorless zero tannin	(c) Whole seed-Visible—(a) Whole seed-Control	-4.42	0.02731
	(e) De-hulled-Visible — (a) Whole seed-Control	-12.57	0.00000
	(e) De-hulled-Visible — (c) Whole seed- Visible	-8.28	0.00032

Table D.22: Multiple Comparison of Δb^*-values of yellow cotyledon lentil under UVA.

Seed Coat Type	Comparison	Estimate	Adj.p-value
Black	(b) Whole seed-UVA — (a)Whole seed-Control	1.37	0.94864
	(d) De-hulled-UVA — (a) Whole seed-Control	-6.86	0.03234
	(d) De-hulled-UVA— (b) Whole seed-UVA	-8.22	0.01084
Grey	(b) Whole seed-UVA — (a)Whole seed-Control	0.06	0.99999
	(d) De-hulled-UVA — (a) Whole seed-Control	-9.51	4.6E-05
	(d) De-hulled-UVA— (b) Whole seed-UVA	-9.57	4.4E-05
Green	(b) Whole seed-UVA — (a)Whole seed-Control	-0.73	0.99415
	(d) De-hulled-UVA — (a) Whole seed-Control	-5.39	0.01582
	(d) De-hulled-UVA— (b) Whole seed-UVA	-4.66	0.16442
Grey Zero tannin	(b) Whole seed-UVA — (a)Whole seed-Control	-0.93	0.95813
	(d) De-hulled-UVA — (a) Whole seed-Control	-12.47	3.23E-05
	(d) De-hulled-UVA— (b) Whole seed-UVA	-11.53	6.42E-05
Colorless zero tannin	(b) Whole seed-UVA — (a)Whole seed-Control	-0.14	0.99995
	(d) De-hulled-UVA — (a) Whole seed-Control	-9.39	0.00010
	(d) De-hulled-UVA— (b) Whole seed-UVA	-9.26	0.00012

Table D.23: Multiple Comparison of ΔE^*-values of yellow cotyledon lentil under visible light.

Seed Coat Type	Comparison	Estimate	Adj.p-value
Black	(c) Whole seed-Visible—(a) Whole seed-Control	1.56	0.90124
	(e) De-hulled-Visible — (a) Whole seed-Control	5.55	0.01144
	(e) De-hulled-Visible — (c) Whole seed- Visible	3.98	0.24642
Grey	(c) Whole seed-Visible—(a) Whole seed-Control	-0.65	0.96478
	(e) De-hulled-Visible — (a) Whole seed-Control	5.91	0.00130
	(e) De-hulled-Visible — (c) Whole seed- Visible	6.56	0.00056
Green	(c) Whole seed-Visible—(a) Whole seed-Control	-1.12	0.77710
	(e) De-hulled-Visible — (a) Whole seed-Control	5.10	0.00264
	(e) De-hulled-Visible — (c) Whole seed- Visible	6.22	0.00057
Grey zero tannin	(c) Whole seed-Visible—(a) Whole seed-Control	-0.89	0.95601
	(e) De-hulled-Visible — (a) Whole seed-Control	7.30	0.00179
	(e) De-hulled-Visible — (c) Whole seed- Visible	8.20	0.00072
Colorless zero tannin	(c) Whole seed-Visible—(a) Whole seed-Control	-1.13	0.82313
	(e) De-hulled-Visible — (a) Whole seed-Control	6.16	0.00128
	(e) De-hulled-Visible — (c) Whole seed- Visible	7.28	0.00033

Table D.24: Multiple Comparison of ΔE^*-values of yellow cotyledon lentil under UVA.

Seed Coat Type	Comparison	Estimate	Adj.p-value
Black	(b) Whole seed-UVA — (a)Whole seed-Control	1.21	0.95725
	(d) De-hulled-UVA — (a) Whole seed-Control	0.84	0.98857
	(d) De-hulled-UVA— (b) Whole seed-UVA	-0.37	0.99951
Grey	(b) Whole seed-UVA — (a)Whole seed-Control	0.19	0.99969
	(d) De-hulled-UVA — (a) Whole seed-Control	0.96	0.87523
	(d) De-hulled-UVA— (b) Whole seed-UVA	0.77	0.93788
Green	(b) Whole seed-UVA — (a)Whole seed-Control	1.13	0.77173
	(d) De-hulled-UVA — (a) Whole seed-Control	3.55	0.02849
	(d) De-hulled-UVA— (b) Whole seed-UVA	2.42	0.16849
Grey zero tannin	(b) Whole seed-UVA — (a)Whole seed-Control	-0.47	0.99607
	(d) De-hulled-UVA — (a) Whole seed-Control	5.49	0.01303
	(d) De-hulled-UVA— (b) Whole seed-UVA	5.95	0.00766
Colorless zero tannin	(b) Whole seed-UVA — (a)Whole seed-Control	0.28	0.99874
	(d) De-hulled-UVA — (a) Whole seed-Control	2.81	0.13458
	(d) De-hulled-UVA— (b) Whole seed-UVA	2.53	0.19776

APPENDIX E: PLOT, ANALYSIS AND MODELING SCRIPTS

E.1: Sample Analysis and Plot R Script for Measurement Repeatability Study.

```
#Set Working Directory

# Assessing Repeatability of the Measuring Instrument


setwd("C:/Users/nij048/Desktop/Preliminary_Study(Spectroscopy)/Instrument
_Repeatability_test")


Indianhead <- read.csv("Black2.csv", header=T)


#Load the Required Package

  install.packages("ggplot2") #Plotting package
  library(ggplot2)
  install.packages("prospectr") #Smoothing package
  library(prospectr)

   #Set Font Type
   windowsFonts(A = windowsFont("Times New Roman"))

 #Load Optical Properties Data
 x<-Indianhead$Wavelength
 y1<-Indianhead$S1
 y2<-Indianhead$S2
 y3<-Indianhead$S3
 y4<-Indianhead$S4
 y5<-Indianhead$S5
 y6<-Indianhead$S6
 y7<-Indianhead$S7
 y8<-Indianhead$S8
 y9<-Indianhead$S9
 y10<-Indianhead$S10

#Apply Moving Average Filter
 x2 <- movav(x,w=11)
 s1 <- movav(y1, w = 11)
 s2 <- movav(y2, w = 11)
 s3 <- movav(y3, w = 11)
 s4 <- movav(y4, w = 11)
 s5 <- movav(y5, w = 11)
 s6 <- movav(y6, w = 11)
 s7 <- movav(y7, w = 11)
 s8 <- movav(y8, w = 11)
 s9 <- movav(y9, w = 11)
 s10 <- movav(y10, w = 11)


#Descriptive Statistics Plots for Indianhead (Black)

 # Create Data frame with smoothed Spectra
 Indianhead2 <- data.frame(x2,s1,s2,s3,s4,s5,s6,s7,s8,s9,s10)
```

```
  View(Indianhead2)

  #Mean and Standard Deviation
  #install.packages("matrixStats")
  library(matrixStats)
  d1<-rowMeans(Indianhead2[,-1]) #Compute means of smoothed spectra
  d2<-rowSds(as.matrix(Indianhead2[,-1])) # Compute Standard deviation of
smoothed spectra

  #Write Mean and SD into the file
  Indianhead3 <- (data.frame(Indianhead2,d1,d2))
  write.csv(Indianhead3,file="Smoothed_Black.csv")

  # Standard Deviation Lines for the plots
  d3<-d1+d2 #  Add standard deviation to the mean
  d4<-d1-d2 #  Subtract standard deviation from the mean

  # Minimum and Maximum Standard Deviation
  min(d2) #0.85, mean = 5.21, Minimum Standard deviation
  max(d2) #1.44, mean = 36.37, Maximum Standard deviation

  #Plotting Mean and Standard Deviations

  library(ggplot2)
  par(mfrow=c(3,2)) #set plot window
  par(mar=c(4,4.5,1,1)) #set margins
  plot(x2,d4,family="A", type="p",lty=c(2,2), xlab="", ylab="Reflectivity
(%)",
         col=c('red', 'red'), cex = 0.1,cex.lab=1.5, lwd = 0.1,
           sub="(a) Indianhead (Black)", ylim = c(-5,50), las=2)#Plot
Upper Standard Deviation
  points(x2,d3,family="A", type="p",lty=c(2,2), xlab="",
ylab="Reflectivity (%)",
       col=c('red', 'red'), cex = 0.1,cex.lab=1.5, lwd = 0.1,
           sub="(a) Indianhead (Black)", ylim = c(-5,50), las=2)#Plot
Lower Standard Deviation
  points(x2,d1, type = 'l', lwd=4, col='black')#Plot Mean
  axis(1, seq(-100,1200,100), las=2) #Granulate x-axis
  names<-c("+/- SD","Mean")#Create legend names
  #Insert Legend
  legend('topleft', legend=names, col=c('red', 'black'),pch=15,
         bg= ("white"), horiz=F)
  text(950,10, labels = "Max. SD = 1.44%", col="black", cex=0.7)
  text(950,6, labels = "Min. SD = 0.85%", col = "black", cex=0.7)
```

E.2: Sample Analysis and Plot R Script for Within-sample Variability Study.

```
#Within-sample Variation

 #Set Working Directory

setwd("C:/Users/nij048/Desktop/Preliminary_Study(Spectroscopy)/Within_Sam
ple_Variation")

 #CDCQG_4(Mottled Green)
 CDCQG_4 <- read.csv("CDCQG_4_MottledGreen.csv", header=T)
 CDCQG_4

 #Load Spectra as Objects
 x<-CDCQG_4 $Wavelength
 x3<-movav(x,w=11)
 y1<- CDCQG_4$S1
 y2<- CDCQG_4$S2
 y3<- CDCQG_4$S3
 y4<- CDCQG_4$S4
 y5<- CDCQG_4$S5
 y6<- CDCQG_4$S6
 y7<- CDCQG_4$S7
 y8<- CDCQG_4$S8
 y9<- CDCQG_4$S9
 y10<- CDCQG_4$S10

 #Applying a Moving Average Filter
 p1 <- movav(y1, w = 11)
 p2 <- movav(y2, w = 11)
 p3 <- movav(y3, w = 11)
 p4 <- movav(y4, w = 11)
 p5 <- movav(y5, w = 11)
 p6 <- movav(y6, w = 11)
 p7 <- movav(y7, w = 11)
 p8 <- movav(y8, w = 11)
 p9 <- movav(y9, w = 11)
 p10 <- movav(y10, w = 11)

 #Store Smoothed spectra in a Data frame
 CDCQG_4_1 <- data.frame(x3,p1,p2,p3,p4,p5,p6,p7,p8,p9,p10)

 #Compute Means and Standard Deviation
 library(matrixStats)
 d5<-rowMeans(CDCQG_4_1[,-1]) #Compute means of smoothed spectra
 d6<-rowSds(as.matrix(CDCQG_4_1[,-1])) # Compute Standard deviation of
smoothes spectra

 #Save mean and Standard Deviation
 CDCQG_4_2  <- (data.frame(CDCQG_4_1 ,d5,d6))
 write.csv( Tan3,file="Smoothed_Dark_tan.csv")

 # Standard Deviation Lines
 d7<-d5+d6 #  Add standard deviation to the mean
 d8<-d5-d6 #  Subtract standard deviation from the mean
```

```
 # Minimum and Maximum Standard Deviation
 min(d6) # Minimum Standard deviation
 max(d6)  #Maximum Standard deviation

 #Plotting Mean and Standard Deviations

 library(ggplot2)
 # par(mfrow=c(1,2)) #set plot window
 #par(mar=c(10,4.5,5,1)) #set margins
 matplot(x3, cbind(d7,d8),family="A",type="p",lty=c(2,2), xlab="",
ylab="",
         col=c('red', 'red'), cex = 0.1,cex.lab=1.5, lwd = 0.1,
           sub="(a) Indianhead(Black)", ylim = c(-5,60), las=2)#Plot +/-
Standard Deviation
 points(x3,d5, type = 'l', lwd=4, col='black')#Plot Mean
 axis(1, seq(-100,1200,100), las=2) #Granulate -axis
 names<-c("+/- SD","Mean")#Create legend names
 #Insert Legend
 legend('topleft', legend=names, col=c('red', 'black'),pch=15,
        bg= ("white"), horiz=F)
 text(950,10, labels = "Max. SD = 3.20%", col="black", cex=0.7)
 text(950,6, labels = "Min. SD = 0.50%", col = "black", cex=0.7)
```

E.3: Sample R Plot Script for Seed Coat Transmission.

```
 # Set Working Directory
 setwd("C:/Users/nij048/Desktop/BACKUP2/MEMORY
CARD/LentilData/Transmission_Rerun")


 # Load Transmission Plot Data file as an object

 transmission <- read.csv('Transmission_plot.csv', header=T)
 names(transmission)

 # Create variables from Seed Coat Transmission
 x<-transmission$Wavelength
 x2<-movav(x,w=11)
 y1<-transmission$ZT4..Zero.tan.
 y2<-transmission$Indianhead..Black.
 y3<-transmission$X7311.1.Black.
 y4<-transmission$X7312.g.Mottled_black.
 y5<-transmission$IBC.1274.2..Light_tan.
 y6<-transmission$X7427_12.Light_tan.
 y7<-transmission$CDC.Kermit.light_tan.
 y8<-transmission$CDC.Rosebud..Tan.
 y9<-transmission$IBC.1264.1.Tan.
 y10<-transmission$IBC.929R..Grey.
 y11<-transmission$SB4.IBC929.Grey..
 y12<-transmission$CDC.KR.2..Grey.
 y13<-transmission$CDC.Marble...Mottled.grey.
 y14<-transmission$CDC.Maxim..Grey.
 y15<-transmission$IBC.1264.3...Light_grey.
 y16<-transmission$CDC.SB.3..Grey.
 y17<-transmission$CDC.Greenstar.Light_green.
 y18<-transmission$CDC.QG.3..Green.
 y19<-transmission$CDC.QG.4.Mottled_green.
 y20<-transmission$CDC.Robin..Brown.

#Create names for Legend and store in a variable
 Genotypes <- c("ZT4 (Zero tannin)","Indianhead (Black)",
"7311-1 (Black)","7312g (Mottled black)", "IBC 1274-2 (Light tan)","7427-
12 (Tan)","CDC Kermit (Light tan)", "CDC Rosebud (Tan)", "IBC 1264-1
(Tan)","IBC 92GR (Grey)", "SB4(IBC 92G) (Grey)","CDC KR-2 (Grey)","CDC
Marble (Mottled grey)","CDC Maxim (Grey)", "IBC 1264-3 (Light grey)","CDC
SB-3 (Grey)", "CDC Greenstar (Light green)", "CDC QG-3 (Green)","CDC QG-4
(Mottled green)", "CDC Robin (Brown)")

# Plots of all Genotypes on one Panel
 #install.packages("ggplot2")
 library(ggplot2)
 par(mfrow=c(1,1)) #Set Plot window
 par(mar=c(5,5,4,4)) #Set Plot margins

matplot(x,cbind(y1,y2,y3,y4,y5,y6,y7,y8,y9,y10,y11,y12,y13,y14,
        y15,y16,y17,y18,y19,y20),
          type="l",lty=c(1,1), xlab="Wavelength (nm)",
ylab="Transmission (%)", lwd=4,
```

```
            col=c('khaki', 'black','turquoise4','slategrey',
'tan2','thistle', 'blue', 'coral', "deeppink", 'grey',
'tan','lightskyblue1', 'gold', 'lightpink4', 'yellow4', 'purple','green',
'darkgreen','darkolivegreen3','brown'),
                cex = 0.5,cex.lab=1.5, yaxs="i",
                 ylim = c(0,5),las=2)
          axis(1, seq(-100,1000,50),las=2) #Customize x-axis
        legend("topleft", legend=Genotypes, text.font=2,
col=c('khaki', 'black','turquoise4','slategrey', 'tan2','thistle',
'blue', 'coral', "deeppink", 'grey',  'tan','lightskyblue1', 'gold',
'lightpink4', 'yellow4', 'purple','green',
'darkgreen','darkolivegreen3','brown'),pch=15,
                      bg= ("white"), horiz=F, cex = 0.5)

 # Make Grouped Plots based on major seed coat classes

  par(mfrow=c(3,2)) #set plot window
  par(mar=c(5,4.5,1,1)) #set margins

  #Plot for Zero Tannin

  matplot(x, cbind(y1),
        type="l",lty=c(1,1), xlab="", cex.sub=1.5,
        sub="(a) Zero  tannin", ylab="Transmission (%)", lwd=4,
        col=c('khaki'), cex = 2,cex.lab=1.5, yaxs="i",
        ylim = c(0,6),las=2)
        axis(1, seq(-100,1000,50),las=2)
    # Create Legend
     legend("topleft",text.font=2, legend="ZT 4 (Zero tannin)",
col='khaki',pch=15,bg= ("white"), horiz=F, cex = 1)

  #Black and its Variants

  matplot(x, cbind(y2,y3,y4),
        type="l",lty=c(1,1), xlab="",
        sub="(b) Black & variants", ylab="", cex.sub=1.5, lwd=4,
        col=c('black','turquoise4','slategrey'),
        cex = 2,cex.lab=1.5, yaxs="i",ylim = c(0,6),las=2)
        axis(1, seq(-100,1000,50),las=2)
  # Create Legend
   legend("topleft", text.font=2,legend=Genotypes[2:4],
col=c('black','turquoise4','slategrey'),pch=15,
       bg= ("white"), horiz=F, cex = 1)

  #Tan and its Variants

  matplot(x, cbind(y5,y6,y7, y8, y9),
        type="l",lty=c(1,1), xlab="", ylab="Transmission (%)",
cex.sub=1.5, sub="(c) Tan & variants", lwd=4,
        col=c( 'cyan','thistle', 'blue', 'coral', "deeppink"), cex =
2,cex.lab=1.5, yaxs="i",ylim = c(0,6),las=2)
        axis(1, seq(-100,1000,50),las=2)
  # Create Legend
```

```
  legend("topleft", text.font=2,legend=Genotypes[5:9],    col=c(
'cyan','thistle', 'blue', 'coral', "deeppink"),pch=15,
       bg= ("white"), horiz=F, cex = 0.8)

  #Grey and its Variants

  matplot(x, cbind(y10,y11,y12, y13, y14,y15,y16),
         type="l",lty=c(1,1), xlab="", cex.sub=1.5,
         sub="(d) Grey & variants", ylab="", lwd=3,
         col=c('grey',  'tan','lightskyblue1', 'gold',   'lightpink4',
'yellow4', 'purple'), cex = 2,cex.lab=1.5, yaxs="i",ylim = c(0,6),las=2)
              axis(1, seq(-100,1000,50),las=2)
 # Create Legend
 legend("topleft", text.font=2,legend=Genotypes[10:16], col=c('grey',
'tan','lightskyblue1', 'gold', 'lightpink4', 'yellow4', 'purple'),pch=15,
       bg= ("white"), horiz=F, cex = 0.7)

  #Green and its Variants

  library(ggplot2)
  matplot(x, cbind(y17,y18,y19),
        type="l",lty=c(1,1), xlab="Wavelength (nm)",   ylab="Transmission
(%)", cex.sub=1.3, sub="(e) Green & variants", lwd=4,
        col=c('green', 'darkgreen','darkolivegreen3'), cex =
2,cex.lab=1.5, yaxs="i",ylim = c(0,6),las=2)
        axis(1, seq(-100,1000,50),las=2)
  legend("topleft", text.font=2,legend=Genotypes[17:19], col=c('green',
'darkgreen','darkolivegreen3'),pch=15,
       bg= ("white"), horiz=F, cex = 0.8)

  #Brown

  library(ggplot2)
  matplot(x, cbind(y20),
        type="l",lty=c(1,1), xlab="Wavelength (nm)", ylab="",
cex.sub=1.3, sub="(f) Brown", lwd=4,
        col=c('brown'), cex = 2,cex.lab=1.5, yaxs="i",
        ylim = c(0,6),las=2)
        axis(1, seq(-100,1000,50),las=2)
   # Create Legend
  legend("topleft", text.font=2,legend=Genotypes[20],
col=c('brown'),pch=15,
         bg= ("white"), horiz=F, cex = 1)
```

E.4: Transmission Analysis R Script.

```
#Set Working Directory
setwd("C:/Users/nij048/Desktop/LentilData/Transmission_Rerun")


#Load Transmission Data as an object
transmission<- read.csv("transmission-contrasts.csv", header=T)
names(transmission) #confirm object is loaded

# Analysis in the UV Region

#Compute Commulative UV Transmission
Cum_UV <- rowSums(transmission[1:nrow(transmission),2:236])
View(Cum_UV) #View computations

Cum_UV <- ifelse(Cum_UV<=0,0.00000000001,Cum_UV) #Remove zero
                                          #inflation

# Write Cumulative UV Transmission to Original Excel File
transmission_2 <- data.frame(transmission,Cum_UV)
write.csv(transmission_2, file = "transmission-2.csv")


#Subset data with only two columns
Line <- transmission$Line
transmission_cum <- data.frame(Line,Cum_UV)

#Data Cleaning
#Boxplot and outlier detection
  par(mar=c(10,4,4,2)) #Set Plot margins
  boxplot(transmission_cum$Cum_UV~transmission_cum$Line,
          las=2, col="tan", xlab= "",
             ylab = "Cummulative UV Transmission")$out

 # Finding which rows the outliers are
  # Store outliers in a vector
  outliers <-
boxplot(transmission_cum$Cum_UV~transmission_cum$Line,las=2, col="tan",
xlab= "",
               ylab = "Cummulative UV Transmission")$out
  #Identify rows containing outliers
  transmission_cum[which(transmission_cum$Cum_UV %in% outliers),]
  #Removing outliers
  transmission_cum <- transmission_cum[-which(transmission_cum$Cum_UV
%in% outliers),]

  #Data Modeling: Effect of Seed Coat Color on NIR Transmission

  # Model Using Glm
  UV_Model1 <- glm(Cum_UV~Line, data=transmission_cum)
  summary(UV_Model1)

  #ANOVA
  anova(UV_Model1, test = "F")#ANOVA with F-test
```

```
   #Highly significant differences in UV Transmission exist    among
genotypes

   #Checking Model Assumptions
   par(mfrow=c(2,2))
   par(mar=c(4,4,4,4))
   plot(UV_Model)
   #Assumption of normality of errors and homogeneity of variance
reasonably met

   #Post-hoc Testing
   TUKEY<-TukeyHSD(aov(UV_Model))

   # Convert Post-hoc Test Results to a Dataframe& export as CSV

   # install.packages("broom") #Install desired package
   library(broom)
   res <- tidy(TUKEY)
   write.csv(res, file="UV1 Tukey.csv") #Export Dataframe

   #Reordered Boxplot with Means
   par(mfrow=c(1,1))#Set Plot Window
   par(mar=c(10,4,2,3))#Set Plot Margin

   # Reorder Data
   transmission_cum$Line <- with(transmission_cum,
reorder(Line,Cum_UV,mean,na.rm=T))
   #Boxplot
   a <- boxplot(transmission_cum$Cum_UV~transmission_cum$Line,
           las=2, col="white", xlab= "", cex.lab=0.9,
           ylab = "Cummulative UV Transmission")

   # Add Means to Plot
    # Get the group means
    means <- by(transmission_cum$Cum_UV, transmission_cum$Line, mean)
    # Plot symbols for each mean, centered
    points(means, pch = 23, cex = 0.8,
          bg = "red")




   # Analysis in the VIS Region

   #Compute Commulative VIS Transmission
   Cum_VIS <-
rowSums(na.omit(transmission)[1:nrow(na.omit(transmission)),236:901])
   View(Cum_VIS)

   Cum_VIS <- ifelse(Cum_VIS<=0,0.00000000001,Cum_VIS)

   # Write Commulative VIS Transmission to Original Excel File
```

```
   transmission_2 <- data.frame(transmission,Cum_VIS)
   write.csv(transmission_2, file = "transmission-2.csv")


   #Subset data with only two columns
   Line <- transmission$Line
   transmission_VIS <- data.frame(Line,Cum_VIS)
   transmission_VIS

   # Data Cleaning

   # Outlier Detection and Removal

   #Boxplot Identifying Outliers
   par(mar=c(9,4,4,2)) #Set Plot margins
   boxplot(transmission_VIS$Cum_VIS~transmission_VIS$Line,
           las=2, col="tan", xlab= "",
           ylab = "Cummulative VIS Transmission")$out

   # Finding which rows the outliers are
   # Store outliers in a vector
   outliers <-
boxplot(transmission_VI$Cum_VIS~transmission_VIS$Line,las=2, col="tan",
xlab="Genotype",
                ylab = "Cummulative VIS Transmission")$out
   #Identify rows containing outliers
   transmission_VIS[which(transmission_VIS$Cum_VIS %in outliers),]
   #Removing outliers
   transmission_VIS <- transmission_VIS[-which(transmission_VIS$Cum_VIS
%in% outliers),]

   #Data Modelling: Effect of Seed Coat Color on NIR #Transmission
   # Model Using Glm
   VIS_Model1 <- glm(Cum_VIS~Line, data= transmission_VIS)
   summary(VIS_Model1)

   #ANOVA
   anova(VIS_Model1, test = "F")
   #Highly significant differences in UV Transmission exist among
genotypes

   #Checking Model Assumptions
   par(mfrow=c(2,2))
   par(mar=c(4,4,4,4))
   plot(VIS_Model1)
   #Assumption of normality of errors and homogeneity of variance
reasonably met

   #Post-hoc Testing
   TUKEY<-TukeyHSD(aov(VIS_Model1))
   # Convert Post-hoc Test Results to a Dataframe& export as Csv

    res <- tidy(TUKEY)
```

```
    write.csv(res, file="VIS Tukey.csv") #Export Dataframe

   #Boxplot
   par(mfrow=c(1,1))
   par(mar=c(10,4,2,3))
   # Reorder Data
   transmission_VIS$Line <- with(transmission_VIS,
reorder(Line,Cum_VIS,mean,na.rm=T))
   a <- boxplot(transmission_VIS$Cum_VIS~transmission_VIS$Line,
               las=2, col="white", xlab= "", cex.lab=0.9,
               ylab = "Cummulative VIS Transmission")

   # Add Means to Plot
   # Get the group means
   means <- by(transmission_VIS$Cum_VIS, transmission_VIS$Line, mean)
   # Plot symbols for each mean, centered
   points(means, pch = 23, cex = 0.8,
          bg = "red")




   # Analysis in the NIR Region

   #Compute Commulative NIR Transmission
   Cum_NIR <-
rowSums(na.omit(transmission)[1:nrow(na.omit(transmission)),902:1240])

   Cum_NIR <- ifelse(Cum_NIR<=0,0.00000000001,Cum_NIR)

   #Subset data with only two columns
   Line <- transmission_2$Line
   transmission_NIR <- data.frame(Line,Cum_NIR)

   # Data Cleaning and Visualizations

   # Outlier Detection and Removal

   #Boxplot Indicating Outliers
   par(mar=c(10,4,4,2)) #Set Plot margins
   boxplot(transmission_NIR$Cum_NIR~transmission_NIR$Line,
           las=2, col="tan", xlab= "",
           ylab = "Cummulative VIS Transmission")$out
   # Store outliers in a vector
   outliers <-
boxplot(transmission_NIS$Cum_NIR~transmission_NIR$Line,las=2, col="tan",
xlab= "",
                        ylab = "Cummulative VIS Transmission")$out
   #Identify rows containing outliers
   transmission_NIR[which(transmission_NIR$Cum_NIR %in% outliers),]
   #Removing outliers
   transmission_NIR <- transmission_NIR[-which(transmission_NIR$Cum_NIR
%in% outliers),]
```

```
   #Data Modeling: Effect of Seed Coat Color on NIR Transmission

   # Model Using Glm
   NIR_Model1 <- glm(Cum_NIR~Line, data= transmission_NIR)
   summary(NIR_Model1)

   #ANOVA
   anova(NIR_Model1, test = "F")
   #Highly significant differences in UV Transmission exist among
genotypes

   #Checking Model Assumptions
   par(mfrow=c(2,2))
   par(mar=c(4,4,4,4))
   plot(NIR_Model1)
   #Assumption of normality of errors and homogeneity of variance
reasonably met

   #Post-hoc Testing
   TUKEY<-TukeyHSD(aov(NIR_Model1))
   # Convert Post-hoc Test Results to a Dataframe &export as Csv

    res <- tidy(TUKEY)

   write.csv(res, file="NIR Tukey.csv") #Export Dataframe

   #Boxplot
   par(mfrow=c(1,1))
   par(mar=c(10,4,2,3))
   # Reorder Data
   transmission_NIR$Line <- with(transmission_NIR,
reorder(Line,Cum_NIR,mean,na.rm=T))
   a <- boxplot(transmission_NIR$Cum_NIR~transmission_NIR$Line,
                las=2, col="white", xlab= "", cex.lab=0.9,
                ylab = "Cummulative NIR Transmission")

   # Add Means to Plot
   # Get the group means
   means <- by(transmission_NIR$Cum_NIR, transmission_NIR$Line, mean)
   # Plot symbols for each mean, centered
   points(means, pch = 23, cex = 0.8,
          bg = "red")



   #
   #
   #
   #
   #
   #
   #
   #
```

E.5: Sample Color Analysis/Plots R Script (Chapter Five).

```
# Set Working Directory

setwd("C:/Users/nij048/Desktop/PHOTODEGRADATION")

# Read in Color Data as an objec

color_data <- read.csv("cot_colorData.csv", header = T)
color_data #Confirm data is stored in object
names(color_data) #Check columns

# Compute Color Differences

# Change in L-value
L_diff <- color_data$L_treated-color_data$L_initial
L_diff

# Change in a-value
a_diff <- color_data$a_treated-color_data$a_initial
a_diff

# Change in b-value
b_diff <- color_data$b_treated-color_data$b_initial
b_diff

#Overall Color Difference
col_diff <- sqrt((L_diff)^2+(a_diff)^2+ (b_diff)^2)
col_diff

# Write Computations into Original File
color_data2 <- data.frame(color_data,L_diff,a_diff,b_diff, col_diff)
write.csv(color_data2, file="Color Diff_Data2.csv")

# Grouped Barplots with Error Bars
  #Using reformatted color data

#Install and Load required packages
#install.packages("plyr")
library(plyr)
library(ggplot2)

par(mfrow=c(2,2)) #set plot window
par(mar=c(4,4,0.5,0.5)) #set margins

# L-Values
L_plot <- read.csv("L_data.csv", header=T)

# Barplot with Error Bars
barCenters <-  barplot(tapply(
L_plot$L_diff,list(L_plot$Treatment,L_plot$Cot_Color),mean),
                       col=c("black", "burlywood4", "Blue", "Green",
"Red","khaki" ),
                       beside=T,ylab="",xlab="", ylim=c(-6,10),cex.axis =
1, cex.lab = 1.5)
# y-axis Label
```

```
         mtext(text = "Mean   L*",
         side = 2, #side 2 = left
         line = 2)
         abline(h=0)#adds line on x axis
          #Add Error Bars
          tabbedMeans <- tapply( L_plot$L_diff,list(L_plot
$Treatment,L_plot$Cot_Color),mean)
          tabbedSd<-  tapply(
L_plot$L_diff,list(L_plot$Treatment,L_plot$Cot_Color),sd)
          arrows(barCenters, tabbedMeans - tabbedSd,
barCenters,tabbedMeans + tabbedSd, lwd = 1.5, angle = 90,code = 3, length
= 0.02)


# a-Values
a_plot <- read.csv("a_data.csv", header=T)

# Barplot with Error Bars
barCenters <-  barplot(tapply(
a_plot$a_diff,list(a_plot$Treatment,a_plot$Cot_Color),mean),
                       col=c("black", "burlywood4", "Blue", "Green",
"Red","khaki" ),
                       beside=T,ylab="",xlab="", ylim=c(-6,16),cex.axis =
1, cex.lab = 1.5)
           # y-axis Label
            mtext(text = "Mean   a*",
            side = 2, #side 2 = left
            line = 2)
            abline(h=0)#adds line on x axis
         #Add Legend
         legend(10,9,c("Control","UV","Blue", "Green", "Red", "F-VIS"),
         fill=c("black", "burlywood4", "Blue", "Green", "Red","khaki"),
cex=0.6)
            #Add Error Bars
            tabbedMeans <- tapply(
a_plot$a_diff,list(a_plot$Treatment,a_plot$Cot_Color),mean)
            tabbedSd<-
tapply(a_plot$a_diff,list(a_plot$Treatment,a_plot$Cot_Color),sd)
            arrows(barCenters, tabbedMeans - tabbedSd,
barCenters,tabbedMeans + tabbedSd, lwd = 1.5, angle = 90,code = 3, length
= 0.02)


# b-Values
b_plot <- read.csv("b_data.csv", header=T)

# Barplot with Error Bars
barCenters <-  barplot(tapply(
b_plot$b_diff,list(b_plot$Treatment,b_plot$Cot_Color),mean),
                      col=c("black", "burlywood4", "Blue", "Green",
"Red","khaki" ), beside=T,ylab="",xlab="Cotyledon Color", ylim=c(-
20,10),cex.axis = 1, cex.lab = 1)
             mtext(text = "Mean   b*",
             side = 2, #side 2 = left
```

```
             line = 2)
             abline(h=0)#adds line on x axis
            #Add Error Bars
            tabbedMeans <- tapply( b_plot$b_diff,list(b_plot
$Treatment,b_plot$Cot_Color),mean)
            tabbedSd<-
tapply(b_plot$b_diff,list(b_plot$Treatment,b_plot$Cot_Color),sd)
            arrows(barCenters, tabbedMeans - tabbedSd,
barCenters,tabbedMeans + tabbedSd, lwd = 1.5, angle = 90,
              code = 3, length = 0.02)

# E-Values
col_plot <- read.csv("col_diff.csv", header=T)

# Barplot with Error Bars
barCenters <-
barplot(tapply(col_plot$col_diff,list(col_plot$Treatment,col_plot$Cot_Col
or),mean),
               col=c("black", "burlywood4", "Blue", "Green",
"Red","khaki" ),beside=T,ylab="",xlab="Cotyledon Color",
ylim=c(0,25),cex.axis = 1, cex.lab = 1)
              mtext(text = "Mean   E*",
              side = 2, #side 2 = left
              line = 2)
              abline(h=0)#adds line on x axis
            #Add Error Bars
            tabbedMeans <- tapply( col_plot$col_diff,
list(col_plot$Treatment,col_plot$Cot_Color),mean)
             tabbedSd<-
tapply(col_plot$col_diff,list(col_plot$Treatment,col_plot$Cot_Color),sd)
             arrows(barCenters, tabbedMeans - tabbedSd,
barCenters,tabbedMeans + tabbedSd, lwd = 1.5, angle = 90,
                    code = 3, length = 0.02)


#Analysis of Green Cotyledon Color Data

#Boxplots

par(mfrow=c(2,2)) #set plot window
par(mar=c(4,4,1,0.5)) #set margins

#L_Value Plot
#Read in Data
# This Data was compiled to contain cleaned L-Value Differences Only
L_plot <- read.csv("L_data.csv", header=T)
boxplot(L_plot[L_plot$Cot_Color=="Green",]$L_diff~L_plot[L_plot$Cot_Color
=="Green",]$Treatment,
        las=2, col="white", cex.lab=1,ylim=c(-5,10), xlab="",
        ylab="",names=c("Control","UV", "Blue", "Green", "Red", "F_VIS"))
        mtext(text = "  L*",
        side = 2, #side 2 = left
        line = 2)
```

```
#a_Value Plot
#Read in Data
# This Data was compiled to contain cleaned a-Value Differences
a_plot <- read.csv("a_data.csv", header=T)
boxplot(a_plot[a_plot$Cot_Color=="Green",]$a_diff~a_plot[a_plot$Cot_Color
=="Green",]$Treatment,
        las=2, col="white", cex.lab=1,ylim=c(-5,20), xlab="",
        ylab="",names=c("Control","UV", "Blue", "Green", "Red", "F_VIS"))
        mtext(text = "  a*",
        side = 2, #side 2 = left
        line = 2)

#b_Value Plot
#Read in Data
# This Data was compiled to contain cleaned b-Value Differences
b_plot <- read.csv("b_data.csv", header=T)
boxplot(b_plot[b_plot$Cot_Color=="Green",]$b_diff~b_plot[b_plot$Cot_Color
=="Green",]$Treatment,
        las=2, col="white", cex.lab=1,ylim=c(-20,10), xlab="Treatment",
        ylab="",names=c("Control","UV", "Blue", "Green", "Red",
"F_VIS"))#x-axis labels
         mtext(text = "  b*",
         side = 2, #side 2 = left
         line = 2)

#E_Value Plot
#Read in Data
# This Data was compiled to contain cleaned E-Value Differences
E_plot <- read.csv("col_diff.csv", header=T)
boxplot(E_plot[E_plot$Cot_Color=="Green",]$col_diff~E_plot[E_plot$Cot_Col
or=="Green",]$Treatment,
        las=2, col="white", cex.lab=1,ylim=c(0,25), xlab="Treatment",
ylab="",names=c("Control","UV", "Blue", "Green", "Red", "F_VIS"))
         mtext(text = "  E*",
         side = 2, #side 2 = left
         line = 2)


# Hypothesis 1: The L-value changes in treated Green Lentils are Not
Different from Control

# GLM Model

green_model <- glm(L_diff ~ Treatment,
data=L_plot[L_plot$Cot_Color=="Green",])

#Output Model Results
summary(green_model)

# Check Model Assumptions
par(mfrow=c(2,2))
par(mar=c(4,4,4,4))
plot(green_model)
```

```
# Hypothesis 2: The a-value changes in treated Green Lentils are Not
Different from Control

# GLM Model

green_model2 <- glm(a_diff ~ Treatment,
data=a_plot[a_plot$Cot_Color=="Green",])

#Output Model Results
summary(green_model2)

# Check Model Assumptions
par(mfrow=c(2,2))
par(mar=c(4,4,4,4))
plot(green_model2)

# Hypothesis 3: The b-value changes in treated Green Lentils are Not
Different from Control

# GLM Model

green_model3 <- glm(b_diff ~ Treatment,
data=b_plot[b_plot$Cot_Color=="Green",])

#Output Model Results
summary(green_model3)

# Check Model Assumptions
par(mfrow=c(2,2))
par(mar=c(4,4,4,4))
plot(green_model3)


# Hypothesis 4: The E-value differences in treated Green Lentils Not are
Different from Control

# GLM Model

green_model4 <- glm(col_diff ~ Treatment,
data=E_plot[E_plot$Cot_Color=="Green",])

#Output Model Results
summary(green_model4)

# Check Model Assumptions
par(mfrow=c(2,2))
par(mar=c(4,4,4,4))
plot(green_model4)
```

E.6: Sample Color Difference Plots (GNUPLOT) Script (Chapter Six).

```
 #set terminal pngcairo  transparent enhanced font "arial,10" fontscale
0.4 size 600, 600
# set output 'sample.png'

#set terminal pdfcairo  enhanced size 5,5 color font "times new #roman,4"
#set output 'sample.png'

set terminal wxt size 1000,2500 enhanced font 'Times New Roman,10'
persist

set datafile separator comma
set style data boxplot
set key off
set xtics  norangelimit
set xtics   ("Control" 1.00000, "W\\\_UVA" 2.00000, "D\\\_UVA" 3.00000,
"W\\\_VIS" 4.00000, "D\\\_VIS" 5.00000)


set xrange [.5:5.5]
set yrange [-2:20]
x = 0.0
set boxwidth 0.3
set errorbars 2 lw 0.5 lt -1

set pointsize 1

set multiplot layout 2,2 rowsfirst scale 1.0,1.0

unset xlabel
set ylabel "{/Symbol D}L*"
#set ylabel "dL*"

unset arrow 1
unset arrow 2
set style arrow 1 nohead

set arrow 1 from 3.5, graph 0 to 3.5, graph 1 nohead dashtype "-"
set arrow 2 from 1.5, graph 0 to 1.5, graph 1 nohead dashtype "-"


plot "Green_colorDatasdn.csv" skip 1 every ::0::4 using 5:7:8 with
errorbars notitle, \
     ''                                    skip 1 every ::0::4 using
5:7:7:7:7 with candlesticks lt -1 lw 2 notitle

unset label 13
unset label 61

unset ylabel

plot "Green_colorDatasdn.csv" skip 1 every ::5::9 using 5:7:8 with
errorbars notitle, \
     ''                                    skip 1 every ::5::9 using
5:7:7:7:7 with candlesticks lt -1 lw 2 notitle
```

```
      set xlabel "Treatment"
      set ylabel "{/Symbol D}L*"
#set ylabel "dL*"

plot "Green_colorDatasdn.csv" skip 1 every ::10::14 using 5:7:8 with
errorbars notitle, \
      ''                                    skip 1 every ::10::14 using
5:7:7:7:7 with candlesticks lt -1 lw 2 notitle

unset ylabel

plot "Green_colorDatasdn.csv" skip 1 every ::15::19 using 5:7:8 with
errorbars notitle, \
      ''                                    skip 1 every ::15::19 using
5:7:7:7:7 with candlesticks lt -1 lw 2 notitle


unset multiplot
#unset output
set terminal wxt size 1000,2500 enhanced font 'Times New Roman,10'
persist
```

E.7: Sample Color Analysis R Script (Chapter Six).

```
# Set Working Directory

setwd("C:/Users/nij048/Desktop/seed_coat_effect")

# Read in Green Cotyledon Color Data as an object

Green_data <- read.csv("Green.csv", header = T)
Green_data #Confirm data is stored in object
 names(Green_data) #Check columns

# Compute Color Differences

  # Change in L-value
  L_diff <- Green_data$L_treated-Green_data$L_initial
  L_diff

  # Change in a-value
  a_diff <- Green_data$a_treated-Green_data$a_initial
  a_diff

  # Change in b-value
  b_diff <- Green_data$b_treated-Green_data$b_initial
  b_diff

  #Overall Color Difference
  col_diff <- sqrt((L_diff)^2+(a_diff)^2+ (b_diff)^2)
  col_diff

# Write Computations into Original File
  Green_colorData <- data.frame(Green_data,L_diff,a_diff,b_diff,
col_diff)
  write.csv(Green_colorData, file="Green_colorData.csv")


 Green_colorData <- read.csv("Green_colorData.csv", header=T)

# BLACK SEED COAT

  #Select Black Seed Coat
   Black <-Green_colorData[Green_colorData$Seed_coat=="Black",]

  #L_Difference
   par(mar=c(9,4,5,1))
   par(mfrow=c(1,2))

  # Model to Compare Changes L*-Values for Black Seed Coat

   Black_model1 <- glm(L_diff ~ Group, data=Black)

   #Output Model Results
   summary(Black_model1)

   # Check Model Assumptions
```

```
par(mfrow=c(2,2))
par(mar=c(4,4,4,4))
plot(Black_model1)
 #Assumptions of normality and homogeneity of variance met.

#Post-hoc Testing
posthoc<-TukeyHSD(aov(Black_model1))
#Output Post-hoc results
library(broom)
res2 <- tidy(posthoc)
write.csv(res2, file="L_Comp(Black).csv")
#
#
#


# Model to Compare Changes in a*-Values for Black Seed Coat

  Black_model2 <- glm(a_diff ~ Group, data=Black)

#Output Model Results
summary(Black_model2)

# Check Model Assumptions
par(mfrow=c(2,2))
par(mar=c(4,4,4,4))
plot(Black_model2)
 #Assumptions of normality and homogeneity of variance met.

#Post-hoc Testing
  posthoc<-TukeyHSD(aov(Black_model2))

#Output post-hoc result
 res3 <- tidy(posthoc)
 write.csv(res3, file="a_Comp(Black).csv")
#
#
#


# Model to Compare Changes in b*-Values for Black Seed Coat

  Black_model3<- glm(b_diff ~ Group, data=Black)

#Output Model Results
  summary(Black_model3)

# Check Model Assumptions
  par(mfrow=c(2,2))
  par(mar=c(4,4,4,4))
  plot(Black_model3)
  #Assumptions of normality and homogeneity of variance met.
```

```
#Post-hoc Testing
  posthoc2<-TukeyHSD(aov(Black_model3))

#Load the required Package to extract results
  library(broom)
  res4 <- tidy(posthoc2)
  write.csv(res4, file="b_Comp(Black).csv")
#
#
#


# Model to Compare changes in E*-Values for Black Seed Coat

  Black_model4<- glm(col_diff ~ Group, data=Black)

#Output Model Results
  summary(Black_model4)

# Check Model Assumptions
  par(mfrow=c(2,2))
  par(mar=c(4,4,4,4))
  plot(Black_model4)
 #Assumptions of normality and homogeneity of variance met.

#Post-hoc Testing
  posthoc3<-TukeyHSD(aov(Black_model4))

#Output Post-hoc results
  res5 <- tidy(posthoc3)
  write.csv(res5, file="E_Comp(Black).csv")


# GREY SEED COAT

#Select Grey Seed Coat
Grey <- Green_colorData[Green_colorData$Seed_coat=="Grey",]

# Model to Compare changes in L*-Values for GREY Seed Coat

 Grey_model1 <- glm(L_diff ~ Group, data=Grey)

#Output Model Results
 summary(Grey_model1)

# Check Model Assumptions
 par(mfrow=c(2,2))
 par(mar=c(4,4,4,4))
 plot(Grey_model1)
 #Assumptions of normality and homogeneity of variance met.

#Post-hoc Testing
 posthoc<-TukeyHSD(aov(Grey_model1))
#Output results
```

```
 res2 <- tidy(posthoc)
 write.csv(res2, file="L_Comp(Grey).csv")
#
#
#

# Model to Compare changes in a*-Values for Grey Seed Coat

 Grey_model2 <- glm(a_diff ~ Group, data=Grey)

#Output Model Results
 summary(Grey_model2 )

# Check Model Assumptions
 par(mfrow=c(2,2))
 par(mar=c(4,4,4,4))
 plot(Grey_model2)
 #Assumptions of normality and homogeneity of variance met.

#Post-hoc Testing
 posthoc<-TukeyHSD(aov(Grey_model2 ))
 res3 <- tidy(posthoc)
 write.csv(res3, file="a_Comp(Grey).csv")
#
#
#


# Model to Compare changes in b*-Values for Grey Seed Coat

  Grey_model3<- glm(b_diff ~ Group, data=Grey)

#Output Model Results
  summary(Grey_model3)

# Check Model Assumptions
  par(mfrow=c(2,2))
  par(mar=c(4,4,4,4))
  plot(Grey_model3)

#Post-hoc Testing
  posthoc2<-TukeyHSD(aov(Grey_model3))

#Output results
  res4 <- tidy(posthoc2)
  write.csv(res4, file="b_Comp(Grey).csv")
#
#
#


# Model to Compare E*-Values for Grey Seed Coat

  Grey_model4<- glm(col_diff ~ Group, data=Grey)
```

```
#Output Model Results
  summary(Grey_model4)

# Check Model Assumptions
  par(mfrow=c(2,2))
  par(mar=c(4,4,4,4))
  plot(Grey_model4)
  #Assumptions of normality and homogeneity of variance met.

#Post-hoc Testing
 posthoc3<-TukeyHSD(aov(Grey_model4))

#Output results
 res5 <- tidy(posthoc3)
 write.csv(res5, file="E_Comp(Grey).csv")



# GREEN SEED COAT

#Select Grey Seed Coat
Green <- Green_colorData[Green_colorData$Seed_coat=="
                           Green ",]

# Model to Compare L Values for Green Seed Coat

  Green_model1 <- glm(L_diff ~ Group, data=Green)

#Output Model Results
  summary(Green_model1)

# Check Model Assumptions
  par(mfrow=c(2,2))
  par(mar=c(4,4,4,4))
  plot(Green_model1)
  #Assumptions of normality and homogeneity of variance met.

#Post-hoc Testing
  posthoc<-TukeyHSD(aov(Green_model1))

#Output result
 res2 <- tidy(posthoc)
 write.csv(res2, file="L_Comp(Green).csv")
#
#
#


# Model to Compare changes in a*-Values for Green Seed Coat

  Green_model2 <- glm(a_diff ~ Group, data=Green)

#Output Model Results
```

```
  summary(Green_model2 )

# Check Model Assumptions
  par(mfrow=c(2,2))
  par(mar=c(4,4,4,4))
  plot(Green_model2)
  #Assumptions of normality and homogeneity of variance met.

#Post-hoc Testing
  posthoc<-TukeyHSD(aov(Green_model2 ))
#Output results
  res3 <- tidy(posthoc)
  write.csv(res3, file="a_Comp(Green).csv")
#
#
#


# Model to Compare b Values for Green Seed Coat

  Green_model3<- glm(b_diff ~ Group, data=Green)

#Output Model Results
  summary(Green_model3)

# Check Model Assumptions
  par(mfrow=c(2,2))
  par(mar=c(4,4,4,4))
  plot(Green_model3)
  #Assumptions of normality and homogeneity of variance met.

#Post-hoc Testing
  posthoc2<-TukeyHSD(aov(Green_model3))

#Output results
  library(broom)
  res4 <- tidy(posthoc2)

write.csv(res4, file="b_Comp(Green).csv")
#
#
#


# Model to Compare E*-Values for Green Seed Coat

  Green_model4<- glm(col_diff ~ Group, data=Green)

#Output Model Results
  summary(Green_model4)

# Check Model Assumptions
  par(mfrow=c(2,2))
  par(mar=c(4,4,4,4))
```

```
  plot(Green_model4)
  #Assumptions of normality and homogeneity of variance met.

#Post-hoc Testing
  posthoc3<-TukeyHSD(aov(Green_model4))

#Output results
  res5 <- tidy(posthoc3)
  write.csv(res5, file="E_Comp(Green).csv")


# GREY ZERO TANNIN SEED COAT

#Select Grey Zero tannin Seed Coat
Grey_ZT <- Green_colorData[Green_colorData$Seed_coat==""
                           Grey_ZT ",]

par(mar=c(9,4,5,1))
par(mfrow=c(1,2))
GreYZT <-Green_colorData[Green_colorData$Seed_coat=="Grey_ZT",]
#Select Grey      Seed Coat

# Model to Compare L Values for GreYZT Seed Coat
  GreYZT_model1 <- glm(L_diff ~ Group, data=GreYZT)

#Output Model Results
  summary(GreYZT_model1)

# Check Model Assumptions
  par(mfrow=c(2,2))
  par(mar=c(4,4,4,4))
  plot(GreYZT_model1)


#Post-hoc Testing
 posthoc<-TukeyHSD(aov(GreYZT_model1))

library(broom)
 res2 <- tidy(posthoc)

write.csv(res2, file="L_Comp(GreYZT).csv")
#
#
#

# Model to Compare a-Values for Grey_ZT Seed Coat
GreYZT_model2 <- glm(a_diff ~ Group, data=GreYZT)

#Output Model Results
summary(GreYZT_model2 )

# Check Model Assumptions
par(mfrow=c(2,2))
par(mar=c(4,4,4,4))
plot(GreYZT_model2)
```

```
#Post-hoc Testing
posthoc<-TukeyHSD(aov(GreYZT_model2 ))

library(broom)
res3 <- tidy(posthoc)

write.csv(res3, file="a_Comp(GreYZT).csv")
#
#
#


# Model to Compare b Values for Grey_ZT Seed Coat
  GreYZT_model3<- glm(b_diff ~ Group, data=GreYZT)

#Output Model Results
 summary(GreYZT_model3)

# Check Model Assumptions
  par(mfrow=c(2,2))
  par(mar=c(4,4,4,4))
  plot(GreYZT_model3)


#Post-hoc Testing
  posthoc2<-TukeyHSD(aov(GreYZT_model3))

#Load the required Package to extract results
 library(broom)
 res4 <- tidy(posthoc2)

write.csv(res4, file="b_Comp(GreYZT).csv")
#
#
#


# Model to Compare changes in E*-Values for Grey_ZT Seed Coat
  GreYZT_model4<- glm(col_diff ~ Group, data=GreYZT)

#Output Model Results
  summary(GreYZT_model4)

# Check Model Assumptions
  par(mfrow=c(2,2))
  par(mar=c(4,4,4,4))
  plot(GreYZT_model4)

#Post-hoc Testing
  posthoc3<-TukeyHSD(aov(GreYZT_model4))


#Output results
  res5 <- tidy(posthoc3)
  write.csv(res5, file="E_Comp(GreYZT).csv")
```